ISTANBUL TECHNICAL UNIVERSITY ★ EARTHQUAKE ENGINEERING AND DISASTER MANAGEMENT INSTITUTE

SOIL-STRUCTURE INTERACTION IN A SEISMICALLY ISOLATED STRUCTURE

M.Sc. THESIS

Yalçıncan ULUS

Earthquake Engineering and Disaster Management Institute

Earthquake Engineering Programme

SEPTEMBER 2019

ISTANBUL TECHNICAL UNIVERSITY ★ EARTHQUAKE ENGINEERING AND DISASTER MANAGEMENT INSTITUTE

SOIL-STRUCTURE INTERACTION IN A SEISMICALLY ISOLATED STRUCTURE

M.Sc. THESIS

Yalçıncan ULUS
(802161224)

Earthquake Engineering and Disaster Management Institute

Earthquake Engineering Programme

Thesis Advisor: Assis. Prof. Dr. Arcan YANIK

SEPTEMBER 2019

ISTANBUL TEKNİK ÜNİVERSİTESİ ★ DEPREM MÜHENDİSLİĞİ VE AFET YÖNETİMİ ENSTİTÜSÜ

TABAN YALITIMLI BİR YAPIDA YAPI ZEMİN ETKİLEŞİMİ

YÜKSEK LİSANS TEZİ

Yalçıncan ULUS
(802161224)

Deprem Mühendisliği Anabilim Dalı

Deprem Mühendisliği Programı

Tez Danışmanı: Dr. Öğr. Üyesi Arcan YANIK

EYLÜL 2019

Yalçıncan ULUS, a M.Sc. student of ITU Earthquake Engineering and Disaster Management Institute student number 802161224 successfully defended the thesis entitled "SOIL-STRUCTURE INTERACTION IN A SEISMICALLY ISOLATED STRUCTURE", which he prepared after fulfilling the requirements specified in the associated legislations, before the jury whose signatures are below.

Thesis Advisor :	**Assis. Prof. Dr. Arcan YANIK** Istanbul Technical University	.....
Jury Members :	**Prof. Dr. Ünal ALDEMİR** Istanbul Technical University	.....
	Assis. Prof. Dr. Yıldırım Serhat ERDOĞAN Yıldız Technical University	.....

Date of Submission : **03 May 2019**
Date of Defense : **13 September 2019**

To my family,

FOREWORD

I would like to thank my thesis advisor Assis. Prof. Dr. Arcan YANIK for his guidance and understanding, this work would not have been possible without his support. I deeply thank my friends from the earthquake engineering graduate program, and my cyclist friends who always helped me in times of need. I am most grateful to AVCI family for their tremendous amount of help.

I would also like to thank my family for their unending support, and my mother for always being there with me.

September 2019

Yalçıncan ULUS
(Civil Engineer)

TABLE OF CONTENTS

Page

FOREWORD ..... **ix**
TABLE OF CONTENTS ..... **xi**
ABBREVIATIONS ..... **xiii**
SYMBOLS ..... **xv**
LIST OF TABLES ..... **xvii**
LIST OF FIGURES ..... **xix**
SUMMARY ..... **xxvii**
ÖZET ..... **xxix**
1. INTRODUCTION **1**
1.1 Base Isolation 1
1.1.1 History of base isolation systems 3
1.1.2 Base isolation systems 4
1.1.2.1 Elastomeric bearings 4
1.1.2.2 Sliding isolation systems 6
1.2 Soil-Structure Interaction 6
1.3 Literature Review 7
2. FORMULATION OF THE PROBLEM **13**
2.1 Soil Model 13
2.2 Structural Matrices 14
2.2.1 Base isolated structures 16
2.2.2 Soil-structure interaction 17
2.2.3 Soil-structure interaction with base isolation 19
2.3 Equations of Motion 20
3. NUMERICAL ANALYSIS **23**
3.1 Analysis Cases 23
3.1.1 Soil Conditions 23
3.1.2 Buildings 24
3.1.3 Base Conditions 25
3.2 Earthquake Records 27
3.3 Time History Analysis 29
3.4 Response Spectrum Analysis 30
4. NUMERICAL RESULTS **33**
4.1 Time Histories 33
4.2 Spectral Analysis 110
5. CONCLUSIONS AND RECOMMENDATIONS **115**
REFERENCES **117**
APPENDICES **121**

CURRICULUM VITAE 123

ABBREVIATIONS

BI : Base Isolation
SSI : Soil Structure Interaction
TBDY : Türkiye Bina Deprem Yönetmeliği
LDRB : Low Damping Rubber Bearing
HDRB : High Damping Rubber Bearing
LRB : Lead Rubber Bearing

SYMBOLS

$\mathbf{a}$	: Length of rectangular foundation
$\mathbf{b}$	: Width of rectangular foundation
$\mathbf{c_r}$	: Rocking damping
$\mathbf{c_s}$	: Swaying damping
$\mathbf{C}$	: Damping matrix
$\mathbf{C_{BI}}$	: Damping matrix considering base isolation
$\mathbf{C_{SSI}}$	: Damping matrix considering soil-structure interaction
$\mathbf{C_{SSI,BI}}$	: Damping matrix considering soil-structure interaction and base isolation
$\mathbf{c_i}$	: Damping of the **i**th floor
$\mathbf{G}$	: Shear modulus of soil
$\mathbf{h_i}$	: Height of the **i**th floor
$\mathbf{I_0}$	: Mass moment of inertia of foundation
$\mathbf{I_i}$	: Mass moment of inertia of the **i**th floor
$\mathbf{k_i}$	: Stiffness of the **i**th floor
$\mathbf{k_r}$	: Rocking stiffness
$\mathbf{k_s}$	: Swaying stiffness
$\mathbf{K}$	: Stiffness matrix
$\mathbf{K_{BI}}$	: Stiffness matrix considering base isolation
$\mathbf{K_{SSI}}$	: Stiffness matrix considering soil-structure interaction
$\mathbf{K_{SSI,BI}}$	: Stiffness matrix considering soil-structure interaction and base isolation
$\mathbf{m_0}$	: Mass of foundation
$\mathbf{m_i}$	: Mass of the **i**th floor
$\mathbf{M}$	: Mass matrix
$\mathbf{M_{BI}}$	: Mass matrix considering base isolation
$\mathbf{M_{SSI}}$	: Mass matrix considering soil-structure interaction
$\mathbf{M_{SSI,BI}}$	: Mass matrix considering soil-structure interaction and base isolation
$\mathbf{r}$	: Foundation radius
$\mathbf{t}$	: time
$\ddot{u_g}$	: Ground acceleration
$\ddot{u}$	: Storey acceleration
$\dot{u}$	: Storey velocity
u	: Storey displacement
$\mathbf{V_S}$	: Shear wave velocity
ν	: Poisson's ratio
ρ	: Soil density

LIST OF TABLES

Page

Table 3.1 : Soil properties. 23
Table 3.2 : Soil properties of five and ten storey buildings. 24
Table 3.3 : Soil properties of forty storey building. 24
Table 3.4 : Properties of the forty-storey building. 24
Table 3.5 : Properties of the five-storey building. 24
Table 3.6 : Properties of the ten-storey building. 25
Table 3.7 : Earthquake events considered in analyses. 28

LIST OF FIGURES

Page

Figure 1.1 : Horizontal elastic design acceleration spectrum from TBDY. 2
Figure 1.2 : Response spectrum of the 1985 Mexico City Earthquake. 2
Figure 1.3 : Drawings from patents "improvement in buildings" (left) and "improved foundation for buildings" (right) 3
Figure 1.4 : Drawings from patent "Building construction to resist the action of earthquakes" 4
Figure 1.5 : Low or High damping rubber bearing. Maurer SE. Downloaded from https://www.maurer.eu/en/products/seismic-devices/isolators/index.html 5
Figure 1.6 : Lead rubber bearing. Maurer SE. Downloaded from https://www.maurer.eu/en/products/seismic-devices/isolators/index.html 5
Figure 1.7 : Sliding pendulum isolator. Maurer SE. Downloaded from https://www.maurer.eu/en/products/seismic-devices/isolators/index.html 6
Figure 2.1 : Spring and dashpot model. 13
Figure 2.2 : Fixed based shear frame structure. 15
Figure 2.3 : Base isolated shear frame structure. 16
Figure 2.4 : Shear frame structure considering SSI. 17
Figure 2.5 : Shear frame structure considering SSI and base isolation together. .. 19
Figure 4.1 : Top storey acceleration-time histories of five-storey building(Imperial Valley, 1979, near fault). 35
Figure 4.2 : Maximum accelerations of each storey for the five-storey building(Imperial Valley, 1979, near fault). 35
Figure 4.3 : Top storey velocity-time histories of five-storey building(Imperial Valley, 1979, near fault). 36
Figure 4.4 : Maximum velocities of each storey for the five-storey building(Imperial Valley, 1979, near fault). 36
Figure 4.5 : Top storey displacement-time histories of five-storey building(Imperial Valley, 1979, near fault). 37
Figure 4.6 : Maximum displacements of each storey for the five-storey building(Imperial Valley, 1979, near fault). 37
Figure 4.7 : Top storey acceleration-time histories of ten-storey building(Imperial Valley, 1979, near fault). 38
Figure 4.8 : Maximum accelerations of each storey for the ten-storey building(Imperial Valley, 1979, near fault). 38
Figure 4.9 : Top storey velocity-time histories of ten-storey building(Imperial Valley, 1979, near fault). 39
Figure 4.10 : Maximum velocities of each storey for the ten-storey building(Imperial Valley, 1979, near fault). 39

Figure 4.11: Top storey displacement-time histories of ten-storey building(Imperial Valley, 1979, near fault). 40
Figure 4.12: Maximum displacements of each storey for the ten-storey building(Imperial Valley, 1979, near fault). 40
Figure 4.13: Top storey acceleration-time histories of forty-storey building(Imperial Valley, 1979, near fault). 41
Figure 4.14: Maximum accelerations of each storey for the forty-storey building(Imperial Valley, 1979, near fault). 41
Figure 4.15: Top storey velocity-time histories of forty-storey building(Imperial Valley, 1979, near fault). 42
Figure 4.16: Maximum velocities of each storey for the forty-storey building(Imperial Valley, 1979, near fault). 42
Figure 4.17: Top storey displacement-time histories of forty-storey building(Imperial Valley, 1979, near fault). 43
Figure 4.18: Maximum displacements of each storey for the forty-storey building(Imperial Valley, 1979, near fault). 43
Figure 4.19: Top storey acceleration-time histories of five-storey building(Imperial Valley, 1979, far fault)..... 44
Figure 4.20: Maximum accelerations of each storey for the five-storey building(Imperial Valley, 1979, far fault). 44
Figure 4.21: Top storey velocity-time histories of five-storey building(Imperial Valley, 1979, far fault)..... 45
Figure 4.22: Maximum velocities of each storey for the five-storey building(Imperial Valley, 1979, far fault)..... 45
Figure 4.23: Top storey displacement-time histories of five-storey building(Imperial Valley, 1979, far fault)..... 46
Figure 4.24: Maximum displacements of each storey for the five-storey building(Imperial Valley, 1979, far fault). 46
Figure 4.25: Top storey acceleration-time histories of ten-storey building(Imperial Valley, 1979, far fault)..... 47
Figure 4.26: Maximum accelerations of each storey for the ten-storey building(Imperial Valley, 1979, far fault). 47
Figure 4.27: Top storey velocity-time histories of ten-storey building(Imperial Valley, 1979, far fault)..... 48
Figure 4.28: Maximum velocities of each storey for the ten-storey building(Imperial Valley, 1979, far fault)..... 48
Figure 4.29: Top storey displacement-time histories of ten-storey building(Imperial Valley, 1979, far fault)..... 49
Figure 4.30: Maximum displacements of each storey for the ten-storey building(Imperial Valley, 1979, far fault). 49
Figure 4.31: Top storey acceleration-time histories of forty-storey building(Imperial Valley, 1979, far fault)..... 50
Figure 4.32: Maximum accelerations of each storey for the forty-storey building(Imperial Valley, 1979, far fault). 50
Figure 4.33: Top storey velocity-time histories of forty-storey building(Imperial Valley, 1979, far fault). 51

Figure 4.34: Maximum velocities of each storey for the forty-storey building(Imperial Valley, 1979, far fault)..... 51
Figure 4.35: Top storey displacement-time histories of forty-storey building(Imperial Valley, 1979, far fault)..... 52
Figure 4.36: Maximum displacements of each storey for the forty-storey building(Imperial Valley, 1979, far fault). 52
Figure 4.37: Top storey acceleration-time histories of five-storey building(Cape Mendocino, 1992, near fault). 54
Figure 4.38: Maximum accelerations of each storey for the five-storey building(Cape Mendocino, 1992, near fault). 54
Figure 4.39: Top storey velocity-time histories of five-storey building(Cape Mendocino, 1992, near fault). 55
Figure 4.40: Maximum velocities of each storey for the five-storey building(Cape Mendocino, 1992, near fault). 55
Figure 4.41: Top storey displacement-time histories of five-storey building(Cape Mendocino, 1992, near fault). 56
Figure 4.42: Maximum displacements of each storey for the five-storey building(Cape Mendocino, 1992, near fault). 56
Figure 4.43: Top storey acceleration-time histories of ten-storey building(Cape Mendocino, 1992, near fault). 57
Figure 4.44: Maximum accelerations of each storey for the ten-storey building(Cape Mendocino, 1992, near fault). 57
Figure 4.45: Top storey velocity-time histories of ten-storey building(Cape Mendocino, 1992, near fault). 58
Figure 4.46: Maximum velocities of each storey for the ten-storey building(Cape Mendocino, 1992, near fault). 58
Figure 4.47: Top storey displacement-time histories of ten-storey building(Cape Mendocino, 1992, near fault). 59
Figure 4.48: Maximum displacements of each storey for the ten-storey building(Cape Mendocino, 1992, near fault). 59
Figure 4.49: Top storey acceleration-time histories of forty-storey building(Cape Mendocino, 1992, near fault). 60
Figure 4.50: Maximum accelerations of each storey for the forty-storey building(Cape Mendocino, 1992, near fault). 60
Figure 4.51: Top storey velocity-time histories of forty-storey building(Cape Mendocino, 1992, near fault). 61
Figure 4.52: Maximum velocities of each storey for the forty-storey building(Cape Mendocino, 1992, near fault). 61
Figure 4.53: Top storey displacement-time histories of forty-storey building(Cape Mendocino, 1992, near fault). 62
Figure 4.54: Maximum displacements of each storey for the forty-storey building(Cape Mendocino, 1992, near fault). 62
Figure 4.55: Top storey acceleration-time histories of five-storey building(Cape Mendocino, 1992, far fault)..... 63
Figure 4.56: Maximum accelerations of each storey for the five-storey building(Cape Mendocino, 1992, far fault). 63

Figure 4.57: Top storey velocity-time histories of five-storey building(Cape Mendocino, 1992, far fault). 64
Figure 4.58: Maximum velocities of each storey for the five-storey building(Cape Mendocino, 1992, far fault)..... 64
Figure 4.59: Top storey displacement-time histories of five-storey building(Cape Mendocino, 1992, far fault)..... 65
Figure 4.60: Maximum displacements of each storey for the five-storey building(Cape Mendocino, 1992, far fault). 65
Figure 4.61: Top storey acceleration-time histories of ten-storey building(Cape Mendocino, 1992, far fault). 66
Figure 4.62: Maximum accelerations of each storey for the ten-storey building(Cape Mendocino, 1992, far fault). 66
Figure 4.63: Top storey velocity-time histories of ten-storey building(Cape Mendocino, 1992, far fault). 67
Figure 4.64: Maximum velocities of each storey for the ten-storey building(Cape Mendocino, 1992, far fault)..... 67
Figure 4.65: Top storey displacement-time histories of ten-storey building(Cape Mendocino, 1992, far fault)..... 68
Figure 4.66: Maximum displacements of each storey for the ten-storey building(Cape Mendocino, 1992, far fault). 68
Figure 4.67: Top storey acceleration-time histories of forty-storey building(Cape Mendocino, 1992, far fault)..... 69
Figure 4.68: Maximum accelerations of each storey for the forty-storey building(Cape Mendocino, 1992, far fault). 69
Figure 4.69: Top storey velocity-time histories of forty-storey building(Cape Mendocino, 1992, far fault). 70
Figure 4.70: Maximum velocities of each storey for the forty-storey building(Cape Mendocino, 1992, far fault)..... 70
Figure 4.71: Top storey displacement-time histories of forty-storey building(Cape Mendocino, 1992, far fault)..... 71
Figure 4.72: Maximum displacements of each storey for the forty-storey building(Cape Mendocino, 1992, far fault). 71
Figure 4.73: Top storey acceleration-time histories of five-storey building(Kocaeli, 1999, near fault). 73
Figure 4.74: Maximum accelerations of each storey for the five-storey building(Kocaeli, 1999, near fault). 73
Figure 4.75: Top storey velocity-time histories of five-storey building(Kocaeli, 1999, near fault). 74
Figure 4.76: Maximum velocities of each storey for the five-storey building(Kocaeli, 1999, near fault). 74
Figure 4.77: Top storey displacement-time histories of five-storey building(Kocaeli, 1999, near fault). 75
Figure 4.78: Maximum displacements of each storey for the five-storey building(Kocaeli, 1999, near fault). 75
Figure 4.79: Top storey acceleration-time histories of ten-storey building(Kocaeli, 1999, near fault). 76

Figure 4.80: Maximum accelerations of each storey for the ten-storey building(Kocaeli, 1999, near fault). 76
Figure 4.81: Top storey velocity-time histories of ten-storey building(Kocaeli, 1999, near fault). 77
Figure 4.82: Maximum velocities of each storey for the ten-storey building(Kocaeli, 1999, near fault). 77
Figure 4.83: Top storey displacement-time histories of ten-storey building(Kocaeli, 1999, near fault). 78
Figure 4.84: Maximum displacements of each storey for the ten-storey building(Kocaeli, 1999, near fault). 78
Figure 4.85: Top storey acceleration-time histories of forty-storey building(Kocaeli, 1999, near fault). 79
Figure 4.86: Maximum accelerations of each storey for the forty-storey building(Kocaeli, 1999, near fault). 79
Figure 4.87: Top storey velocity-time histories of forty-storey building(Kocaeli, 1999, near fault). 80
Figure 4.88: Maximum velocities of each storey for the forty-storey building(Kocaeli, 1999, near fault). 80
Figure 4.89: Top storey displacement-time histories of forty-storey building(Kocaeli, 1999, near fault). 81
Figure 4.90: Maximum displacements of each storey for the forty-storey building(Kocaeli, 1999, near fault). 81
Figure 4.91: Top storey acceleration-time histories of five-storey building(Kocaeli, 1999, far fault). 82
Figure 4.92: Maximum accelerations of each storey for the five-storey building(Kocaeli, 1999, far fault). 82
Figure 4.93: Top storey velocity-time histories of five-storey building(Kocaeli, 1999, far fault). 83
Figure 4.94: Maximum velocities of each storey for the five-storey building(Kocaeli, 1999, far fault). 83
Figure 4.95: Top storey displacement-time histories of five-storey building(Kocaeli, 1999, far fault). 84
Figure 4.96: Maximum displacements of each storey for the five-storey building(Kocaeli, 1999, far fault). 84
Figure 4.97: Top storey acceleration-time histories of ten-storey building(Kocaeli, 1999, far fault). 85
Figure 4.98: Maximum accelerations of each storey for the ten-storey building(Kocaeli, 1999, far fault). 85
Figure 4.99: Top storey velocity-time histories of ten-storey building(Kocaeli, 1999, far fault). 86
Figure 4.100 Maximum velocities of each storey for the ten-storey building(Kocaeli, 1999, far fault). 86
Figure 4.101 Top storey displacement-time histories of ten-storey building(Kocaeli, 1999, far fault). 87
Figure 4.102 Maximum displacements of each storey for the ten-storey building(Kocaeli, 1999, far fault). 87

Figure 4.103 Top storey acceleration-time histories of forty-storey building(Kocaeli, 1999, far fault). 88
Figure 4.104 Maximum accelerations of each storey for the forty-storey building(Kocaeli, 1999, far fault). 88
Figure 4.105 Top storey velocity-time histories of forty-storey building(Kocaeli, 1999, far fault). 89
Figure 4.106 Maximum velocities of each storey for the forty-storey building(Kocaeli, 1999, far fault). 89
Figure 4.107 Top storey displacement-time histories of forty-storey building(Kocaeli, 1999, far fault). 90
Figure 4.108 Maximum displacements of each storey for the forty-storey building(Kocaeli, 1999, far fault). 90
Figure 4.109 Top storey acceleration-time histories of five-storey building(Manjil, 1990, near fault). 92
Figure 4.110 Maximum accelerations of each storey for the five-storey building(Manjil, 1990, near fault). 92
Figure 4.111 Top storey velocity-time histories of five-storey building(Manjil, 1990, near fault). 93
Figure 4.112 Maximum velocities of each storey for the five-storey building(Manjil, 1990, near fault). 93
Figure 4.113 Top storey displacement-time histories of five-storey building(Manjil, 1990, near fault). 94
Figure 4.114 Maximum displacements of each storey for the five-storey building(Manjil, 1990, near fault). 94
Figure 4.115 Top storey acceleration-time histories of ten-storey building(Manjil, 1990, near fault). 95
Figure 4.116 Maximum accelerations of each storey for the ten-storey building(Manjil, 1990, near fault). 95
Figure 4.117 Top storey velocity-time histories of ten-storey building(Manjil, 1990, near fault). 96
Figure 4.118 Maximum velocities of each storey for the ten-storey building(Manjil, 1990, near fault). 96
Figure 4.119 Top storey displacement-time histories of ten-storey building(Manjil, 1990, near fault). 97
Figure 4.120 Maximum displacements of each storey for the ten-storey building(Manjil, 1990, near fault). 97
Figure 4.121 Top storey acceleration-time histories of forty-storey building(Manjil, 1990, near fault). 98
Figure 4.122 Maximum accelerations of each storey for the forty-storey building(Manjil, 1990, near fault). 98
Figure 4.123 Top storey velocity-time histories of forty-storey building(Manjil, 1990, near fault). 99
Figure 4.124 Maximum velocities of each storey for the forty-storey building(Manjil, 1990, near fault). 99
Figure 4.125 Top storey displacement-time histories of forty-storey building(Manjil, 1990, near fault). 100

Figure 4.126 Maximum displacements of each storey for the forty-storey building(Manjil, 1990, near fault). 100
Figure 4.127 Top storey acceleration-time histories of five-storey building(Manjil, 1990, far fault). 101
Figure 4.128 Maximum accelerations of each storey for the five-storey building(Manjil, 1990, far fault). 101
Figure 4.129 Top storey velocity-time histories of five-storey building(Manjil, 1990, far fault). 102
Figure 4.130 Maximum velocities of each storey for the five-storey building(Manjil, 1990, far fault). 102
Figure 4.131 Top storey displacement-time histories of five-storey building(Manjil, 1990, far fault). 103
Figure 4.132 Maximum displacements of each storey for the five-storey building(Manjil, 1990, far fault). 103
Figure 4.133 Top storey acceleration-time histories of ten-storey building(Manjil, 1990, far fault). 104
Figure 4.134 Maximum accelerations of each storey for the ten-storey building(Manjil, 1990, far fault). 104
Figure 4.135 Top storey velocity-time histories of ten-storey building(Manjil, 1990, far fault). 105
Figure 4.136 Maximum velocities of each storey for the ten-storey building(Manjil, 1990, far fault). 105
Figure 4.137 Top storey displacement-time histories of ten-storey building(Manjil, 1990, far fault). 106
Figure 4.138 Maximum displacements of each storey for the ten-storey building(Manjil, 1990, far fault). 106
Figure 4.139 Top storey acceleration-time histories of forty-storey building(Manjil, 1990, far fault). 107
Figure 4.140 Maximum accelerations of each storey for the forty-storey building(Manjil, 1990, far fault). 107
Figure 4.141 Top storey velocity-time histories of forty-storey building(Manjil, 1990, far fault). 108
Figure 4.142 Maximum velocities of each storey for the forty-storey building(Manjil, 1990, far fault). 108
Figure 4.143 Top storey displacement-time histories of forty-storey building(Manjil, 1990, far fault). 109
Figure 4.144 Maximum displacements of each storey for the forty-storey building(Manjil, 1990, far fault). 109
Figure 4.145 Spectral acceleration, velocity and displacement values for very soft soil conditions. 111
Figure 4.146 Spectral acceleration, velocity and displacement values for soft soil conditions. 112
Figure 4.147 Spectral acceleration, velocity and displacement values for medium soil conditions. 113
Figure 4.148 Spectral acceleration, velocity and displacement values for dense soil conditions. 114

SOIL-STRUCTURE INTERACTION
IN A SEISMICALLY ISOLATED STRUCTURE

SUMMARY

Seismic base isolation is a structural control technique which is being used in the seismic protection of civil engineering structures. Additionally, soil-structure interaction (SSI) is an important concept that is usually neglected in practical applications because its effect on structures is believed to be beneficial. However, studies show that the effects of soil structure interaction can also be detrimental. The aim of this study is to analytically implement base isolation with SSI to an example structure and to develop a very simple solution to add these combined effects into the mass, damping and stiffness matrices of the structure. After applying this solution, these matrices are used in the dynamic equations of the motion of the structure under earthquake effect. Dynamic analysis is carried out using a computer program developed in MATLAB environment. This program performs dynamic analysis using Newmark's method under the effect of earthquake excitation with and without SSI. In these simulations, three shear frame structures with different properties are considered. The strong ground motions selected for these analyses are eighteen different events with far fault and near fault components. In addition, four different base and soil-structure combination cases are taken into account. These four analytical cases are; a fixed based structure and a seismically isolated structure with or without the SSI. The results of these numerical dynamic analyses are presented graphically and comparatively in time domain. The results consist of storey displacements, accelerations and velocities. With the help of the numerical results, effects of SSI in seismically isolated structures are discussed.

TABAN YALITIMLI BİR YAPIDA
YAPI ZEMİN ETKİLEŞİMİ

ÖZET

Taban yalıtımı, yapıların deprem etkisine karşı korunmasında kullanılan yapısal kontrol tekniklerinden biridir. Ek olarak, yapı-zemin etkileşimi, yapılar üzerindeki etkisinin yararlı olduğuna inanıldığı için genellikle ihmal edilen önemli bir kavramdır. Bununla birlikte, yapı zemin etkileşiminin yapı üzerindeki etkilerinin zararlı da olabileceği araştırmalar tarafından ortaya konmuştur. Bu çalışmanın amaçlarından biri, yapı zemin etkileşimi ve taban yalıtımı etkilerinin tüm kombinasyonlarını örnek yapıların kütle, sönüm ve rijitlik matrislerine basit olarak ekleyen bir çözüm üretmektir. Bu matrisler elde edildikten sonra, deprem etkisindeki yapının hareket denklemlerinde kullanılmıştır.

Taban yalıtımı, 19. yüzyıldan itibaren araştırılan ve kullanılan, yapıları depremden koruma yöntemlerinden biridir. Bu sistemler hastaneler, havalimanları gibi kesintisiz hizmet vermesi beklenen binalarda ve viyadüklerde sıklıkla kullanılmaktadır. Taban yalıtımının ana fikri; üst yapı ve bina temeli arasına konumlanarak birbirlerinden ayrı hareket edebilmelerine olanak sağlamaktır. Taban yalıtımları, binanın yükünü taşıyabilmeleri için yüksek dikey rijitliğe, serbest yatay hareket sağlayabilmek için ise düşük yatay rijitliğe sahiptirler. Deprem esnasında üst yapı ve bina temeli birbirinden ayrı hareket edebilir ve bu sayede normalden daha az taban kesme kuvveti ve daha az göreli kat ötelenmeleri ile karşılaşılır.

Taban yalıtımı her zaman yapının doğal titreşim periyodunu uzatmaktadır ve bu taban yalıtımının en önemli özelliğidir. Doğal titreşim periyodunun uzaması, yapının daha az spektral ivmeye maruz kalmasını sağlamaktadır ve bu sayede yapısal elemanlarda oluşan iç kuvvetler azalmaktadır.

Üstyapı ve bina temelinin birbirinden ayrılması fikri 19. yüzyılın sonlarında Amerika Birleşik Devletleri'nde alınan patentlerde görülmüştür. Bu patentlerde mucitler, yapıların metal küreler veya elastik yaylar üzerine inşa edilmesini tavsiye etmişlerdir. Tokyo Üniversitesi'nde görev yapan İngiliz yerbilimci John Milne, kaymaya dayalı taban yalıtım sistemlerinin ilk örneği üzerinde çalışmıştır.

Birçok farklı çeşidi olsa da, taban yalıtım sistemleri; elastomer mesnetler ve kaymaya dayalı sistemler olarak iki ana gruba ayrılabilir. Elastomer mesnetler, üst üste sıralı olarak dizilmiş kauçuk ve çelik levhalardan oluşmaktadır. Kauçuk levhalar gerekli olan düşük yatay rijitliği sağlamakta iken, çelik levhalar da gerekli olan yüksek dikey rijitliği sağlamaktadır. Çelik levhalar ek olarak kauçuk levhaların şişmesine ve ezilmesine engel olmaktadır. Elastomer mesnetler, kullanılan malzemeler değiştirilerek düşük sönümlü veya yüksek sönümlü olarak üretilebilirler. Elastomer mesnetler içerisine bir veya birden fazla kurşun çekirdek konularak da üretilebilirler. Kurşun çekirdekler bu mesnetlere enerji sönümleme yeteneği kazandırmaktadır.

Diğer bir tür olan kaymaya dayalı mesnetler, elastomer mesnetlerden daha ekonomiktir. Bu mesnetlerde sürtünme oluştuğundan, az miktarda kesme kuvveti yapıya iletilmektedir. Bu mesnetlerin sürtünme özellikleri enerji tüketimine de katkı sağlamaktadır. Geleneksel kayma mesnetlerinin deprem hareketinden sonra eski konumuna gelme özellikleri mevcut değildir. Bu tarz mesnetlerin eski konumlarına gelmelerine yardımcı olacak elemanlar kullanılması gerekmektedir. Ancak bu özelliğe sahip olan kayma mesnetleri de mevcuttur. Konkav geometrileri sayesinde, sarkaç mesnetler yer çekimi yardımıyla gerekli olan geri dönme kuvvetlerinin oluşmasını sağlamaktadır.

Yapı-zemin etkileşimi; yapı, temel ve zeminin etkilerinin birlikte hesaba katıldığı bir tasarım yöntemidir. Geleneksel olarak yapılar zemine sabitlenmiş olarak tasarlanmaktadır ve yapının altındaki zeminin etkileri göz ardı edilmektedir. Bunun genel sebebi, yapı-zemin etkileşiminin yapıya faydalı olduğu görüşüdür.

Dinamik analizler, MATLAB ortamında geliştirilen bir bilgisayar programı kullanılarak yapılmıştır. Bu program deprem etkisi altındaki yapıların dinamik analizlerini yapı zemin etkileşimi etkisi eklenmiş ve eklenmemiş şekilde gerçekleştirmektedir. Bu analizlerde kullanılan örnek yapılar; beş, on ve kırk katlı kayma binalarıdır. Bu analizler için yakın fay ve uzak fay bileşenleri dahil olmak üzere onsekiz farklı yer hareketi seçilmiştir. Ek olarak dört farklı temel ve yapı zemin kombinasyonu hesaba katılmıştır. Bu dört farklı kombinasyon; taban yalıtımlı ve taban yalıtımsız, yapı zemin etkileşimi hesaba katılmış ve katılmamış yapılardan oluşmaktadır. Bu nümerik dinamik analizlerin sonuçları grafiksel ve karşılaştırmalı olarak zaman tanım alanında sunulmuştur. Nümerik sonuçların yardımıyla, taban yalıtımlı yapılarda yapı zemin etkileşimi etkileri tartışılmıştır.

Yapı-zemin etkileşimi problemlerinin çözümünde iki ana yaklaşım kullanılmaktadır. Bunlardan biri zeminin yapının devamı olarak modellendiği direkt metottur. Diğeri ise zeminin yaylar ve sönümleyiciler ile modellendiği altyapı metodudur. Bu çalışmada altyapı metodu kullanılmıştır.

Zeminin özelliklerini içeren rijitlik ve sönüm değerleri, empedans fonksiyonlarından hesaplanmıştır. Bu rijitlik ve sönüm değerleri, yapı-zemin etkileşimini içeren yapısal matrislerde kullanılmıştır.

Yapının kütle, sönüm ve rijitlik matrisleri, yapı-zemin etkileşimi ve taban yalıtımını dahil edecek şekilde kurulmuştur. Bu işlemler için Matlab ortamında yardımcı fonksiyonlar geliştirilmiştir. Yapı-zemin etkileşimini ve taban yalıtımını içeren bu matrisler hareket denklemlerinin çözümünde kullanılmıştır. Hareket denklemlerinin çözümünde Newmark yöntemi kullanılmıştır. Çok katlı yapılarda Newmark yöntemini uygulayan bir Matlab programı da geliştirilmiştir ve analizler bu programla yapılmıştır.

Her bina, deprem ve zemin koşulu için ayrı ayrı analiz yapılmıştır. Sonuçlar, yapıların katlarında oluşan ivme, hız ve yer değiştirmelerin zamana dayalı değerleridir.

Analizler sonucu şu sonuçlara ulaşılmıştır:

Taban yalıtımı binaya gelen ivme, hız ve yer değiştirme isteklerini önemli ölçüde azaltmaktadır. Toplam yer değiştirmeler normal yapılardan daha fazla olsa da, bu yer değiştirme yalıtım sisteminde odaklandığı için üst yapı birlikte hareket ederek normalden çok daha düşük göreli kat ötelenmelerine maruz kalmaktadır.

Yapı-zemin etkileşimi, yapıda oluşan ivme, hız ve yer değiştirmeleri etkilemektedir. Yapı-zemin etkileşiminin genellikle deprem etkilerini azalttığı ve yapıya faydalı olduğu görülmektedir. Yönetmelikler güvenli tarafta kalma adına yapı-zemin etkileşimi için detaylı çözüm yöntemleri sunmamaktadır. Bu çalışmanın sonuçları da bu varsayımlarla örtüşmektedir. Ancak bazı sonuçlarda yapı-zemin etkileşiminin az da olsa deprem etkilerini artırdığı da görülmektedir.

Yapı-zemin etkileşimi etkileri daha çok yumuşak zemin koşullarında ortaya çıkmaktadır. Sert zemin koşullarında, yapı zemine sabit kabul edilen durumla aynı tepkiyi vermektedir.

Yapı-zemin etkileşiminin, taban yalıtımının performansına etki ettiği görülmüştür. Taban yalıtımının tesirliği yapı-zemin etkileşimi hesaba katıldığından azalmaktadır.

Depremlerin yakın veya uzak fay olması sonuçların niteliğini etkilememiştir. Aynı şekilde, yapı yüksekliği de sonuçlarda dikkate değer değişikliğe sebep olmamıştır.

1. INTRODUCTION

1.1 Base Isolation

Base isolation (BI), also known as dynamic isolation or seismic base isolation, is a widely used technique for protecting structures from earthquake effects. It is mostly used in important structures that continuous operation is needed even after large earthquakes such as hospitals, airports, nuclear power plants and government buildings. It is also used in highway engineering structures such as bridges and viaducts [1].

The main idea behind base isolation is to simply form an interface between the superstructure and the foundation of the building. This interface has high vertical stiffness so that it can support the weight of the building, but a very low horizontal stiffness enabling free horizontal movement of the foundation. During earthquakes the superstructure and the foundation are effectively decoupled from each other with the help of base isolation systems, resulting much lower base shear forces and inter-storey drifts [2].

Base isolation will always increase the natural vibration period of the structure. This is the single most important feature of base isolation systems. By lengthening the natural vibration period, the structure will usually experience less acceleration on storey levels therefore internal forces that structural elements encounter will also be smaller [2].

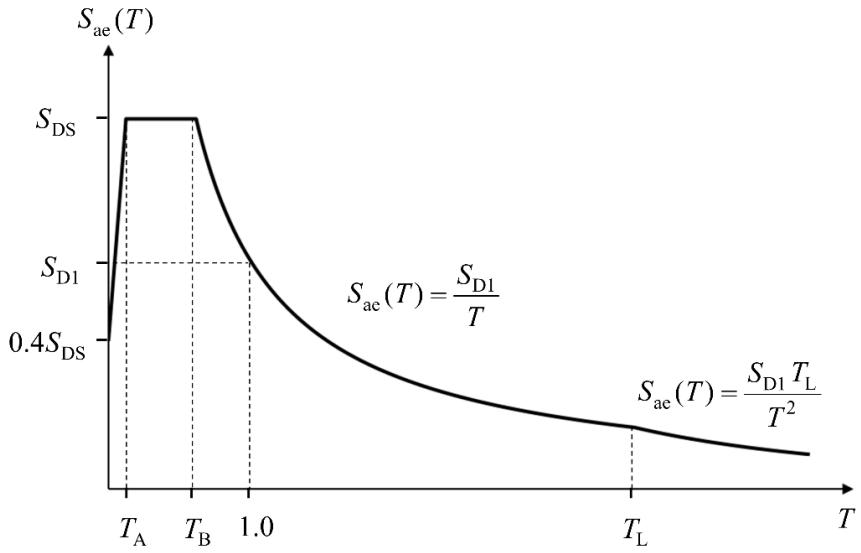

Figure 1.1 : Horizontal elastic design acceleration spectrum from TBDY.

Basic shape of a design acceleration spectrum can be seen in figure 1.1 [3]. Although details about these design spectra varies from country to country, overall shape of the spectrum remains nearly the same. Beneficialness of base isolation systems becomes more evident when design spectra are considered. Bigger natural period of isolated structures means they will experience less spectral acceleration. However, because these design spectra are composed by averaging response of multiple ground motion data, they can hide detrimental effects of base isolation systems that can rarely be manifested.

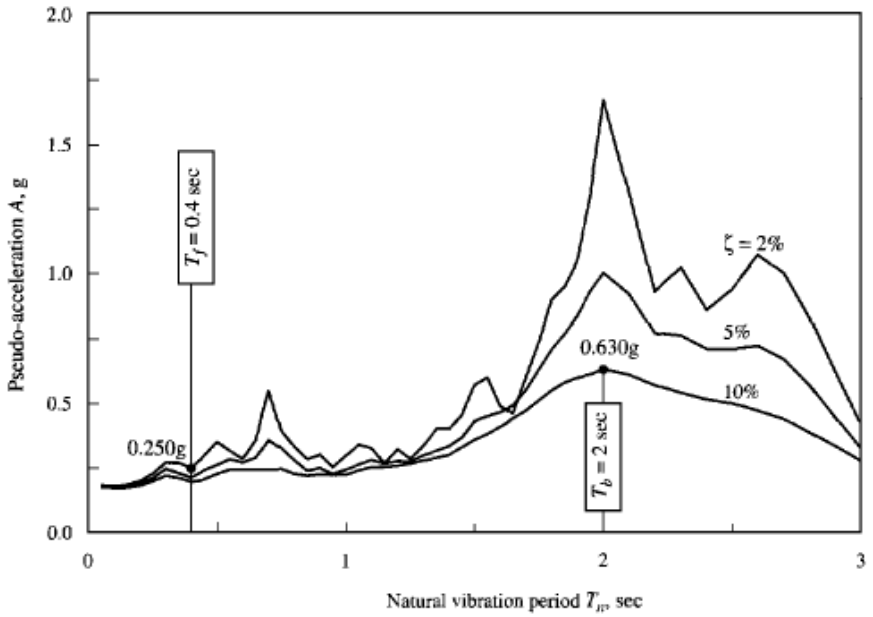

Figure 1.2 : Response spectrum of the 1985 Mexico City Earthquake.

As is seen from figure 1.2 [2], some earthquakes can have different response spectra that contradict every design spectrum. In the case of the 19 September 1985 Mexico City earthquake, unlike most other earthquakes, spectral response is actually increases towards higher period values. In cases like this, a base isolation system will be detrimental to the structure instead of being beneficial.

1.1.1 History of base isolation systems

First known documents that possess the idea of decoupling superstructures from their foundations are two US patents from 1870s. First one is called "improvement in buildings" by Jules Touaillon dated February 15, 1870. He suggested that buildings should to be constructed with their superstructure and foundation separate from each other by using balls [4].

Few days later, Almond F. Cooper patented his invention called "Improved foundation for buildings". Rather than balls, he suggested using "elastic cushions or springs" for decoupling the superstructure [5].

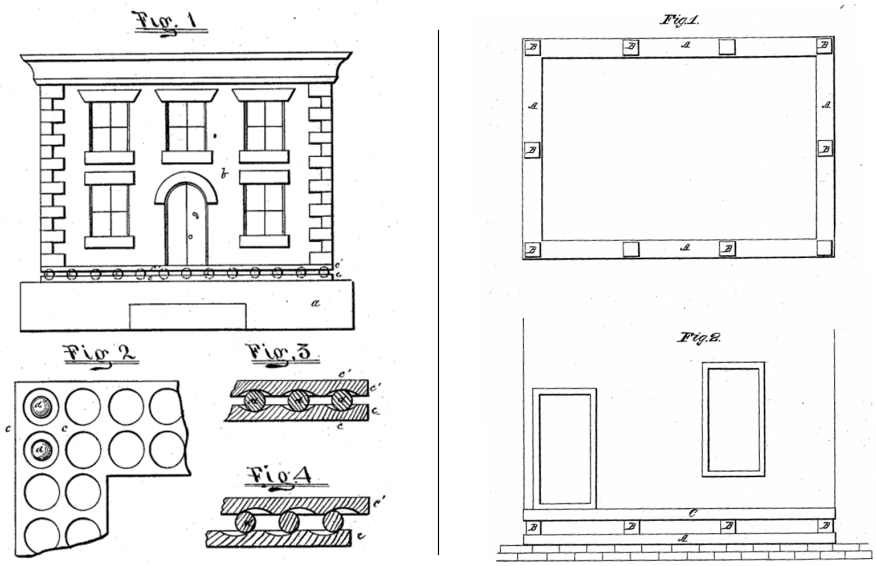

Figure 1.3 : Drawings from patents "improvement in buildings" (left) and "improved foundation for buildings" (right)

A geologist and mining engineer from England, John Milne, has built the first known base isolated structure while he was working at the University of Tokyo in 1885. This structure was built on cast iron balls and on top of those, slightly concave plates. He wasn't satisfied with the wind performance of the structure so he experimented with cast iron balls with different sizes until he landed on 0.25 inch balls which were

performing well on wind loads and the structure's performance under actual earthquake motion was satisfactory [6].

Jacob Bechtold from Munich, Germany suggested using a container filled with "spherical bodies of hard material" for decoupling purposes [7].

Compared to the aforementioned patents, a more complex decoupling system is the work of Johannes Avetician Calantarients, a medical doctor from Scarborough, England. He suggested using a layered surface between superstructure and foundation that consists of variety of materials including metal plates, soapstone, mica, talc and sand, thus allowing horizontal movement of the foundation [8].

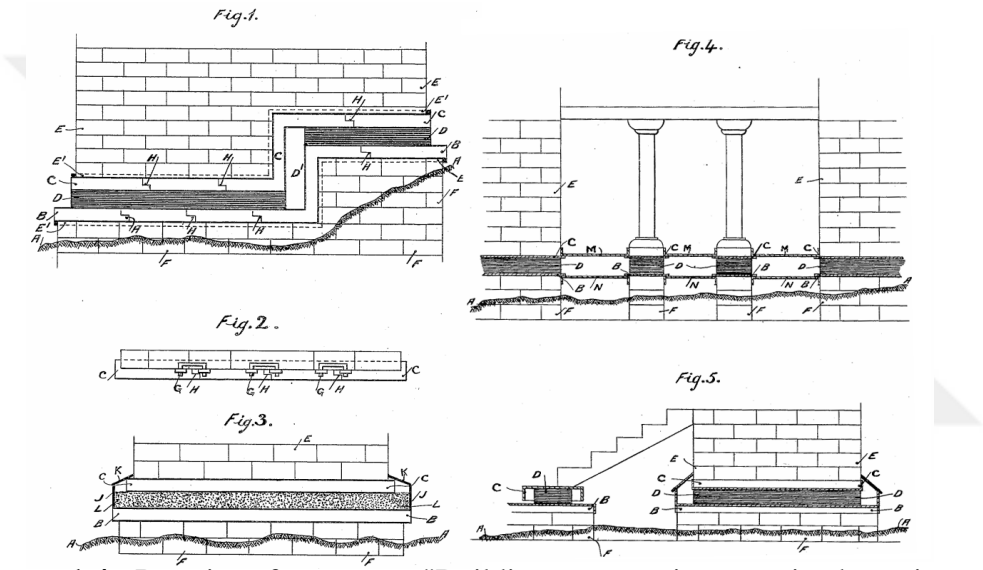

Figure 1.4 : Drawings from patent "Building construction to resist the action of earthquakes"

1.1.2 Base isolation systems

Although there are many different designs for base isolation systems, they can be represented within two main categories.

1.1.2.1 Elastomeric bearings

Elastomeric bearings are the most commonly used base isolation systems. They consist of multiple layers of steel plates and elastomeric rubber material stacked on top of each other. Rubber and steel plates are bonded together by application of pressure and heat. While steel plates provide the necessary vertical stiffness and vertical load capacity, rubber layers provide low horizontal stiffness that is needed for the decoupling effect.

Steel plates also help prevent rubber plates from swelling and deflecting under vertical loads.

Figure 1.5 : Low or High damping rubber bearing. Maurer SE. Downloaded from https://www.maurer.eu/en/products/seismic-devices/isolators/index.html

There are different types of elastomeric bearings. Naturally, rubber has low viscous damping. Bearings that are only made with rubber and steel plates are called low-damping rubber bearings (LDRB). It is possible to manufacture high-damping rubber bearings (HDRB) by adding extra materials such as carbon, oil and resin. While low-damping bearings have 2-3% ratios, high-damping bearings have 10-20%. Low-damping bearings might need additional devices for damping e.g., viscous dampers. Manufacturing bearings with no damping is also possible [6].

Figure 1.6 : Lead rubber bearing. Maurer SE. Downloaded from https://www.maurer.eu/en/products/seismic-devices/isolators/index.html

Elastomeric bearings can also include one or more lead cores. Lead cores are fitted tightly into a hole in rubber bearings. While rubber provides centering capabilities, lead cores provide energy dissipation.

1.1.2.2 Sliding isolation systems

Sliding bearings are more economical than their elastomeric counterparts. Because this type of bearings have friction, a small amount of shear force is inflicted on the structure. Friction is a feature of the sliding systems which provides energy dissipation capabilities. Traditional sliding bearings do not have re-centering features, meaning the structure will not restore its position after an earthquake. These type of bearings need to be supplemented with additional elements that provide re-centering abilities. However, there is one other type of sliding bearings that does have re-centering capabilities. Thanks to their concave geometry, friction pendulum bearings generate the necessary re-centering forces. In addition to moving horizontally, the structure also moves vertically, naturally generating forces that moves the structure to its original position thanks to gravity.

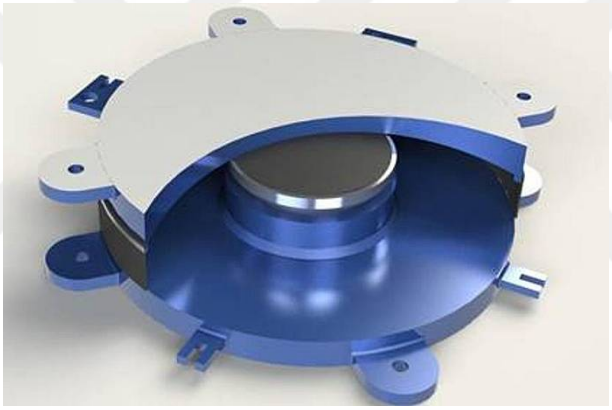

Figure 1.7 : Sliding pendulum isolator. Maurer SE. Downloaded from https://www.maurer.eu/en/products/seismic-devices/isolators/index.html

1.2 Soil-Structure Interaction

Soil-structure interaction (SSI), also known as soil-foundation-structure interaction, is a design concept that takes responses of structure, foundation and soil medium into account. Soil-structure interaction is a concept that is often neglected when it comes to designing structures. Conventionally, structures are considered fixed to the ground and response of underlying soil is neglected. This is because effects of soil are usually considered beneficial to the structure, so neglecting soil can be considered conservative and safe. In FEMA 356 [9], soil-structure interaction is classified as a rare case that may modify the spectral response of the structure, particularly in soft soil conditions.

There are two main approaches for evaluating soil-structure interaction. One of which is the direct approach, where the soil is modelled as a continuum of the structure. The other is called the substructure approach where properties of soil are calculated via simple impedance functions or springs and dashpots. Soil properties that are calculated include stiffness and damping characteristics of the soil-structure interaction. The substructure approach with impedance functions requires the foundation to be rigid, and allows for formulation of soil-structure interaction. In this dissertation, the substructure approach is used.

1.3 Literature Review

One of the first studies that investigates the effect of SSI in base isolated structures is by Constantinou and Kneifati [10], which conducted a parametric study on a linear 1-degree-of-freedom structure. They concluded that SSI does not effect the structure significantly in base isolated structures than it does on conventional structures.

Bycroft [11], introduced approaching solutions and analysis for the SSI when high-frequencies are involved. He stimulates forced vibrations to a stiff circular platform connected to the area of a flexible half space. This model, considering high frequencies, can be parallelized to an earthquake and an analysis can be done to a stiff foundation resting on soft soil.

Novak and Henderson [12], made use of the equations of motion for a structure by evaluating the SSI effect, especially in foundations consisting of joint or spread footings. They analyzed the SSI on buildings by taking into account the modal characteristics.

Pappin et al. [13], highlighted the importance of the site effects on performance based design. They chose to work on three different soil profiles. It was concluded that in dense soil, the design ground motion differs depending on the seismic rate, while for soft soils results are not affected.

Mylonakis and Gazetas [14], investigated the beneficialness of SSI. They found that the effects of SSI are not necessarily beneficial and can be detrimental instead. Actual response spectrum for some earthquakes can be different from design spectra found in

design codes. Elongation of the natural period of structures does not necessarily mean reduced response thus SSI effects can be detrimental to structures.

Tongaonkar and Jangid [15] studied the effects of SSI in bridges. They concluded that considering SSI effects in isolated bridges are beneficial to the bridge and may result in cost reduction in design. They also found that SSI effects are more significant in stiff bridges and in bridges that have stiff isolation systems than flexible bridges and flexible isolation systems, respectively.

When analyzing the damaging earthquake of 1999 in Athens, Mylonakis et al. [16], reached to a conclusion that the effects of surface layer made of soft rock and stiff soil were a detrimental factor.

Syngros [17] has gone through history of two different cases related to seismic response of piles supporting bridges and piles group, the Ohba Ohashi bridge and the Fukae Section of Hanshin Expressway. He concluded that the type of soil changed the seismic waves and the ground surface motion encountered by the specific bridge was greater, also a higher frequency was measured in that portion.

During the study of a 3D nonlinear model of base isolation, Deb [18] takes SSI into consideration and from a near fault earthquake he introduced the results. He related SSI with the stiffness of isolation system, if the isolators have a greater stiffness compared to the soil, SSI has a negligible effect. In opposite cases, an effect should be expected in the structure.

A detailed study related to an isolated structure and SSI with an unbounded section was conducted by Tsai et al. [19], where they underlined that the performance of the base isolation is dependent on the stiffness and damping of the soil.

Dicleli et al. [20], studied the effects of SSI in two different types of brides, ones that the superstructure is heavy and the substructure part is light and vice versa. They concluded that SSI effects should be investigated in soft soil conditions, regardless of the bridge type. Also on stiff soil conditions, SSI effects are negligible for isolated bridges with heavy superstructures.

Liu et al. [21], conducted a study in time domain that investigates the effects of wind in high-rise structures with tuned mass dampers, considering SSI effects. They found

that SSI affects the effectiveness of the dampers in soft soil conditions, tuned mass dampers are more effective in stiff soil conditions.

Spyrakos et al. [22], studied the effects of SSI in buildings in frequency domain. They found that SSI effects on damping of the isolated structures are negligible and damping is dependent on base isolation damping characteristics. They also found that SSI effects are more pronounced in relatively stiff structures.

Jeremic et al. [23], investigated the effects of SSI with varying soil properties on a four span bridge. They concluded that SSI has significant effects on response of elements and should be simulated whenever possible. They also found that stiff soil conditions are not always beneficial for the structures.

Karabörk et al. [24], conducted a study which investigates the effects of SSI on an isolated structure with HDRB. They used the direct approach and used finite element method to model the structure. They found that on soft soil conditions, stiffer isolation systems are more effective when it comes to reducing the earthquake effects.

Kausel [25], investigated the SSI history and phenomena. He introduced the authors that have studied the SSI before and their detailed explanations as it concern the static SSI, dynamic SSI and the interaction effect within or in the nearby areas of the structure.

Geneş et al [26]., conducted a study in order to analyze SSI effects in two different reinforced concrete buildings. They concluded that SSI has a fluctuating effect and the type of soil, where the structure is found, building dimensions and the earthquake magnitudes should be always taken in consideration.

Matinmanesh and Asheghabadi [27], took into consideration a plane finite element, and used three different earthquake data with different frequency contents. In their analysis they also evaluated the type of soil and height of the structure. They concluded that all types of soil have an effect in bedrock movement, but with different rates.

Manolis and Markous [28] presented a combination of base isolation and SSI. They took into consideration a cantilever beam, representing a system of distributed mass. By analyzing it with modal analysis and finite element methods and evaluating the mechanical properties of SSI and base isolation together, they concluded that base isolation performance depends on the type of soil the structure rests.

Giarlelis and Mylonakis [29], conducted a study related to the role of SSI in elastic performance of multi-storey buildings, they concluded that the distribution of internal forces is also affected by SSI.

Li et al. [30], studied SSI in base isolated structures in frequency domain using the substructure approach. They concluded that considering stiffer isolation systems in soft soil conditions, SSI effects are significant. This conclusion is inline with the study performed by Karabörk et al. [24]. They also found that the properties of soil can modify the damping and natural period of the structure.

Luco [31] studied the effects of SSI on a structure that has a nonlinear base isolation system. He concluded that SSI amplifies the response of the isolated structures. He also found that SSI increases the ductility of isolation systems in soft soil conditions.

Tsai et al. [32], investigated the effects of SSI and damping in isolated structures. They found that the first mode of the structure is controlled by the base isolation system, and higher modes are controlled by soil parameters. They concluded that SSI has no effect on base isolation performance.

Ashiquzzaman and Hong [33], studied the SSI effects on isolated nuclear power plant containment buildings. They concluded that SSI effects are negligible in tall structures but the effects are significant in stiffer structures. They also found that SSI changes the modal attributes of structures.

Zhou and Wei [34], conducted a similar study to Ashiquzzaman and Hong [33] where they studied SSI effects on nuclear power plants and they discovered that SSI mostly amplify responses near resonant frequencies. They concluded that SSI directly affects the performance of isolation systems.

Forcellini [35], studied the SSI effects on base isolated buildings using OpenSees [36] framework. He found that SSI effects are more pronounced in softer soil conditions. SSI effects include elongation of the natural period of the structure, reduction in base shear and increase in displacements.

Dai et al. [37], studied the effects of SSI in a specific base isolated bridge and observed that SSI effects are more distinct in transverse direction as opposed to longitudinal direction. They also found that in isolated structures, SSI effects are more pronounced.

Zhenxia and Haiping [38], studied SSI effects on base isolated structures using finite element method with the software called LS-DYNA [39]. They found that the performance of base isolation systems are correlated with soil conditions.

To this day, there are limited amount of studies that investigate SSI and base isolation together, and results of these studies are not always consistent with each other.

2. FORMULATION OF THE PROBLEM

This study aims to analyze SSI and base isolation effects on two dimensional shear frame structures with the assumption of storeys being rigid diaphragms. Analyses are conducted on three different shear frame structures which are five, ten and forty storeys high. Newmark average acceleration method is used for dynamic analysis.

2.1 Soil Model

In order to take into account SSI in analyses, "spring and dashpot method" is used. Spring and dashpot analysis replaces the soil with springs and dashpots with horizontal, vertical, rotational and torsional degrees of freedom. In this study, only horizontal and rotational degrees of freedom are considered, vertical and torsional degrees of freedom are neglected.

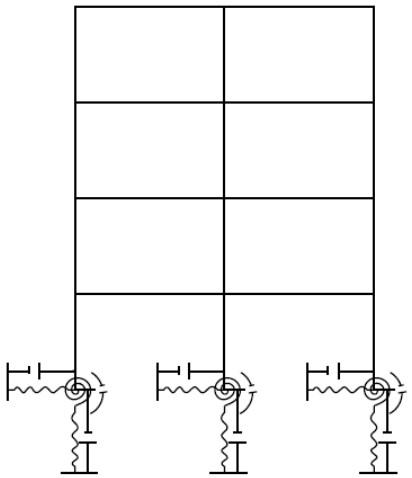

Figure 2.1 : Spring and dashpot model.

Illustration of springs and dashpots in place of soil can be seen in figure 2.1 [40]. Calculation of stiffness and damping coefficients of springs and dashpots are done by using frequency independent impedance functions [40]. As seen from the equations below, both structure and soil properties contribute to calculation of the values.

$$k_s = \frac{8Gr}{2-\nu} \tag{2.1}$$

$$k_r = \frac{8Gr^3}{3(1-\nu)} \tag{2.2}$$

$$c_s = \frac{4.6}{2-\nu}\rho V_S r^2 \tag{2.3}$$

$$c_r = \frac{0.4}{1-\nu}\rho V_S r^4 \tag{2.4}$$

In the equations above, "s" subscript denotes "swaying" which is the horizontal component, and the "r" subscript denotes "rocking" which is the rotational component. k_s and k_r are swaying and rocking stiffness of the soil, respectively. Similarly, c_s and c_r are swaying and rocking damping of the soil, respectively. V_S, ρ and ν are the shear wave velocity, mass density and poisson's ratio of soil. G is the shear modulus of the soil which can be calculated with the following equation:

$$G = \rho V_S^2 \tag{2.5}$$

r is the radius of the circular foundation. For a rectangular foundation with the dimensions a and b, an equivalent r value can be calculated by equalizing areas of the rectangle and the circle, such as:

$$\pi r^2 = ab \tag{2.6}$$

$$r = \sqrt{\frac{ab}{\pi}} \tag{2.7}$$

2.2 Structural Matrices

In this section, formulation of mass, stiffness and damping matrices of structures are presented. In order to represent soil properties and base isolation in mass, stiffness and damping matrices, corresponding values must be embedded into the matrices.

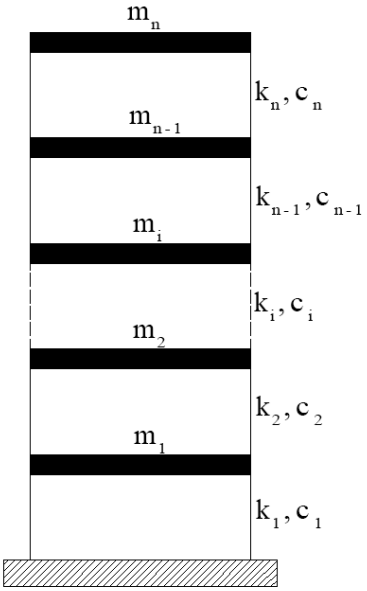

Figure 2.2 : Fixed based shear frame structure.

Conventional mass, damping and stiffness matrices for a fixed based shear frame structure can be written as:

$$\mathbf{M} = \begin{bmatrix} m_1 & 0 & 0 & \cdots & 0 \\ 0 & m_2 & 0 & \cdots & 0 \\ 0 & 0 & \ddots & \cdots & 0 \\ \vdots & \vdots & \vdots & m_{n-1} & 0 \\ 0 & 0 & 0 & 0 & m_n \end{bmatrix}_{n\times n} \tag{2.8}$$

$$\mathbf{C} = \begin{bmatrix} c_1+c_2 & -c_2 & 0 & \cdots & 0 \\ -c_2 & c_2+c_3 & -c_3 & \cdots & 0 \\ 0 & -c_3 & \ddots & \cdots & 0 \\ \vdots & \vdots & \vdots & c_{n-1}+c_n & -c_n \\ 0 & 0 & 0 & -c_n & c_n \end{bmatrix}_{n\times n} \tag{2.9}$$

$$\mathbf{K} = \begin{bmatrix} k_1+k_2 & -k_2 & 0 & \cdots & 0 \\ -k_2 & k_2+k_3 & -k_3 & \cdots & 0 \\ 0 & -k_3 & \ddots & \cdots & 0 \\ \vdots & \vdots & \vdots & k_{n-1}+k_n & -k_n \\ 0 & 0 & 0 & -k_n & k_n \end{bmatrix}_{n\times n} \tag{2.10}$$

k_1 to k_n are storey stiffnesses, c_1 to c_n are storey dampings and m_1 to m_n are storey masses of an n-storey structure. **M** is the mass matrix, **C** is the damping matrix and **K** is the stiffness matrix of fixed based shear frame structure.

2.2.1 Base isolated structures

Properties of the base isolation can be added to the matrices by simply taking the base isolation layer as the first storey of the structure.

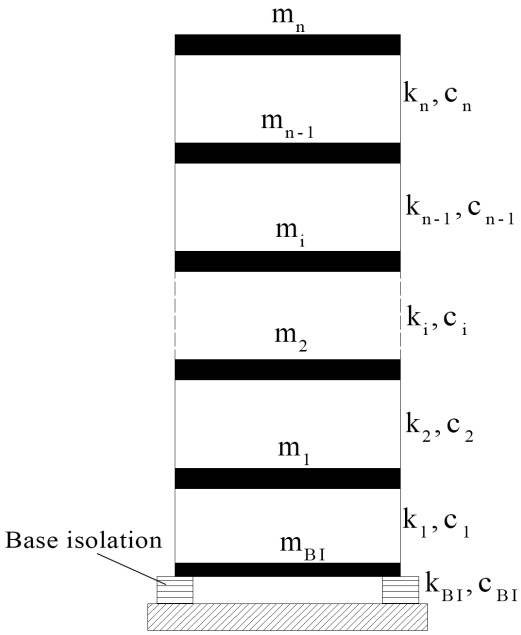

Figure 2.3 : Base isolated shear frame structure.

k_{BI} is the stiffness, c_{BI} is the damping and m_{BI} is the mass of the base isolation system.

Mass, damping and stiffness matrices for a base isolated n-storey shear frame structure can be written as:

$$\mathbf{M_{BI}} = \begin{bmatrix} m_{BI} & 0 & 0 & 0 & \cdots & 0 \\ 0 & m_1 & 0 & 0 & \cdots & 0 \\ 0 & 0 & m_2 & 0 & \cdots & 0 \\ 0 & 0 & 0 & \ddots & \cdots & 0 \\ \vdots & \vdots & \vdots & \vdots & m_{n-1} & 0 \\ 0 & 0 & 0 & 0 & 0 & m_n \end{bmatrix}_{(n+1)\times(n+1)} \tag{2.11}$$

$$\mathbf{C_{BI}} = \begin{bmatrix} c_{BI}+c_1 & -c_1 & 0 & 0 & \cdots & 0 \\ -c_1 & c_1+c_2 & -c_2 & 0 & \cdots & 0 \\ 0 & -c_2 & c_2+c_3 & -c_3 & \cdots & 0 \\ 0 & 0 & -c_3 & \ddots & \cdots & 0 \\ \vdots & \vdots & \vdots & \vdots & c_{n-1}+c_n & -c_n \\ 0 & 0 & 0 & 0 & -c_n & c_n \end{bmatrix}_{(n+1)\times(n+1)} \tag{2.12}$$

$$\mathbf{K_{BI}} = \begin{bmatrix} k_{BI}+k_1 & -k_1 & 0 & 0 & \cdots & 0 \\ -k_1 & k_1+k_2 & -k_2 & 0 & \cdots & 0 \\ 0 & -k_2 & k_2+k_3 & -k_3 & \cdots & 0 \\ 0 & 0 & -k_3 & \ddots & \cdots & 0 \\ \vdots & \vdots & \vdots & \vdots & k_{n-1}+k_n & -k_n \\ 0 & 0 & 0 & 0 & -k_n & k_n \end{bmatrix}_{(n+1)\times(n+1)} \tag{2.13}$$

The subscript "BI" denotes "base isolation". $\mathbf{M_{BI}}$ is the mass matrix, $\mathbf{C_{BI}}$ is the damping matrix and $\mathbf{K_{BI}}$ is the stiffness matrix of base isolated shear frame structure. Base isolation adds one degree of freedom to the fixed base structure, therefore dimensions of all matrices are increased by one.

2.2.2 Soil-structure interaction

Spring-dashpot model of an n-storey shear frame structure is shown in figure 2.4:

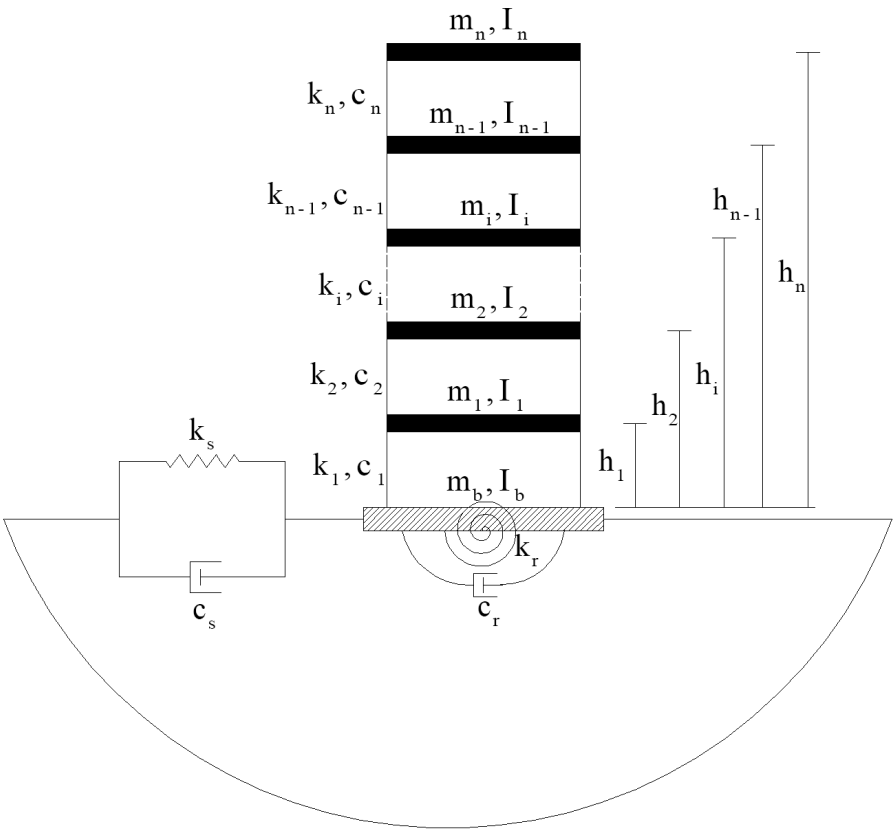

Figure 2.4 : Shear frame structure considering SSI.

m_b and I_b are the mass and the mass moment of inertia of the foundation, respectively. I_1 to I_n are the mass moment of inertia of each floor. k_s is the swaying stiffness, k_r is the rocking stiffness, c_s is the swaying damping and c_r is the rocking damping of

foundation-soil medium. h_1 to h_n are storey heights with respect to ground. Swaying values are the horizontal components of foundation-soil medium, whereas rocking values are rotational components.

Mass, damping and stiffness matrices can be written as follows [41]:

$$\mathbf{M_{SSI}} = \begin{bmatrix} \mathbf{M} & \mathbf{M_v} & \mathbf{M_h} \\ \mathbf{M_v^T} & \left(m_b + \sum_{i=1}^{n} m_i\right) & \left(\sum_{i=1}^{n} m_i h_i\right) \\ \mathbf{M_h^T} & \left(\sum_{i=1}^{n} m_i h_i\right) & \left(\sum_{i=1}^{n} m_i h_i^2 + I_b + \sum_{i=1}^{n} I_i\right) \end{bmatrix}_{(n+2)\times(n+2)} \tag{2.14}$$

$$\mathbf{C_{SSI}} = \begin{bmatrix} \mathbf{C} & \mathbf{0} & \mathbf{0} \\ \mathbf{0} & c_s & 0 \\ \mathbf{0} & 0 & c_r \end{bmatrix}_{(n+2)\times(n+2)} \tag{2.15}$$

$$\mathbf{K_{SSI}} = \begin{bmatrix} \mathbf{K} & \mathbf{0} & \mathbf{0} \\ \mathbf{0} & k_s & 0 \\ \mathbf{0} & 0 & k_r \end{bmatrix}_{(n+2)\times(n+2)} \tag{2.16}$$

The subscript "SSI" denotes soil-structure interaction. $\mathbf{M_{SSI}}$ is the mass matrix, $\mathbf{C_{SSI}}$ is the damping matrix and $\mathbf{K_{SSI}}$ is the stiffness matrix of shear frame structure considering SSI.

$\mathbf{M}$, $\mathbf{C}$ and $\mathbf{K}$ are conventional mass, damping and stiffness matrices for fixed base structures. $\mathbf{M_v}$ and $\mathbf{M_h}$ are defined as follows:

$$\mathbf{M_v} = \begin{bmatrix} m_1 \\ m_2 \\ \vdots \\ m_{n-1} \\ m_n \end{bmatrix}_{n\times 1} \tag{2.17}$$

$$\mathbf{M_h} = \begin{bmatrix} m_1 h_1 \\ m_2 h_2 \\ \vdots \\ m_{n-1} h_{n-1} \\ m_n h_n \end{bmatrix}_{n\times 1} \tag{2.18}$$

SSI introduces two additional degrees of freedom to the fixed base structure, therefore dimensions of all matrices are increased by two.

2.2.3 Soil-structure interaction with base isolation

SSI in base isolated structures can be represented by adjusting SSI matrix formulation. Fixed based **M**, **C** and **K** matrices that are used in SSI matrices can be substituted with base isolated $\mathbf{M_{BI}}$, $\mathbf{C_{BI}}$ and $\mathbf{K_{BI}}$ matrices. Height of the base isolation system, h_{BI} must be included in the mass matrix considering SSI and base isolation together.

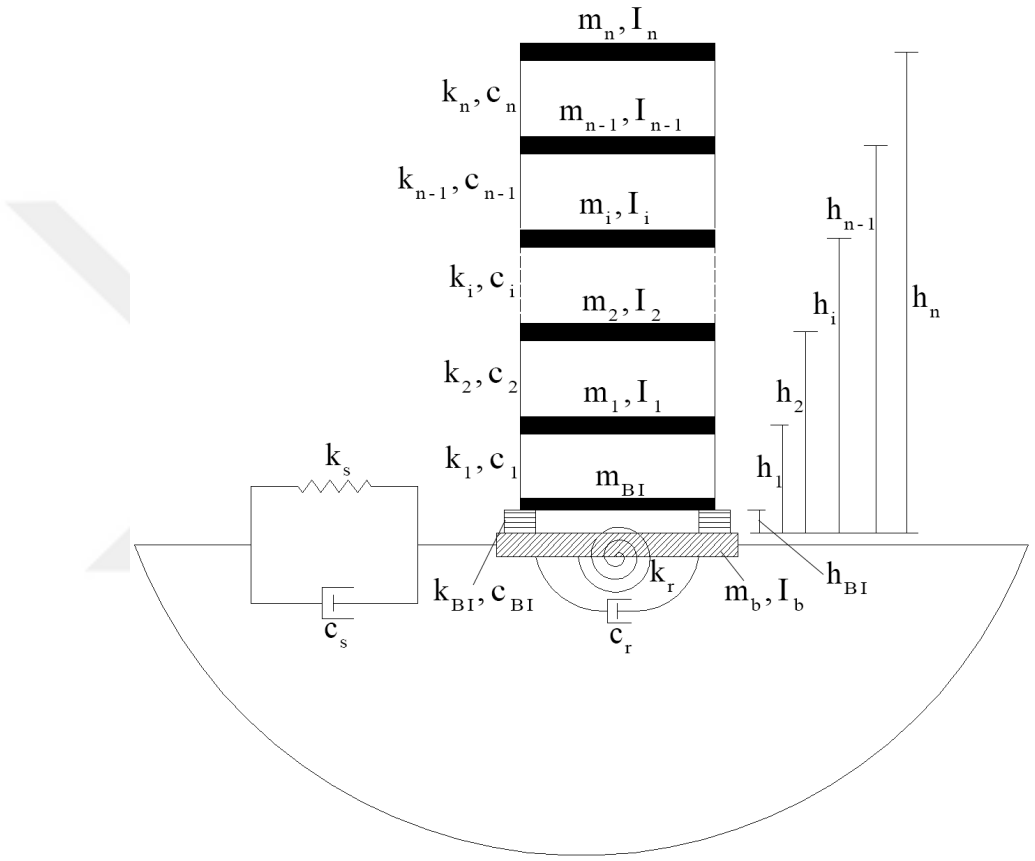

Figure 2.5 : Shear frame structure considering SSI and base isolation together.

Mass, damping and stiffness matrices considering SSI and base isolation together, can be written as follows:

$$\mathbf{M_{SSI,BI}} = \begin{bmatrix} \mathbf{M_{BI}} & \mathbf{M_{v,BI}} & \mathbf{M_{h,BI}} \\ \mathbf{M_{v,BI}^T} & \left(m_b + \sum_{i=1}^{n} m_i\right) & \left(\sum_{i=1}^{n} m_i h_i\right) \\ \mathbf{M_{h,BI}^T} & \left(\sum_{i=1}^{n} m_i h_i\right) & \left(\sum_{i=1}^{n} m_i h_i^2 + I_b + \sum_{i=1}^{n} I_i\right) \end{bmatrix}_{(n+3)\times(n+3)} \tag{2.19}$$

$$\mathbf{C_{SSI,BI}} = \begin{bmatrix} \mathbf{C_{BI}} & \mathbf{0} & \mathbf{0} \\ \mathbf{0} & c_s & 0 \\ \mathbf{0} & 0 & c_r \end{bmatrix}_{(n+3)\times(n+3)} \tag{2.20}$$

$$\mathbf{K_{SSI,BI}} = \begin{bmatrix} \mathbf{K_{BI}} & \mathbf{0} & \mathbf{0} \\ \mathbf{0} & k_s & 0 \\ \mathbf{0} & 0 & k_r \end{bmatrix}_{(n+3)\times(n+3)} \tag{2.21}$$

The subscript "SSI, BI" denotes soil-structure interaction with base isolation. $\mathbf{M_{SSI,BI}}$ is the mass matrix, $\mathbf{C_{SSI,BI}}$ is the damping matrix and $\mathbf{K_{SSI,BI}}$ is the stiffness matrix of shear frame structure considering SSI and base isolation together.

$\mathbf{M_{v,BI}}$ and $\mathbf{M_{h,BI}}$ are defined as follows:

$$\mathbf{M_{v,BI}} = \begin{bmatrix} m_{BI} \\ m_1 \\ m_2 \\ \vdots \\ m_{n-1} \\ m_n \end{bmatrix}_{(n+1)\times 1} \tag{2.22}$$

$$\mathbf{M_{h,BI}} = \begin{bmatrix} m_{BI}h_{BI} \\ m_1h_1 \\ m_2h_2 \\ \vdots \\ m_{n-1}h_{n-1} \\ m_nh_n \end{bmatrix}_{(n+1)\times 1} \tag{2.23}$$

While SSI introduces two additional degrees of freedom to the fixed base structure, base isolation adds one, therefore dimensions of all matrices are increased by three in total.

2.3 Equations of Motion

Four different equations of motion are needed in order to cover all four analysis cases, these cases being; fixed base, base isolated, fixed base considering SSI and structure with base isolation considering SSI.

Equation of motion for the fixed base analysis case can be written as:

$$\mathbf{M}\ddot{u}(t) + \mathbf{C}\dot{u}(t) + \mathbf{K}u(t) = -\mathbf{m}^*\ddot{u_g}(t) \tag{2.24}$$

M, **C** and **K** are conventional fixed base mass, damping and stiffness matrices. $\mathbf{m}^*$ is a vector containing the diagonal of **M**, which happens to be the mass values.

$$\mathbf{m}^* = \begin{bmatrix} m_1 \\ m_2 \\ \vdots \\ m_{n-1} \\ m_n \end{bmatrix}_{n\times 1} \tag{2.25}$$

Equation of motion for the base isolated analysis case can be written by substituting conventional fixed base matrices with base isolated matrices:

$$\mathbf{M_{BI}}\ddot{u}(t) + \mathbf{C_{BI}}\dot{u}(t) + \mathbf{K_{BI}}u(t) = -\mathbf{m^*_{BI}}\ddot{u_g}(t) \tag{2.26}$$

$\mathbf{m^*_{BI}}$ is a vector containing the diagonal elements of $\mathbf{M_{BI}}$:

$$\mathbf{m^*_{BI}} = \begin{bmatrix} m_{BI} \\ m_1 \\ m_2 \\ \vdots \\ m_{n-1} \\ m_n \end{bmatrix}_{(n+1)\times 1} \tag{2.27}$$

Equation of motion for the SSI analysis case can be written by substituting conventional fixed base matrices with SSI matrices:

$$\mathbf{M_{SSI}}\ddot{u}(t) + \mathbf{C_{SSI}}\dot{u}(t) + \mathbf{K_{SSI}}u(t) = -\mathbf{m^*_{SSI}}\ddot{u_g}(t) \tag{2.28}$$

$\mathbf{m^*_{SSI}}$ is a vector containing the diagonal elements of **M** with $(m_b + \sum_{i=1}^{n} m_i)$ and $(\sum_{i=1}^{n} m_i h_i)$ from $\mathbf{M_{SSI}}$ [41]:

$$\mathbf{m^*_{SSI}} = \begin{bmatrix} m_1 \\ m_2 \\ \vdots \\ m_{n-1} \\ m_n \\ (m_b + \sum_{i=1}^{n} m_i) \\ (\sum_{i=1}^{n} m_i h_i) \end{bmatrix}_{(n+2)\times 1} \tag{2.29}$$

For the joint case of SSI and base isolation, the equation of motion is written as follows:

$$\mathbf{M_{SSI,BI}}\ddot{u}(t) + \mathbf{C_{SSI,BI}}\dot{u}(t) + \mathbf{K_{SSI,BI}}u(t) = -\mathbf{m^*_{SSI,BI}}\ddot{u_g}(t) \tag{2.30}$$

$\mathbf{m^*_{SSI,BI}}$ is a vector containing the diagonal of $\mathbf{M_{BI}}$ with the additions of $(m_b + \sum_{i=1}^{n} m_i)$ and $(\sum_{i=1}^{n} m_i h_i)$ from $\mathbf{M_{SSI,BI}}$ [41]:

$$\mathbf{m^*_{SSI,BI}} = \begin{bmatrix} m_{BI} \\ m_1 \\ m_2 \\ \vdots \\ m_{n-1} \\ m_n \\ (m_b + \sum_{i=1}^{n} m_i) \\ (\sum_{i=1}^{n} m_i h_i) \end{bmatrix}_{(n+3)\times 1} \tag{2.31}$$

In the equations defined above, $\ddot{u_g}(t)$ is the horizontal ground motion acceleration. $u(t)$, $\dot{u}(t)$, and $\ddot{u}(t)$ are the displacement, velocity and acceleration vectors of the structure.

3. NUMERICAL ANALYSIS

For the sake of compatibility and convenience, units are displayed with kilonewtons, meters and seconds wherever possible.

3.1 Analysis Cases

Analyses are carried out by considering following cases. Three different buildings with five, ten and forty storeys are considered. For each building, four different base conditions are considered. These conditions consist of a fixed base, an isolated base, an SSI included base and an isolated base considering SSI. For base isolated cases, two different isolation systems with low damping and high damping are also considered. For SSI cases, four different soil conditions; very soft, soft, medium and dense are considered. All cases are tested with a suit of earthquakes with different rupture distances.

3.1.1 Soil Conditions

Soil properties of each building can be calculated with the equations listed in section 2.1. Soil properties are taken and adapted from [21], which are used in different studies previously [41–43]

Soil properties of five and ten storey buildings are the same because the foundation dimensions are the same.

Soil properties are given in table 3.1. Soil properties of five and ten storey buildings are given in table 3.2. Soil properties of forty storey building is given in table 3.3.

Table 3.1 : Soil properties.

Soil	ν	ρ kNs^2/m^4	V_S m/s^2	G kN/m^2
Very Soft	0.49	1.60	50	4000
Soft	0.49	1.80	100	18000
Medium	0.48	1.90	300	171000
Dense	0.33	2.40	500	600000

Table 3.2 : Soil properties of five and ten storey buildings.

Soil	k_s kN/m	k_r kNm	c_s kNs/m	c_r $kNsm$
Very Soft	2.12×10^5	2.09×10^7	2.44×10^4	6.27×10^5
Soft	9.54×10^5	9.41×10^7	5.48×10^4	1.41×10^6
Medium	9.00×10^6	8.77×10^8	1.73×10^5	4.38×10^6
Dense	2.87×10^7	2.39×10^9	3.31×10^5	7.16×10^9

Table 3.3 : Soil properties of forty storey building.

Soil	k_s kN/m	k_r kNm	c_s kNs/m	c_r $kNsm$
Very Soft	4.24×10^5	1.67×10^8	9.74×10^4	1.00×10^7
Soft	1.91×10^6	7.53×10^8	2.19×10^5	2.26×10^7
Medium	1.80×10^7	7.02×10^9	6.90×10^8	7.02×10^7
Dense	5.75×10^5	1.91×10^{10}	1.32×10^6	1.15×10^8

3.1.2 Buildings

Three different shear frame buildings are used in analyses. Properties of the forty-storey building is given in table 3.4.

Table 3.4 : Properties of the forty-storey building.

storey height, h_i (m)	4 to 160
storey mass, $m_i(kNs^2/m)$	980
storey stiffness, $k_i(kN/m)$	2.1×10^6 to 0.99×10^6
storey damping, $c_i(kNs/m)$	42.6×10^3 to 20×10^3
storey inertia, $I_i(kNs^2m)$	1.31×10^5
foundation mass, $m_0(kNs^2/m)$	1960
foundation inertia, $I_0(kNs^2m)$	1.96×10^5

In table 3.4, stiffness and damping values are linearly decreasing between listed values.

Table 3.5 : Properties of the five-storey building.

storey height, h_i (m)	4 to 20
storey mass, $m_i(kNs^2/m)$	300
storey stiffness, $k_i(kN/m)$	3.5×10^5 to 1.50×10^5
storey inertia, $I_i(kNs^2m)$	7.5×10^3
foundation mass, $m_0(kNs^2/m)$	300
foundation inertia, $I_0(kNs^2m)$	7.5×10^5

Stiffness vector of the five-storey building is $[7k\ 5k\ 3k\ 3k\ 3k]$ in which $k = 5 \times 10^4 kN/m$. Damping of the structure is calculated as Rayleigh damping which is proportional to its mass and stiffness matrices [2].

Table 3.6 : Properties of the ten-storey building.

storey height, h_i (m)	4 to 40
storey mass, $m_i(kNs^2/m)$	300
storey stiffness, $k_i(kN/m)$	7.0×10^5 to 3.00×10^5
storey inertia, $I_i(kNs^2m)$	7.5×10^3
foundation mass, $m_0(kNs^2/m)$	300
foundation inertia, $I_0(kNs^2m)$	7.5×10^5

Properties of five and ten-storey buildings are given in tables 3.5 and 3.6. Stiffness vector of the ten-storey building is $[7k\ 7k\ 5k\ 5k\ 3k\ 3k\ 3k\ 3k\ 3k\ 3k]$ in which $k = 1.0 \times 10^5 kN/m$. Damping of the structure is calculated as Rayleigh damping which is proportional to its mass and stiffness matrices [2]. A Matlab [44] function for calculating rayleigh damping is developed. The function takes damping ratio, mass and stiffness matrices of the structure. Another helper function that performs an eigenvalue analysis for calculating natural periods and mod shapes is also written and given below.

```
function C = rayleigh(M, K, damping_ratio)

[natural_periods, omega, mod_shapes] = findProperties(M,K);

a0 = damping_ratio *  ( (2*omega(1)*omega(2)) / ...
(omega(1)+omega(2)) );
a1 = damping_ratio * ( 2 / (omega(1) + omega(2)) );
C = (a0 * M) + (a1 * K);

function [natural_periods, omega, mod_shapes] = findProperties(M,K)

[mod_shapes, omega2] = eig(K,M);
omega = sqrt(diag(omega2)); % rad/sec
natural_periods = 2*pi./omega; % seconds
for i=1:size(mod_shapes,1)
    mod_shapes(:,i) = mod_shapes(:,i)./mod_shapes(end,i);
end
```

Listing 3.1: Rayleigh damping implementation in Matlab.

3.1.3 Base Conditions

Considered base conditions consist of;

- fixed base
- base isolation
- SSI
- SSI and base isolation

In order to calculate necessary matrices for every case mentioned in section 2.2, Matlab functions are developed. For the conventional damping and stiffness matrices, following function is written.

```
function K = kcMat(k_vect)

superDiagonal = zeros(1,(size(k_vect,2)-1));
theDiagonal = zeros(size(k_vect));
theDiagonal(size(k_vect)) = k_vect(size(k_vect,2));

for i = 1:size(superDiagonal,2)
    superDiagonal(1,i) = -1 * k_vect(i+1);
    theDiagonal(1,i) = k_vect(i) + k_vect(i+1);
end

K1 = diag(superDiagonal,1);
K2 = diag(superDiagonal,-1);
K3 = diag(theDiagonal,0);

K = K1 + K2 + K3;
```

Listing 3.2: Matlab function for calculation damping and stiffness matrices.

The function takes a vector of storey stiffnesses or dampings, and then outputs the correct stiffness and damping matrices. The function can calculate both stiffness and damping matrices. For the base isolated case, Matlab functions that add base isolation to the conventional fixed base matrices are written and given below.

```
function M_bi = addBItoM(M, mb)

story = size(M,2);

temp = zeros(story+1);
temp(1,1) = mb;
temp(2:end,2:end) = M;
M_bi = temp;

function K_bi = addBItoKC(K, kb, first_story)

story = size(K,2);

temp = zeros(story+1);
temp(1,1) = kb + first_story;
temp(1,2) = -1 * first_story;
temp(2,1) = -1 * first_story;
temp(2:end,2:end) = K;

K_bi = temp;
```

Listing 3.3: Matlab functions for adding base isolation to conventional matrices.

These functions take conventional matrices and base isolation properties, then outputs the desired matrices with base isolation.

Adding SSI to the conventional matrices is done by the following developed functions.

```
function M = mass_ssi(mass_vect, story_spcng, I_base, m_base, Ii)

M_ = diag(mass_vect);
Zi = cumsum(story_spcng);

MiZi = (mass_vect .* Zi).';
MiZi_sq = sum(MiZi .* Zi.');

M = [ M_ mass_vect.' MiZi;
    mass_vect (m_base + sum(mass_vect)) (sum(MiZi));
    MiZi.' (sum(MiZi)) (MiZi_sq + I_base + size(mass_vect,2)*Ii) ];

function kc_ssi = kcToSSI(k, k_swaying, k_rocking)

posS = size(k,2) + 1;
posR = posS + 1;

k(posS, posS) = k_swaying;
k(posR, posR) = k_rocking;

kc_ssi = k;
```

Listing 3.4: Matlab functions for adding SSI to conventional matrices.

These functions take soil properties, mass moment of inertia of foundation and storeys, foundation mass, storey heights, mass vector of storeys and conventional stiffness or damping matrices, then outputs matrices with SSI addition.

For the joint case of SSI and base isolation, same functions can be used. Instead of using conventional matrices as inputs, base isolated matrices can be used as inputs. SSI with base isolation implementation are obtained by this way.

3.2 Earthquake Records

A large number of earthquakes are used in analyses. All earthquake data is downloaded from PEER Ground Motion Database [45]. Corresponding earthquakes include near field records which their rupture distances are less than 20 kilometers, and far field records which their rupture distances are more than 20 kilometers. Details of the records are listed in table3.7:

Table 3.7 : Earthquake events considered in analyses.

Event	Year	Magnitude (M_w)	Mechanism
Imperial Valley, US	1940	6.95	Strike Slip
Imperial Valley, US	1979	6.53	Strike Slip
Loma Prieta, US	1989	6.93	Reverse Oblique
Manjil, IR	1990	7.37	Strike Slip
Cape Mendocino, US	1992	7.01	Reverse
Erzincan, TR	1992	6.69	Strike Slip
Landers, US	1992	7.28	Strike Slip
Northridge, US	1994	6.69	Reverse
Dinar, TR	1995	6.40	Normal
Kobe, JP	1995	6.90	Strike Slip
Chi-Chi, TW	1999	7.62	Reverse Oblique
Düzce, TR	1999	7.14	Strike Slip
Hector Mine, US	1999	7.13	Strike Slip
Kocaeli, TR	1999	7.51	Strike Slip
Iwate, JP	2008	6.90	Reverse
Darfield, NZ	2010	7.00	Strike Slip
El Mayor Cucapah, MX	2010	7.20	Strike Slip
Christchurch, NZ	2011	6.20	Reverse Oblique

Multiple earthquake records for each event is used in the analysis. For loading earthquake acceleration data from the files that are downloaded from PEER, a Matlab function is written and given below.

```
function [timeacc, dt] = peer(filename)

out = GetNumsInAsciiFile(filename);
possible = [0.005 0.01 0.02 0.0029 0.0024 0.0025 ...
0.004 0.0039 0.0078];

for i = 1:size(possible,2)
    for j = 1:5
        if possible(i) == out(j)
            delta = j;
        end
    end
end

dt = out(delta);
accBegins = delta + 1;
cleanAccValues = out(accBegins:end);
clear out
total = size(cleanAccValues,2);
timeacc = zeros(2,total);
timeacc(1,:) = dt:dt:dt*total;
timeacc(2,:) = 9.80665*cleanAccValues; % g units to m/s2
timeacc = timeacc.';
```

Listing 3.5: Matlab function for loading PEER earthquake data.

This function takes the file name of the PEER formatted earthquake acceleration record and loads it into Matlab for future use. The function automatically parses the file and detects the time step without user input.

3.3 Time History Analysis

Analyses are carried out by using Newmark's average acceleration time stepping method. For this task, a Matlab function is developed. Given an earthquake motion, the function solves the equations of motion and calculates the acceleration, velocity and displacement time histories of each story. The function can use both linear acceleration method and average acceleration method.

```
function [t,a, displ, acc, vel] = mdofNewmark(Mass, Stiffness, ...
Damping, earthquake, damp_ratio, useRatio, isSSI, M_conv)
modAmount = 2;
[omega, phi] = mods(Mass, Stiffness, modAmount);

M = phi' * Mass * phi;
K = phi' * Stiffness * phi;

if(useRatio)
    C = 2 * M * omega * damp_ratio;
else
    C = phi' * Damping * phi;
end

if isSSI
    P = phi' * diag(-M_conv);
else
    P = phi' * diag(-Mass);
end

[timeacc, dt] = peer(earthquake);
beta = 1/4;
gamma = 1/2;

a1 = (1/(beta * dt^2)) * M + (gamma/(beta * dt)) * C;
a2 = (1/(beta * dt)) * M + ((gamma / beta) - 1) * C;
a3 = ((1/(2 * beta)) - 1) * M + dt * (gamma/(2 * beta) - 1) * C;

q_acc = zeros(modAmount,size(timeacc,1) + 1);
q_vel = zeros(modAmount,size(timeacc,1) + 1);
q_dsp = zeros(modAmount,size(timeacc,1) + 1);

displ = zeros(size(timeacc,1) + 1 ,size(Mass,1));
acc = zeros(size(timeacc,1) + 1 ,size(Mass,1));
vel = zeros(size(timeacc,1) + 1 ,size(Mass,1));

t = zeros(size(timeacc,1) + 1,1);
t(2:end,1) = timeacc(:,1);

a = zeros(size(timeacc,1) + 1,1);
```

```
a(2:end,1) = timeacc(:,2);

K_hat = K + a1;

for i=1:size(timeacc,1)

    q_dsp(:,i+1) = K_hat \ (P*timeacc(i,2) + a1*q_dsp(:,i) ...
    + a2*q_vel(:,i) + a3*q_acc(:,i));

    q_vel(:,i+1) = (gamma/(beta * dt))*(q_dsp(:,i+1)-q_dsp(:,i)) ...
        + (1 - (gamma / beta)) * q_vel(:,i) ...
        + dt * (1 - gamma/(2 * beta)) * q_dsp(:,i);

    q_acc(:,i+1) = (1/(beta * dt^2)) * (q_dsp(:,i+1)-q_dsp(:,i)) ...
        - (1/(beta * dt)) * q_vel(:,i) ...
        - ((1/(2 * beta)) - 1) * q_acc(:,i);

    displ(i+1,:) = (phi * q_dsp(:,i+1))';
    acc(i+1,:) = (phi * q_acc(:,i+1))';
    vel(i+1,:) = (phi * q_vel(:,i+1))';

end
```

Listing 3.6: Matlab function for newmark's time stepping method

The function can also handle the unusual case of SSI.

3.4 Response Spectrum Analysis

Besides time history analysis, spectrum analysis is also conducted. A Matlab function is written for this task and given below.

```
function [ SD , SV , SA ] = RSpectPWExact(data,Period,ksi,dt)
clear SD SV SA
n=length(Period);
w=2*pi./Period;
wd=w*sqrt(1-ksi^2);
a11=exp((-ksi)*w*dt).*(cos(wd*dt)+...
(ksi*w.*exp((-ksi)*w*dt).*sin(wd*dt))./wd);
a12=(exp(-ksi*w*dt).*sin(wd*dt))./wd;
a21=-((w.^2).*a12);
a22=exp((-ksi)*w*dt).*(cos(wd*dt)-...
(ksi*w.*exp((-ksi)*w*dt).*sin(wd*dt))./wd);
b11=(a11-1.0)./(w.^2);
b12=(a12-2.0*ksi*w.*b11-dt)./((w.^2)*dt);
b21=-(a12);
b22=b11/dt;
u0(1:n)=0.0;
v0(1:n)=0.0;
umax(1:n)=0.0;
for i=2:length(data)
    u(1:n)=a11.*u0(1:n)+a12.*v0(1:n)+b11*data(i) ...
    b12*(data(i)-data(i-1));
    v(1:n)=a21.*u0(1:n)+a22.*v0(1:n)+b21*data(i)+ ...
    b22*(data(i)-data(i-1));
    u0=u;
```

```
    v0=v;
    umax=max(umax,abs(u0));
end
SD=umax;
SV=w.*umax;
SA=w.^2.*umax;
return
```

Listing 3.7: Matlab function for calculating spectral responses.

This function takes the earthquake record, desired period range, damping ratio and time step of the earthquake record, then outputs the spectral acceleration, velocity and displacement values.

4. NUMERICAL RESULTS

4.1 Time Histories

The results consist of acceleration, velocity and displacement time histories of structures. Analyses are conducted for every soil condition and the results are presented separately for each soil condition. The comparisons are carried out between conventional structure and for the structure with base isolation.

Three different buildings with different properties are taken into account. Maximum acceleration, velocity and displacement values for each storey are presented. Near and far fault earthquake records are used and the results are presented.

Results for 1979 Imperial Valley Earthquake can be seen from figure 4.1 to figure 4.36. Considering the acceleration results for five, ten and forty storey buildings; base isolation reduces responses considerably in all cases. It can also be said that SSI reduces the acceleration values, but these effects are only pronounced in softer soil conditions. In very soft soil conditions, SSI effects can be observed clearly, but moving towards denser soil, effects disappear and structures behave like they are fixed based. These effects can be seen by comparing figures 4.2, 4.8, 4.14, 4.20, 4.26 and 4.32.

Looking at the velocity results for five, ten and forty storey buildings results are same as acceleration results; base isolation reduces responses considerably. It can also be said that SSI reduces the velocity values, but again, these effects are only pronounced in softer soil conditions. In very soft soil conditions, SSI effects can be observed clearly, but moving towards denser soil, effects disappear and structures behave like they are fixed based. These effects can be seen by comparing figures 4.4, 4.10, 4.16, 4.22, 4.28 and 4.34.

Considering the displacement results for five, ten and forty storey buildings; although base isolated displacements might be higher than fixed cases, large displacements occur at base isolation layer, providing low inter-storey displacements and structures

behave linearly. It can also be said that SSI reduces the displacement values, like in previous acceleration and velocity results, these effects are only pronounced in softer soil conditions. In very soft soil conditions, SSI effects can be observed clearly, but moving towards denser soil, effects disappear and structures behave like they are fixed based. This is the expected result as the dense soil case has the closest behaviour to a fixed base case among all the soil cases studied in this paper. These effects can be seen by comparing figures 4.6, 4.12, 4.18, 4.24, 4.30 and 4.36.

Additional results are provided with the added DVD.

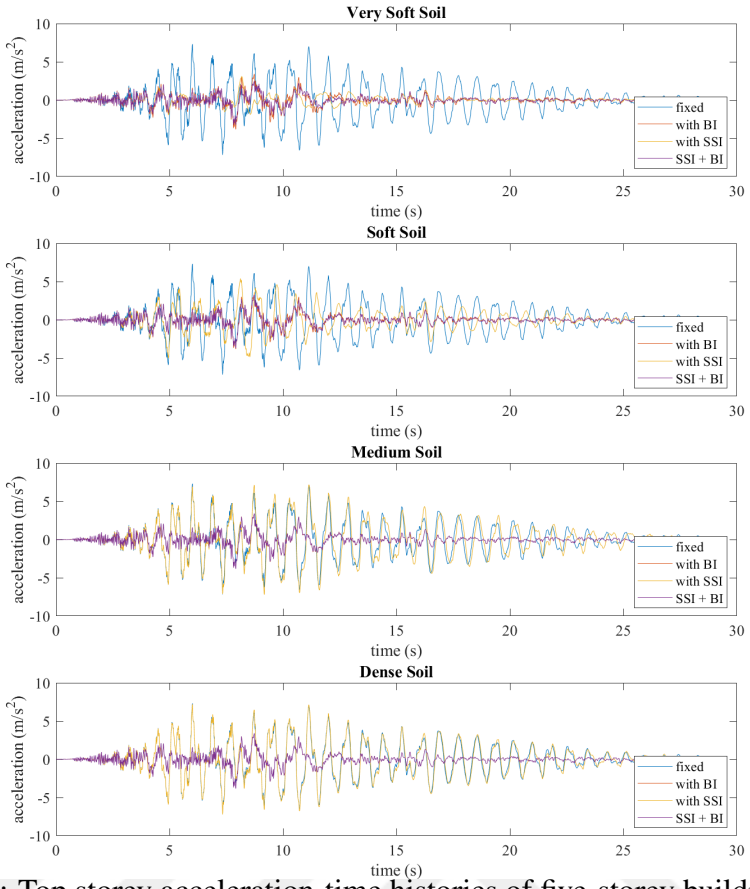

Figure 4.1 : Top storey acceleration-time histories of five-storey building(Imperial Valley, 1979, near fault).

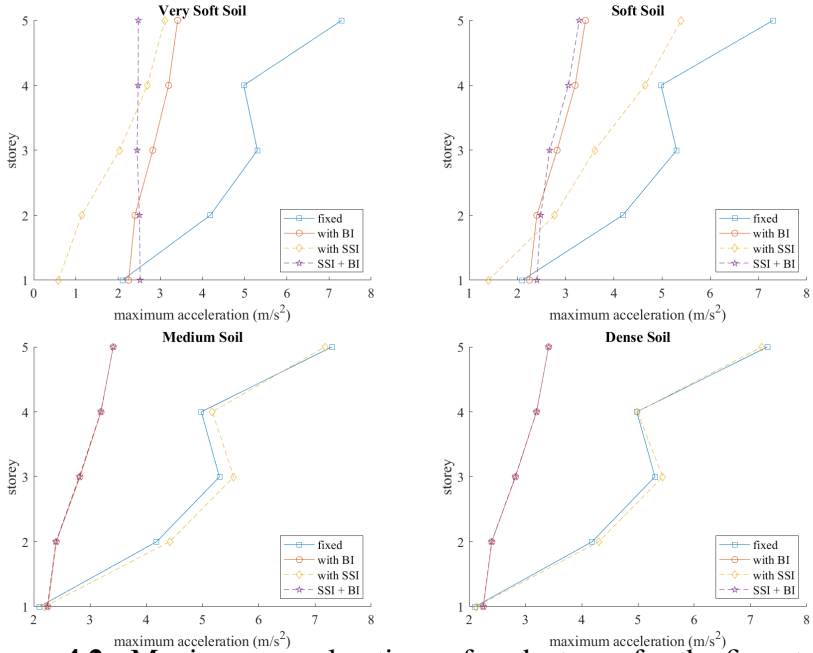

Figure 4.2 : Maximum accelerations of each storey for the five-storey building(Imperial Valley, 1979, near fault).

Figure 4.1 shows comparative acceleration-time histories of the five-storey building for each soil type. Figure 4.2 shows maximum acceleration values for each storey.

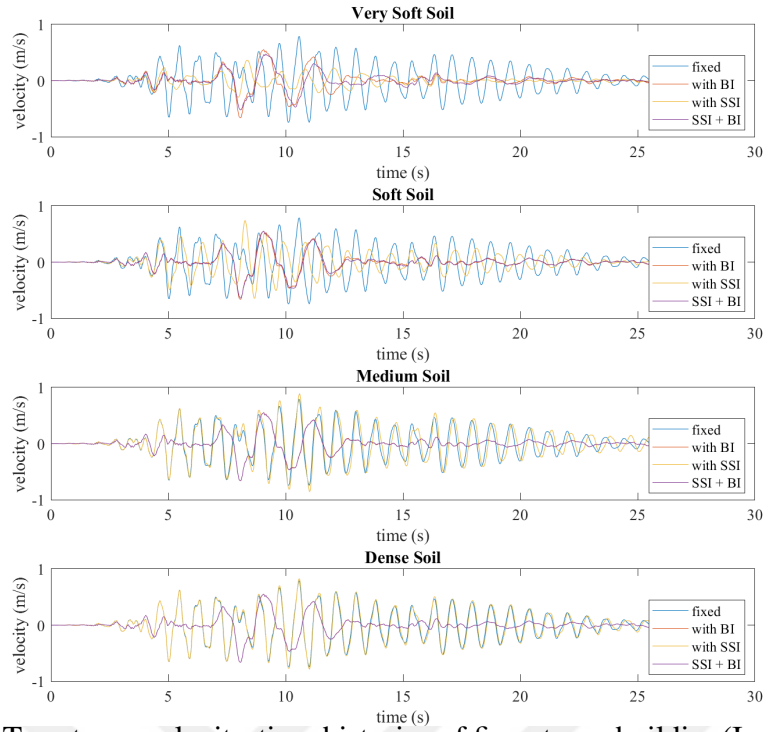

Figure 4.3 : Top storey velocity-time histories of five-storey building(Imperial Valley, 1979, near fault).

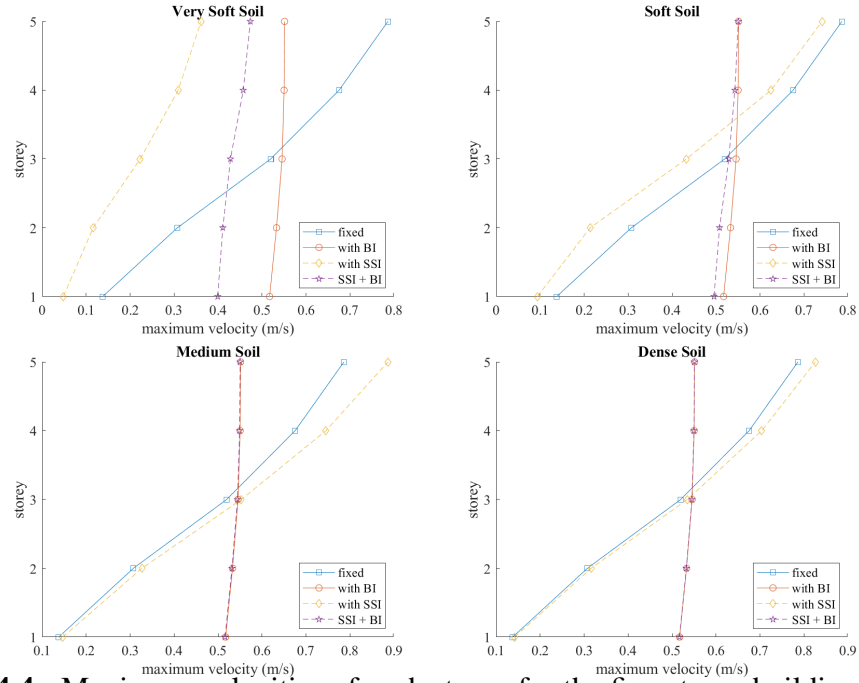

Figure 4.4 : Maximum velocities of each storey for the five-storey building(Imperial Valley, 1979, near fault).

Figure 4.3 shows comparative velocity-time histories of the five-storey building for each soil type. Figure 4.4 shows maximum velocity values for each storey.

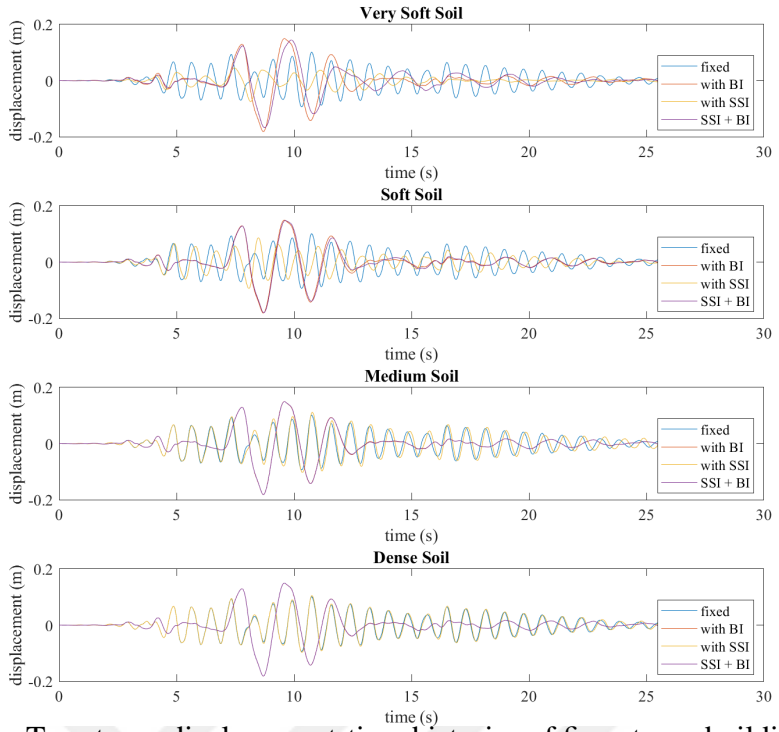

Figure 4.5 : Top storey displacement-time histories of five-storey building(Imperial Valley, 1979, near fault).

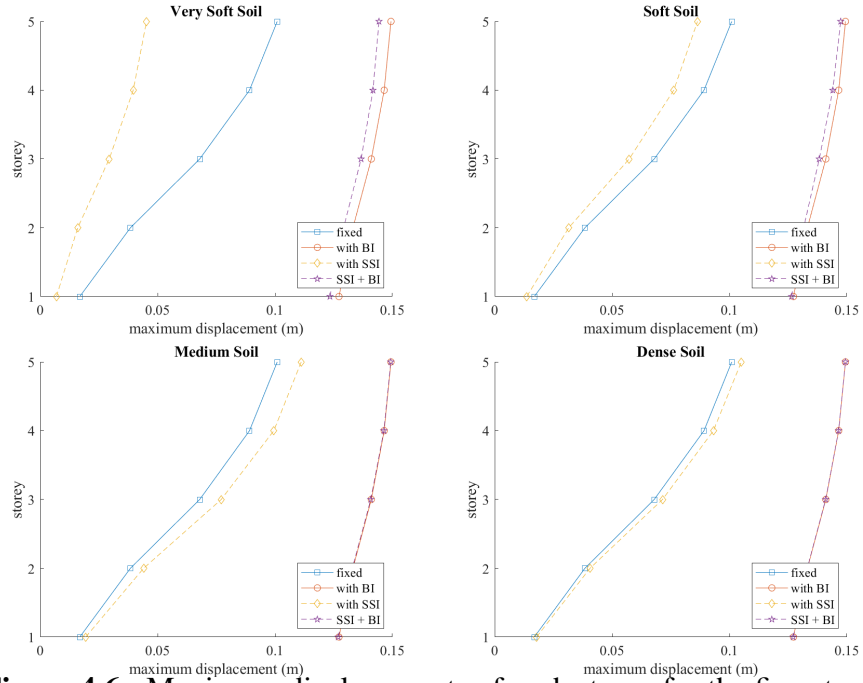

Figure 4.6 : Maximum displacements of each storey for the five-storey building(Imperial Valley, 1979, near fault).

Figure 4.5 shows comparative displacement-time histories of the five-storey building for each soil type. Figure 4.6 shows maximum displacement values for each storey.

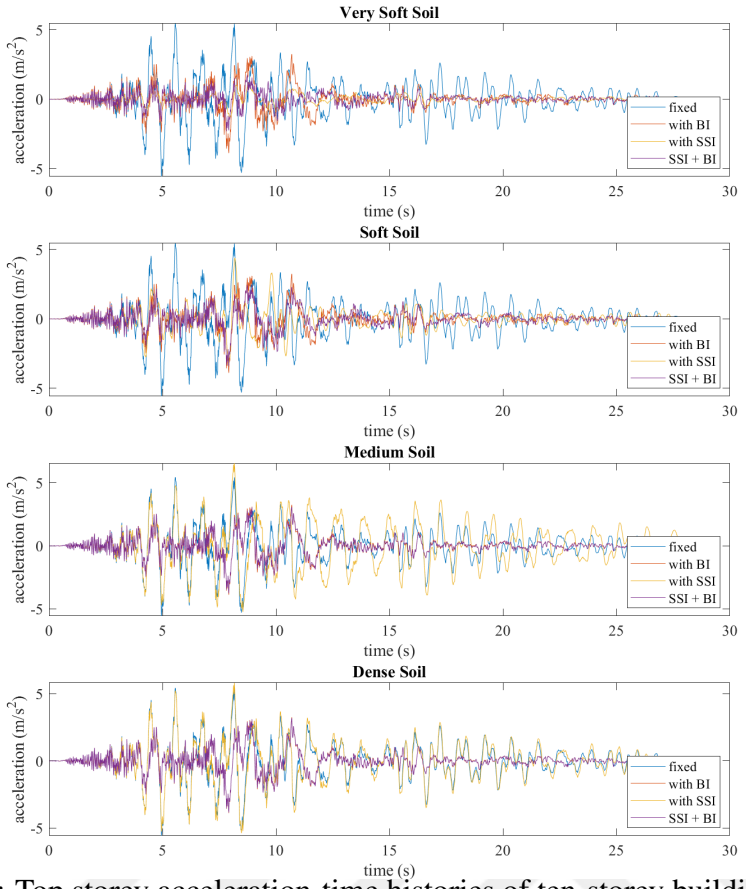

Figure 4.7 : Top storey acceleration-time histories of ten-storey building(Imperial Valley, 1979, near fault).

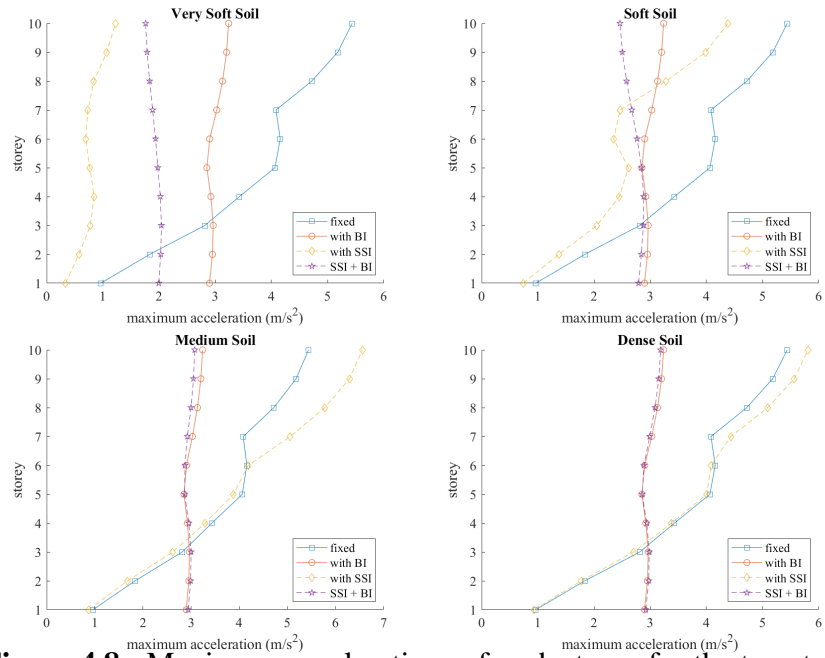

Figure 4.8 : Maximum accelerations of each storey for the ten-storey building(Imperial Valley, 1979, near fault).

Figure 4.7 shows comparative acceleration-time histories of the five-storey building for each soil type. Figure 4.8 shows maximum acceleration values for each storey.

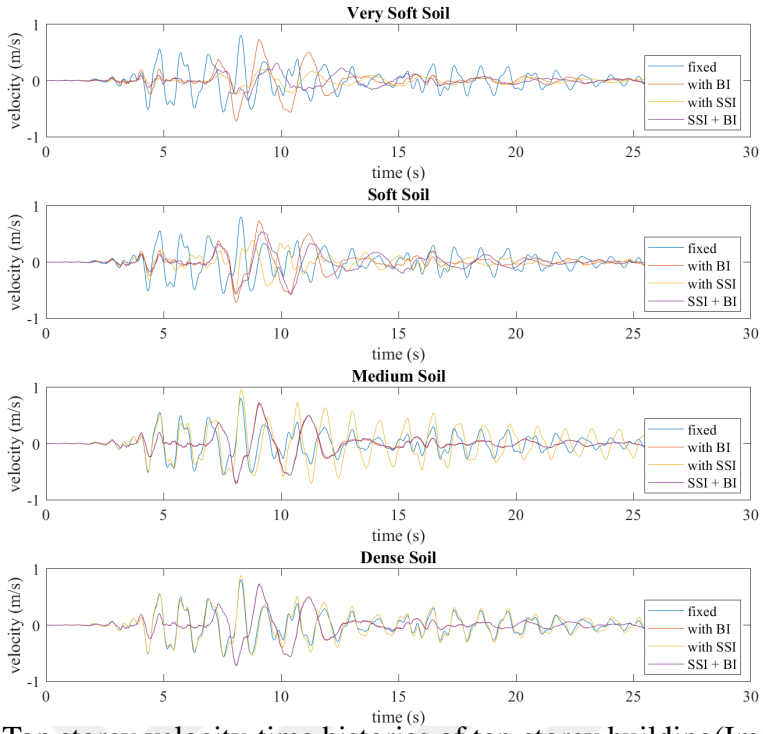

Figure 4.9 : Top storey velocity-time histories of ten-storey building(Imperial Valley, 1979, near fault).

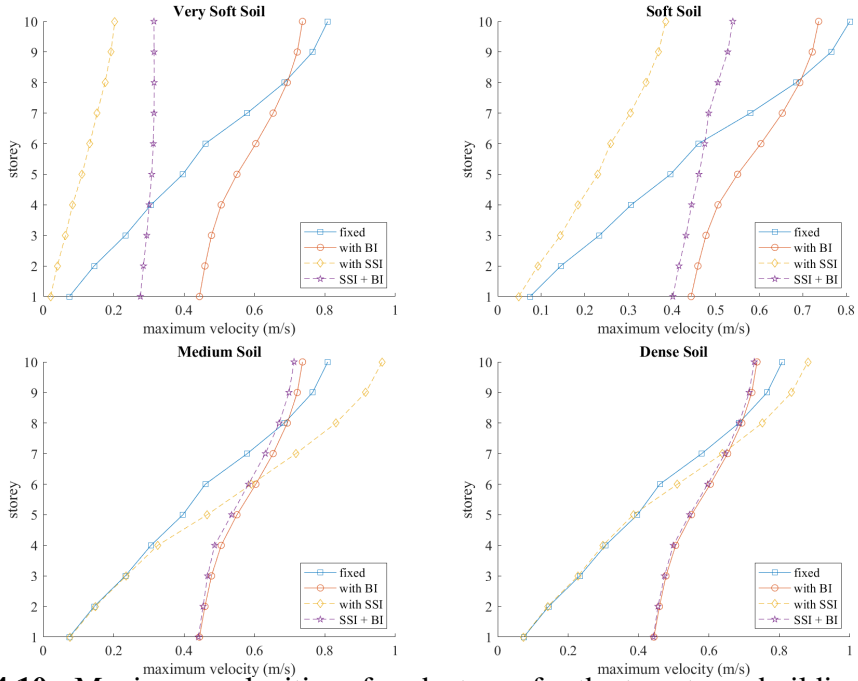

Figure 4.10 : Maximum velocities of each storey for the ten-storey building(Imperial Valley, 1979, near fault).

Figure 4.9 shows comparative velocity-time histories of the ten-storey building for each soil type. Figure 4.10 shows maximum velocity values for each storey.

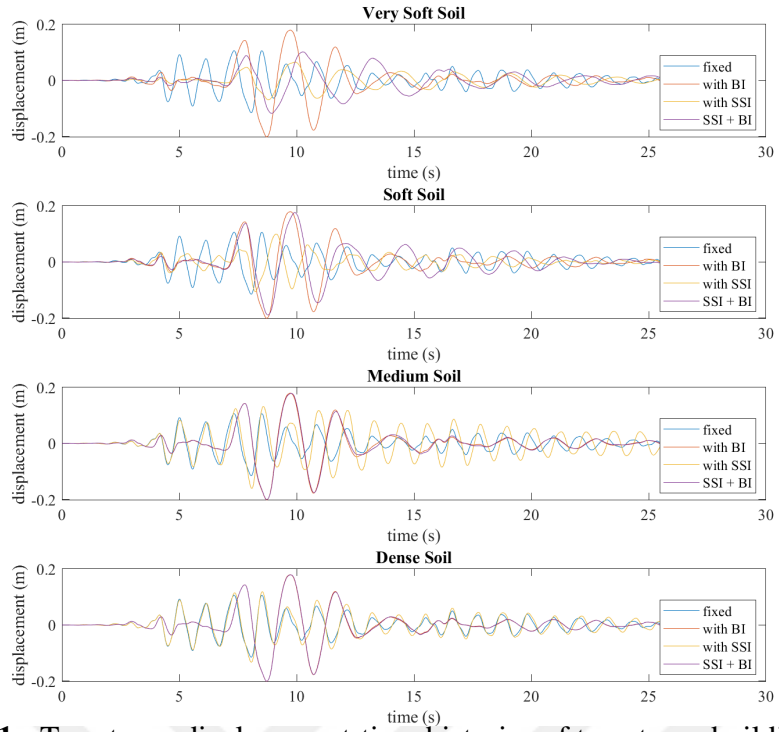

Figure 4.11 : Top storey displacement-time histories of ten-storey building(Imperial Valley, 1979, near fault).

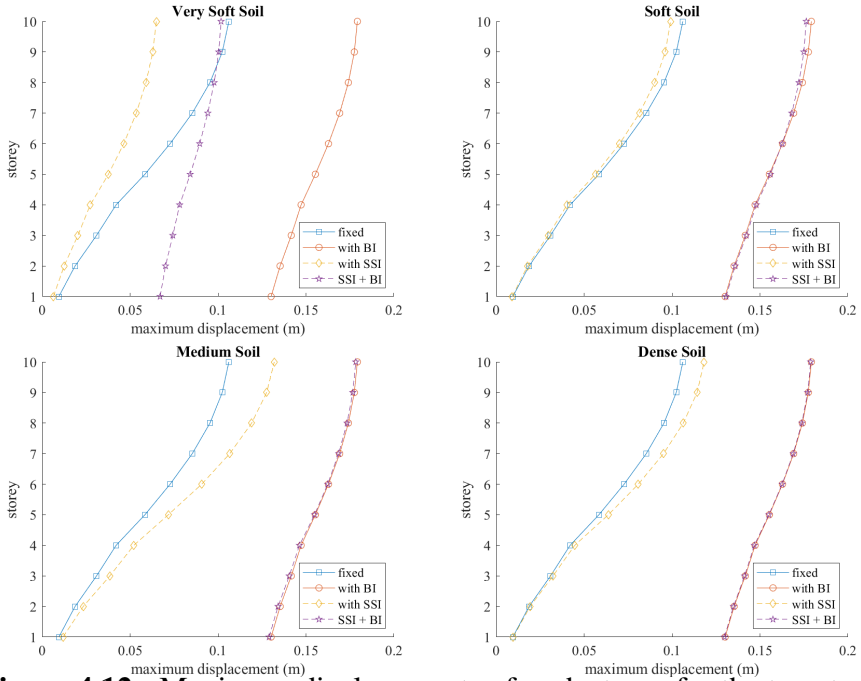

Figure 4.12 : Maximum displacements of each storey for the ten-storey building(Imperial Valley, 1979, near fault).

Figure 4.11 shows comparative displacement-time histories of the ten-storey building for each soil type. Figure 4.12 shows maximum displacement values for each storey.

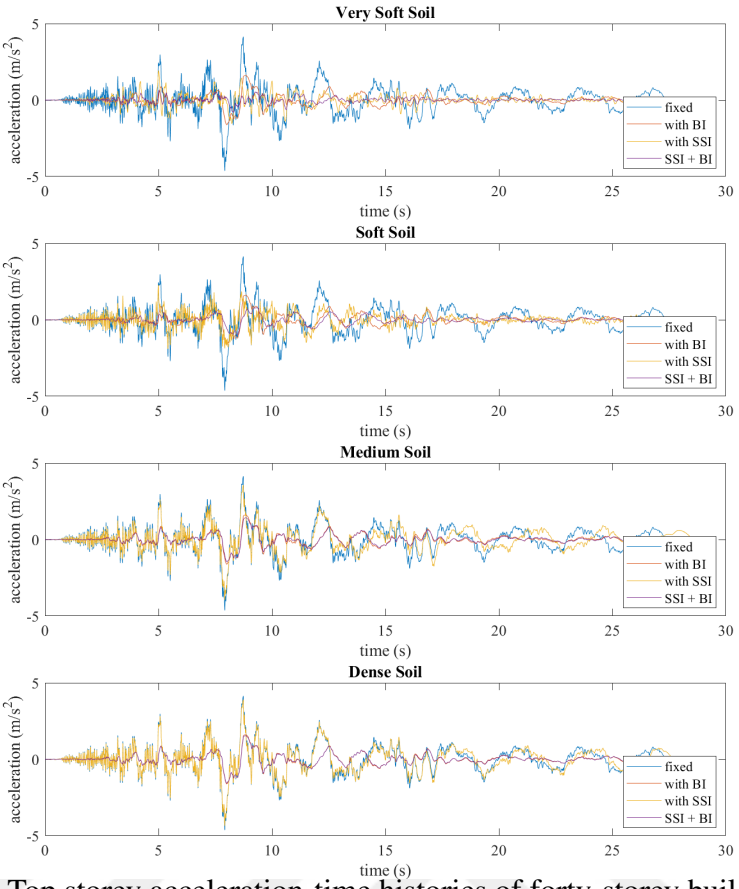

Figure 4.13 : Top storey acceleration-time histories of forty-storey building(Imperial Valley, 1979, near fault).

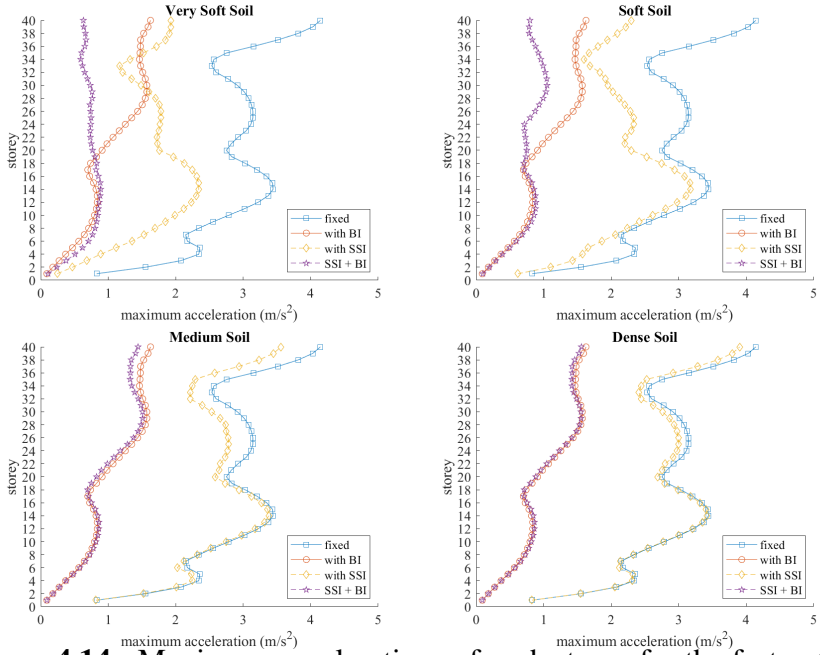

Figure 4.14 : Maximum accelerations of each storey for the forty-storey building(Imperial Valley, 1979, near fault).

Figure 4.13 shows comparative acceleration-time histories of the forty-storey building for each soil type. Figure 4.14 shows maximum acceleration values for each storey.

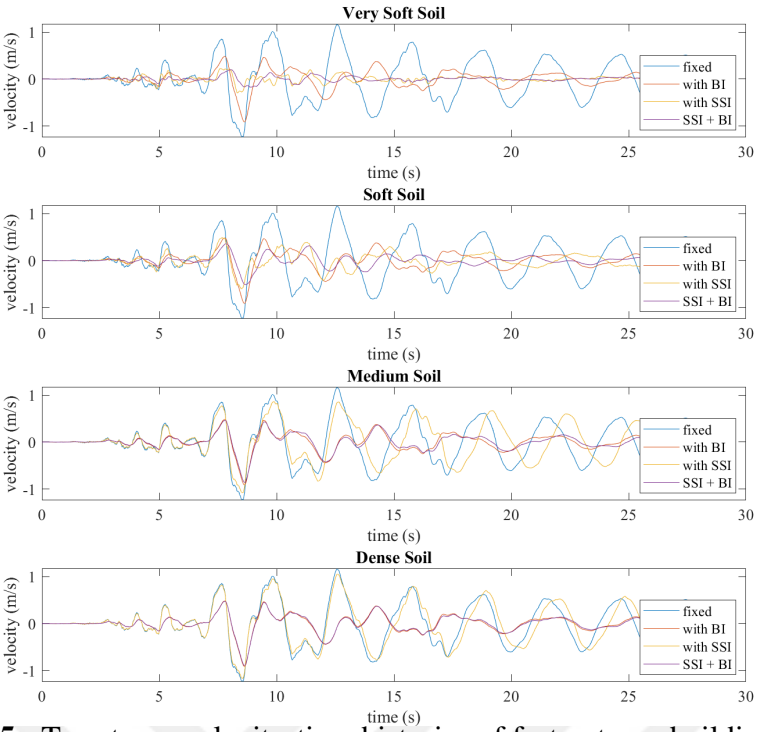

Figure 4.15 : Top storey velocity-time histories of forty-storey building(Imperial Valley, 1979, near fault).

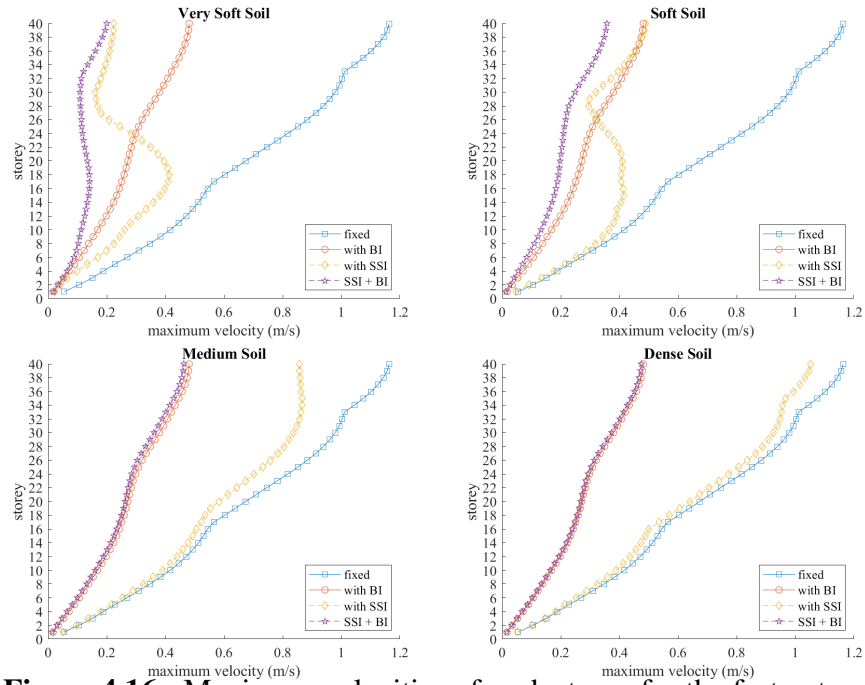

Figure 4.16 : Maximum velocities of each storey for the forty-storey building(Imperial Valley, 1979, near fault).

Figure 4.15 shows comparative velocity-time histories of the forty-storey building for each soil type. Figure 4.16 shows maximum velocity values for each storey.

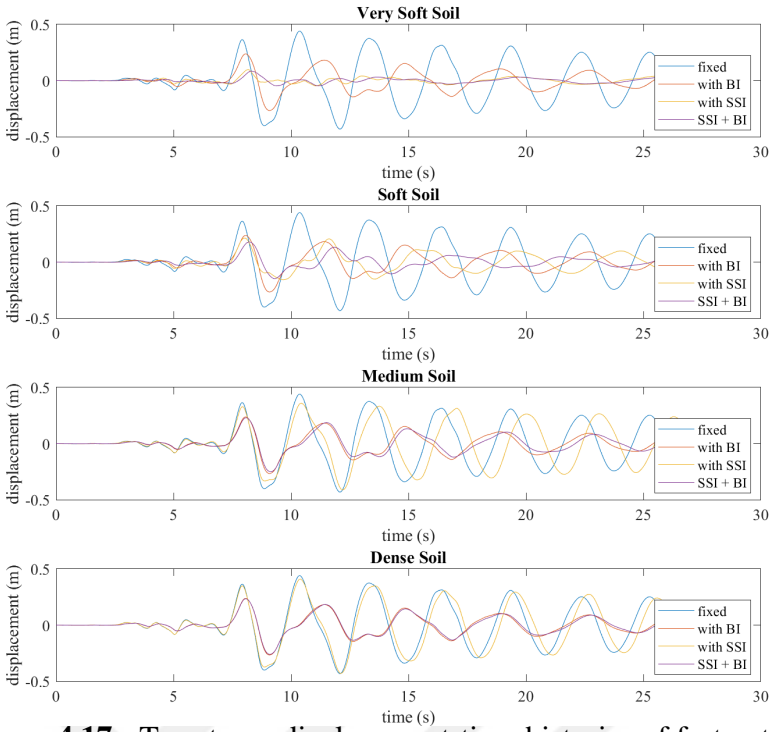

Figure 4.17 : Top storey displacement-time histories of forty-storey building(Imperial Valley, 1979, near fault).

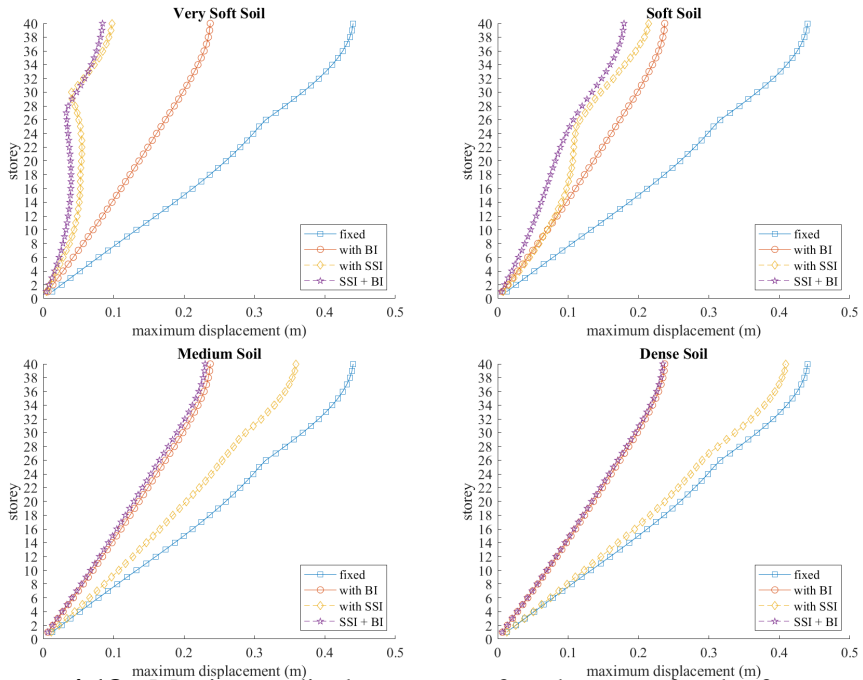

Figure 4.18 : Maximum displacements of each storey for the forty-storey building(Imperial Valley, 1979, near fault).

Figure 4.17 shows comparative displacement-time histories of the forty-storey building for each soil type. Figure 4.18 shows maximum displacement values for each storey.

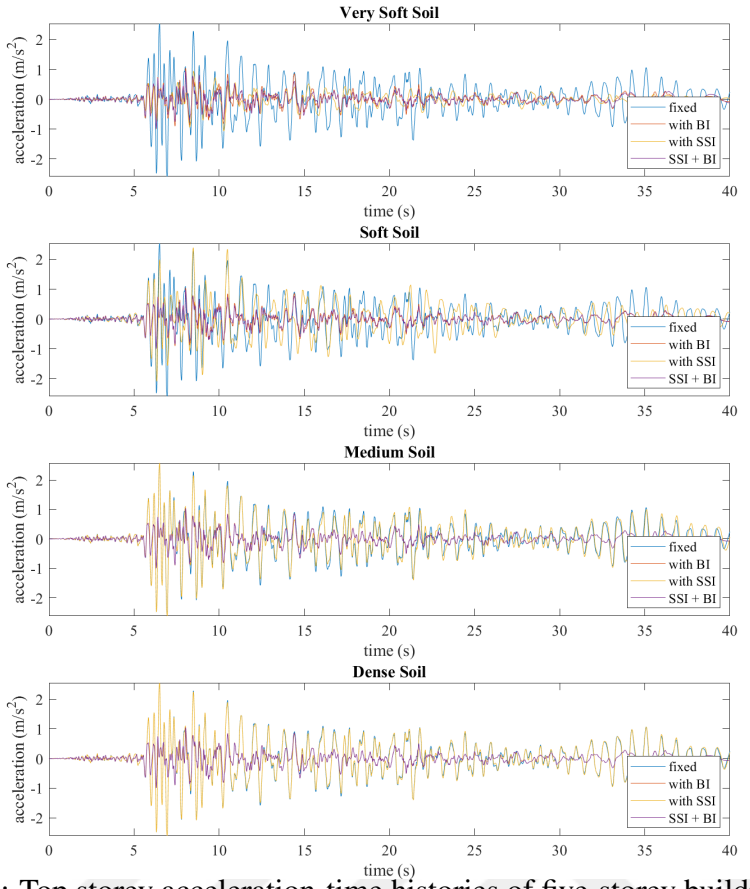

Figure 4.19 : Top storey acceleration-time histories of five-storey building(Imperial Valley, 1979, far fault).

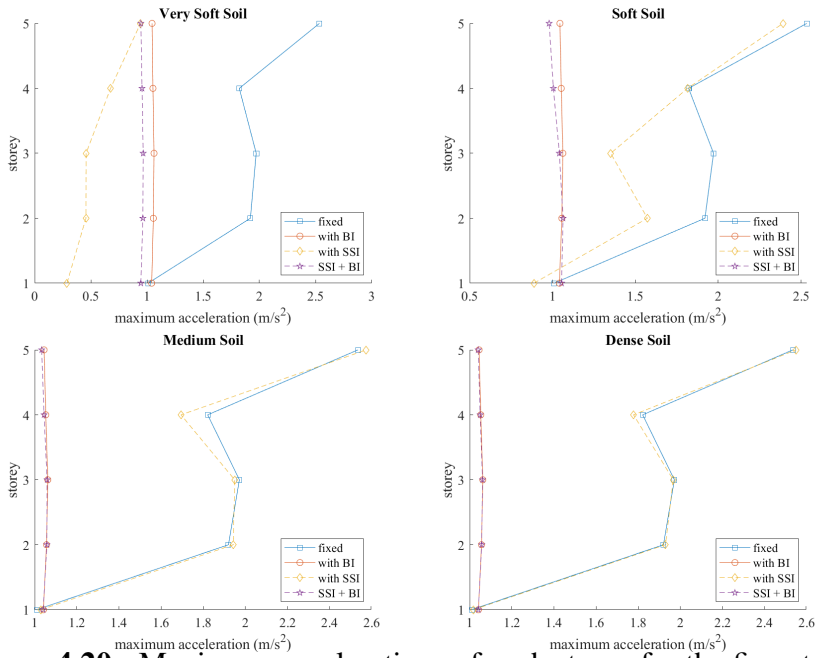

Figure 4.20 : Maximum accelerations of each storey for the five-storey building(Imperial Valley, 1979, far fault).

Figure 4.19 shows comparative acceleration-time histories of the five-storey building for each soil type. Figure 4.20 shows maximum acceleration values for each storey.

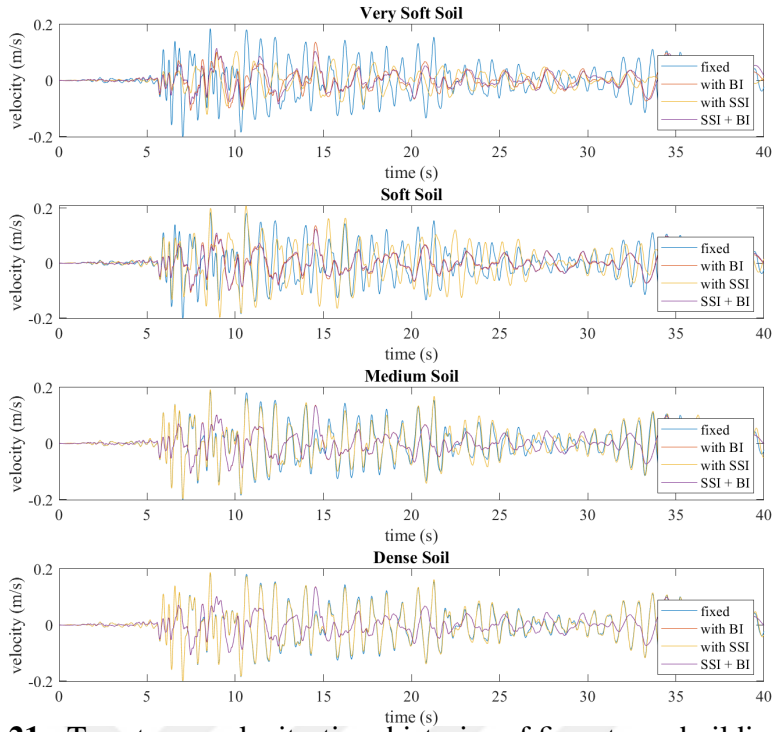

Figure 4.21 : Top storey velocity-time histories of five-storey building(Imperial Valley, 1979, far fault).

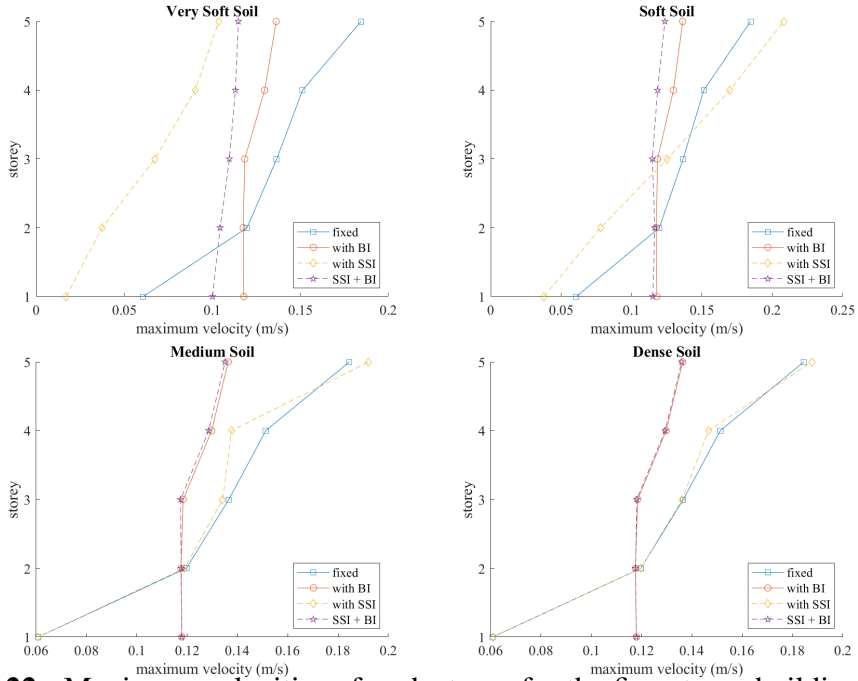

Figure 4.22 : Maximum velocities of each storey for the five-storey building(Imperial Valley, 1979, far fault).

Figure 4.21 shows comparative velocity-time histories of the five-storey building for each soil type. Figure 4.22 shows maximum velocity values for each storey.

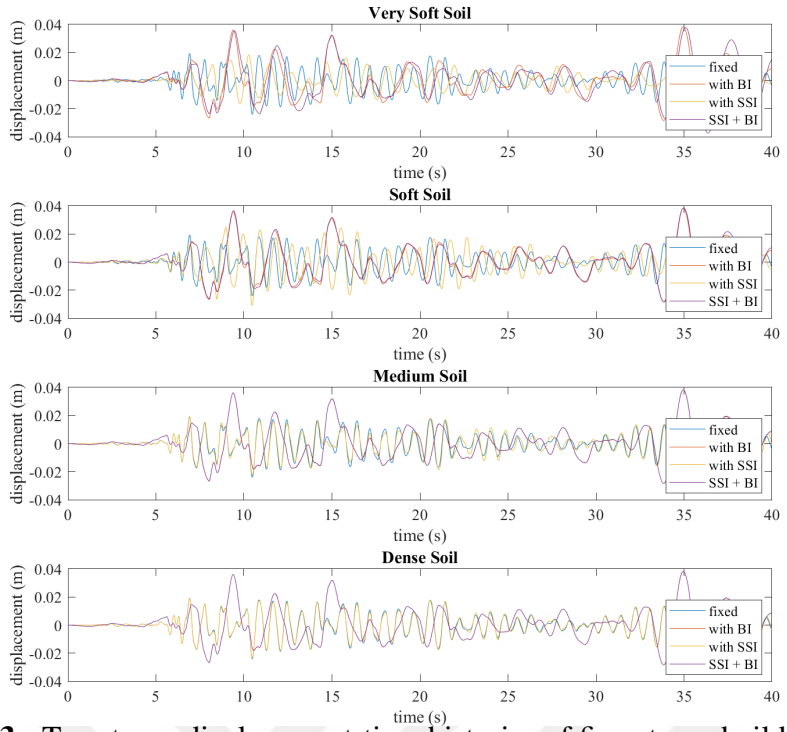

Figure 4.23 : Top storey displacement-time histories of five-storey building(Imperial Valley, 1979, far fault).

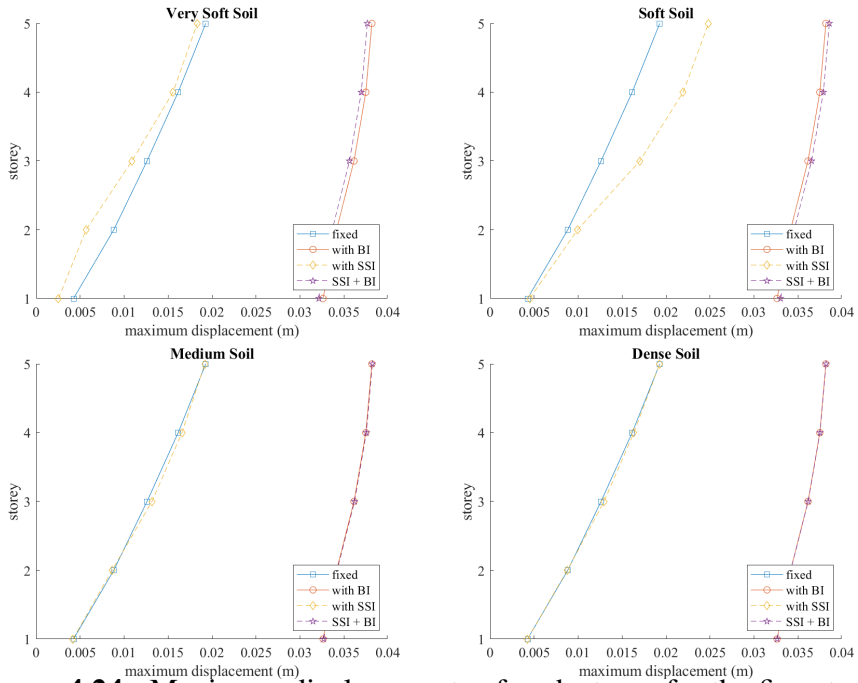

Figure 4.24 : Maximum displacements of each storey for the five-storey building(Imperial Valley, 1979, far fault).

Figure 4.23 shows comparative displacement-time histories of the five-storey building for each soil type. Figure 4.24 shows maximum displacement values for each storey.

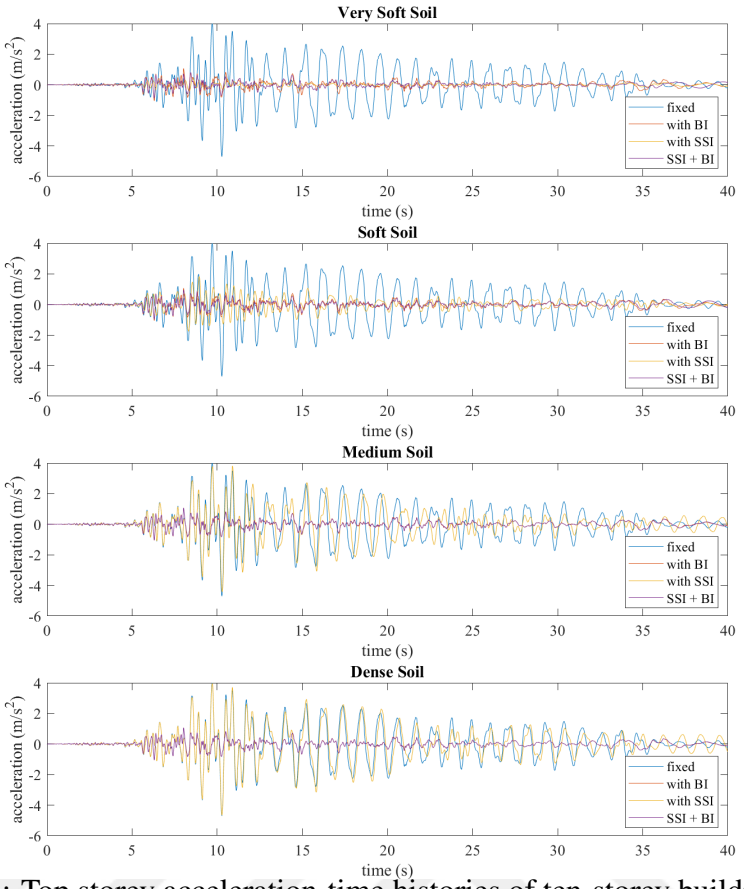

Figure 4.25 : Top storey acceleration-time histories of ten-storey building(Imperial Valley, 1979, far fault).

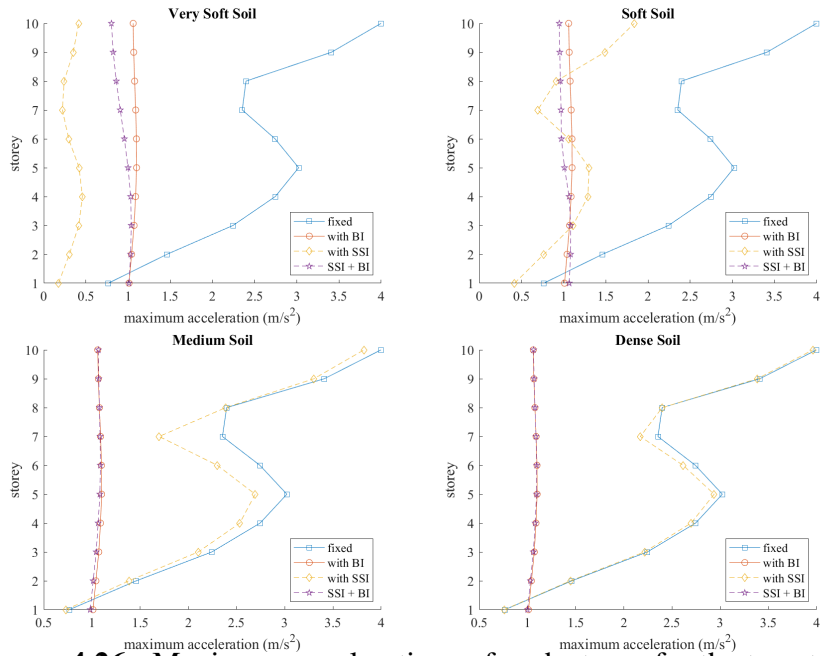

Figure 4.26 : Maximum accelerations of each storey for the ten-storey building(Imperial Valley, 1979, far fault).

Figure 4.25 shows comparative acceleration-time histories of the ten-storey building for each soil type. Figure 4.26 shows maximum acceleration values for each storey.

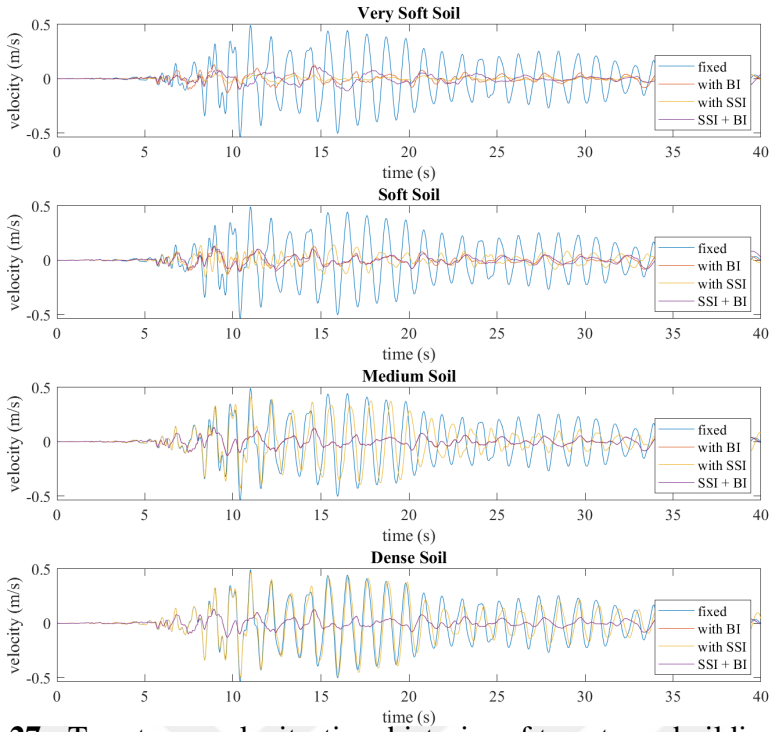

Figure 4.27 : Top storey velocity-time histories of ten-storey building(Imperial Valley, 1979, far fault).

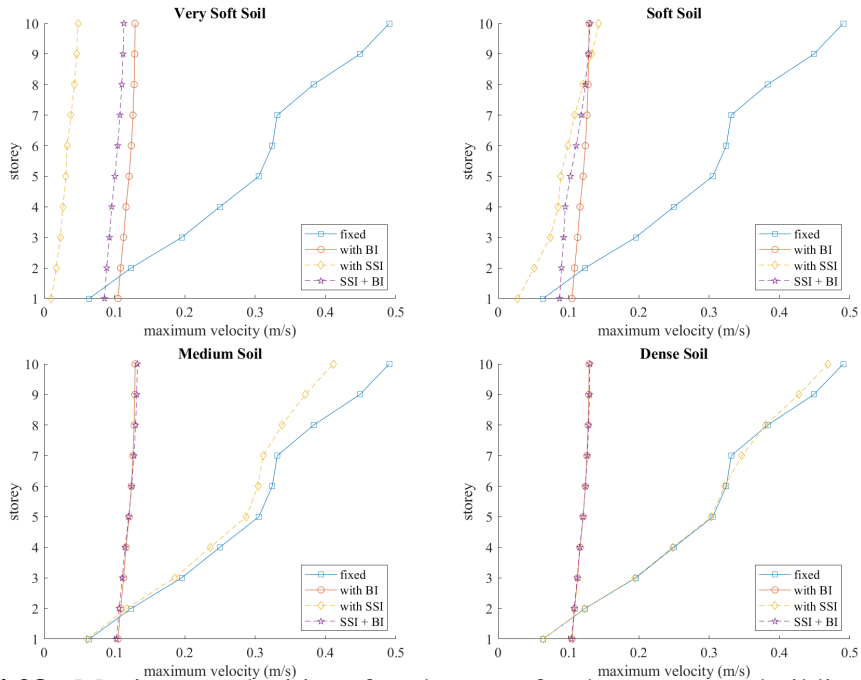

Figure 4.28 : Maximum velocities of each storey for the ten-storey building(Imperial Valley, 1979, far fault).

Figure 4.27 shows comparative velocity-time histories of the ten-storey building for each soil type. Figure 4.28 shows maximum velocity values for each storey.

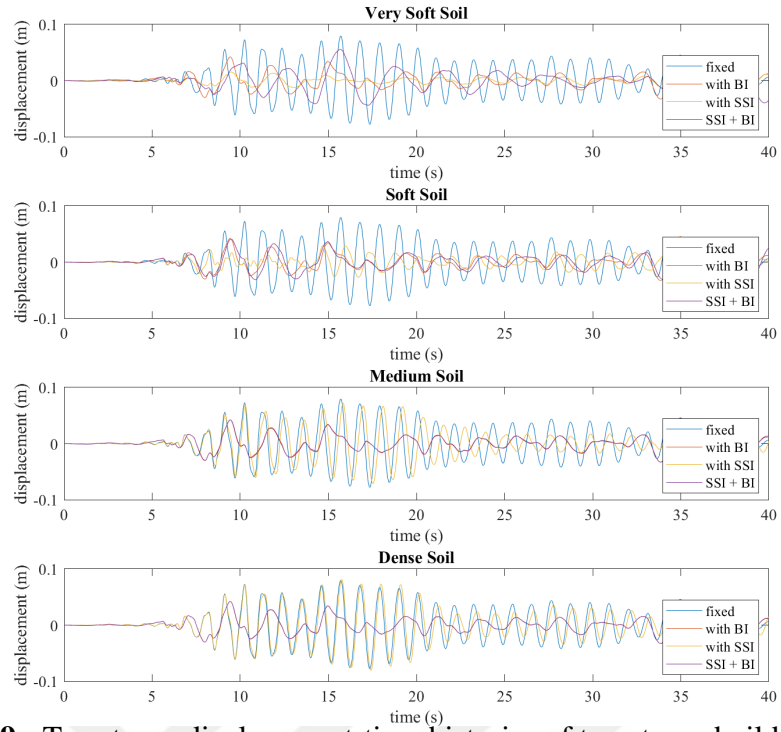

Figure 4.29 : Top storey displacement-time histories of ten-storey building(Imperial Valley, 1979, far fault).

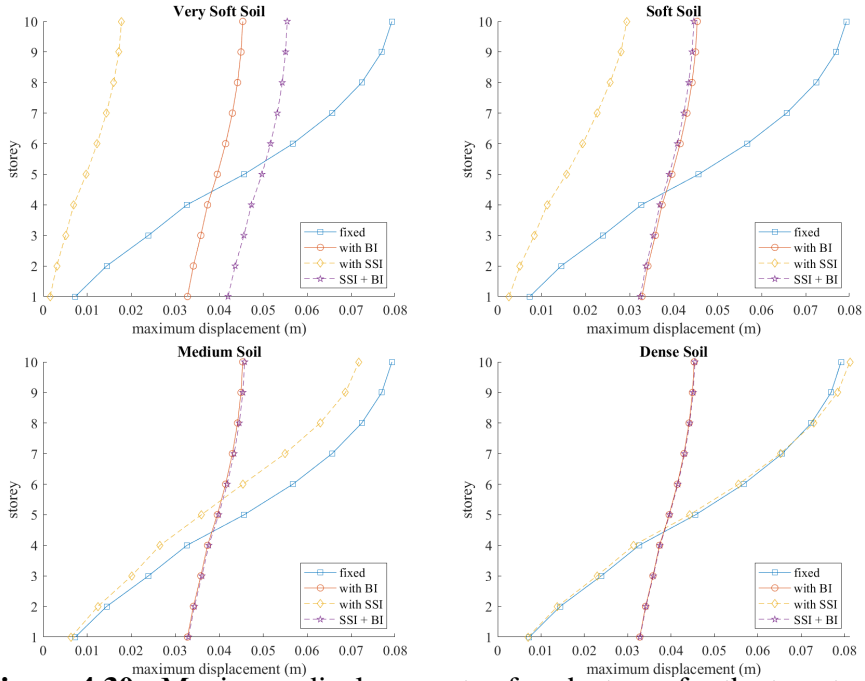

Figure 4.30 : Maximum displacements of each storey for the ten-storey building(Imperial Valley, 1979, far fault).

Figure 4.29 shows comparative displacement-time histories of the ten-storey building for each soil type. Figure 4.30 shows maximum displacement values for each storey.

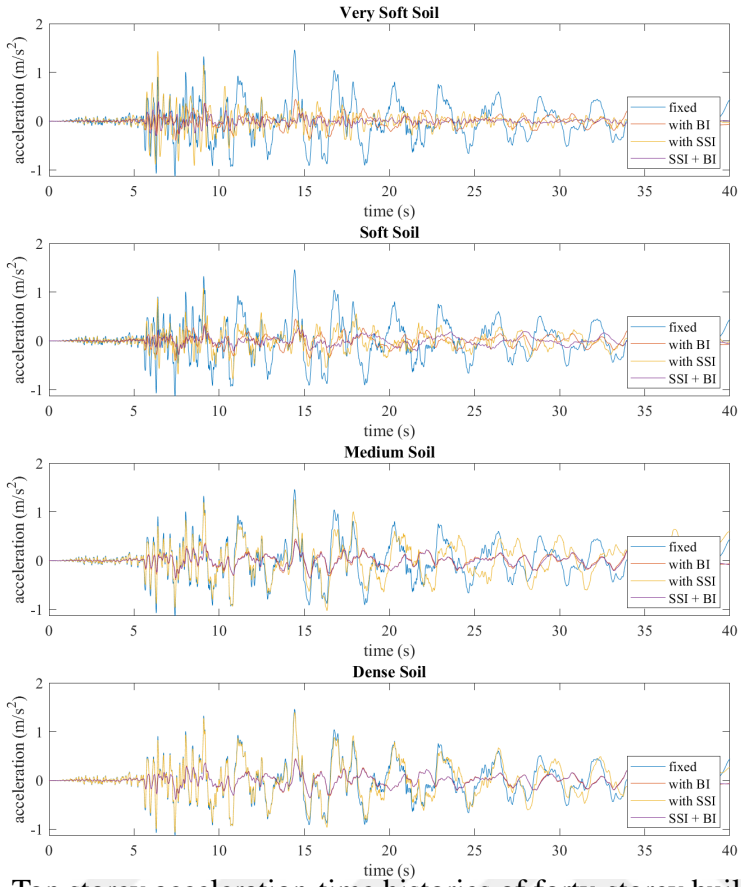

Figure 4.31 : Top storey acceleration-time histories of forty-storey building(Imperial Valley, 1979, far fault).

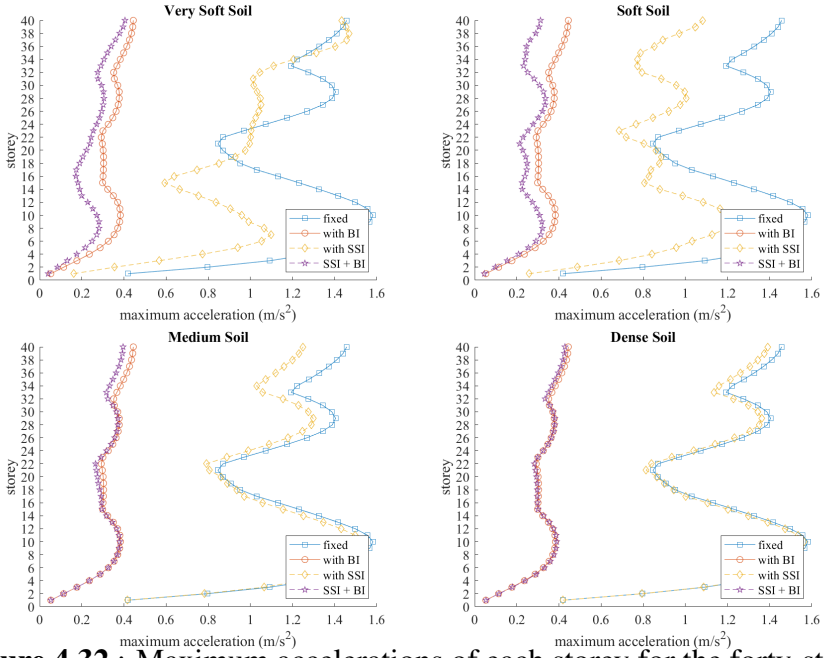

Figure 4.32 : Maximum accelerations of each storey for the forty-storey building(Imperial Valley, 1979, far fault).

Figure 4.31 shows comparative acceleration-time histories of the forty-storey building for each soil type. Figure 4.32 shows maximum acceleration values for each storey.

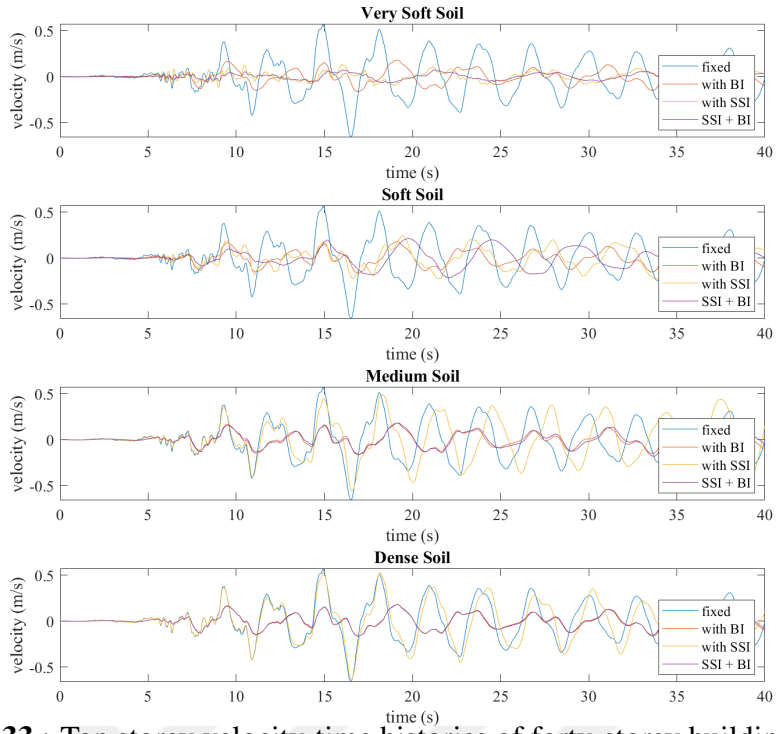

Figure 4.33 : Top storey velocity-time histories of forty-storey building(Imperial Valley, 1979, far fault).

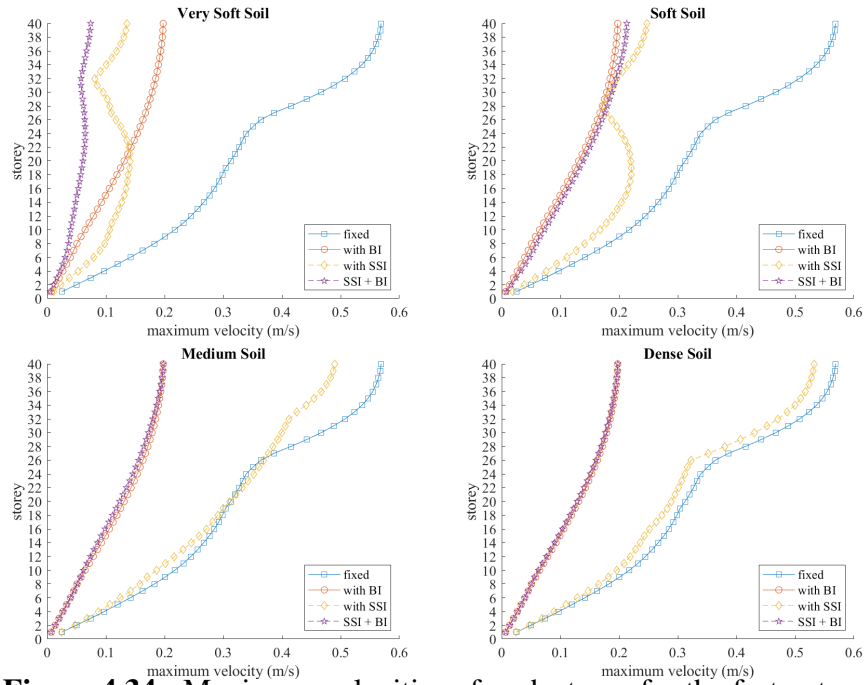

Figure 4.34 : Maximum velocities of each storey for the forty-storey building(Imperial Valley, 1979, far fault).

Figure 4.33 shows comparative velocity-time histories of the forty-storey building for each soil type. Figure 4.34 shows maximum velocity values for each storey.

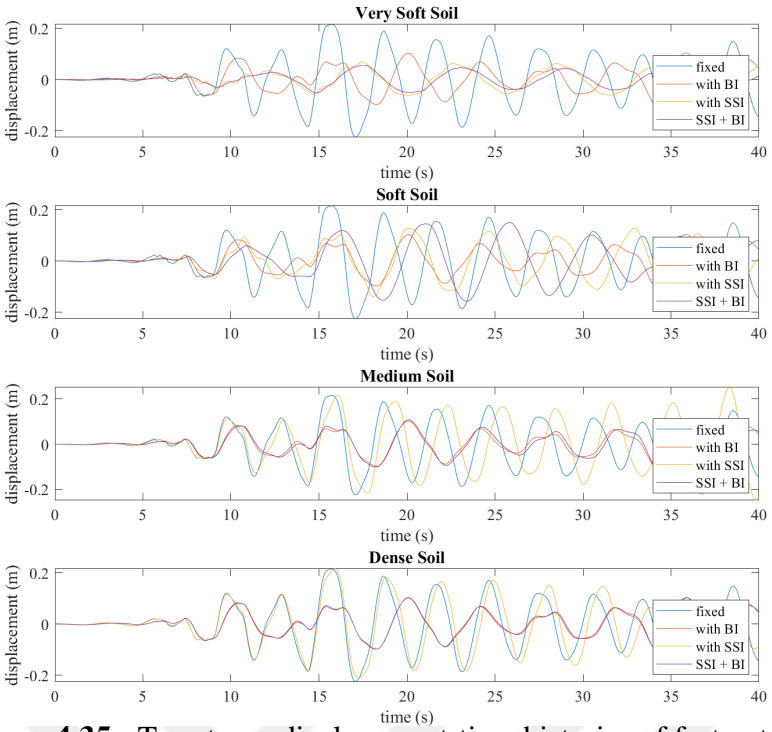

Figure 4.35 : Top storey displacement-time histories of forty-storey building(Imperial Valley, 1979, far fault).

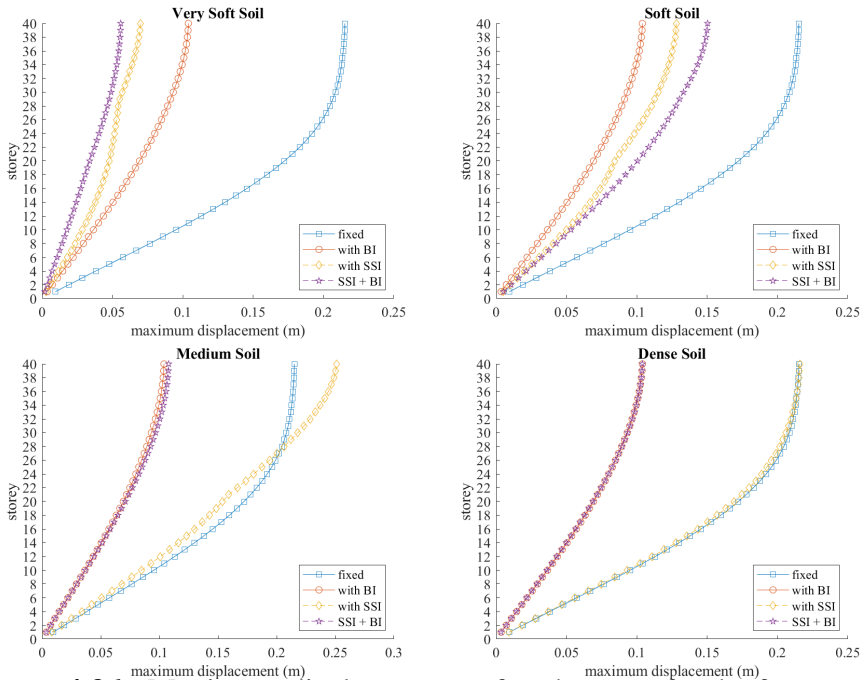

Figure 4.36 : Maximum displacements of each storey for the forty-storey building(Imperial Valley, 1979, far fault).

Figure 4.35 shows comparative displacement-time histories of the forty-storey building for each soil type. Figure 4.36 shows maximum displacement values for each storey.

Results for 1992 Cape Mendocino Earthquake can be seen from figure 4.37 to figure 4.72. Considering the acceleration results for five, ten and forty storey buildings; base isolation reduces responses considerably in all cases. It can also be said that SSI reduces the acceleration values, but these effects are only pronounced in softer soil conditions. In very soft soil conditions, SSI effects can be observed clearly, but moving towards denser soil, effects disappear and structures behave like they are fixed based. The disappearance of SSI effects while shifting from very soft soil to dense soil and eventually to fixed base case is the expected result. As it has been stated before in this thesis, dynamic behaviour of dense soil approaches to fixed base case. These effects can be seen by comparing figures 4.38, 4.44, 4.50, 4.56, 4.62 and 4.68.

If we consider the velocity graphics for five, ten and forty storey buildings results are same as acceleration results; base isolation reduces responses considerably. In addition it has been presented in velocity figures that SSI reduces velocity values. However this is valid only in softer soil conditions. In very soft soil conditions, SSI effects can be observed clearly, but moving towards denser soil, effects disappear and structures behave like they are fixed based. This conclusion has been reached many times in this study. These effects can be seen by comparing figures 4.40, 4.46, 4.52, 4.58, 4.64 and 4.70.

If we investigate the results obtained from all buildings studied in this section, it has been found that base isolated displacements might be higher than fixed base case. However base isolation layer has the large displacements which leads to linear behaviour of the structure and low inter-storey displacements. It can also be said that SSI reduces the displacement values, like in Imperial Valley earthquake, these effects are only pronounced in softer soil conditions. In very soft soil conditions, SSI effects can be observed clearly, in dense soil it is observed that SSI effects are almost invisible. And their behaviour is nearly similar to the fixed base structures. All these findings are obtained from the comparison figures 4.42, 4.48, 4.54, 4.60, 4.66 and 4.72.

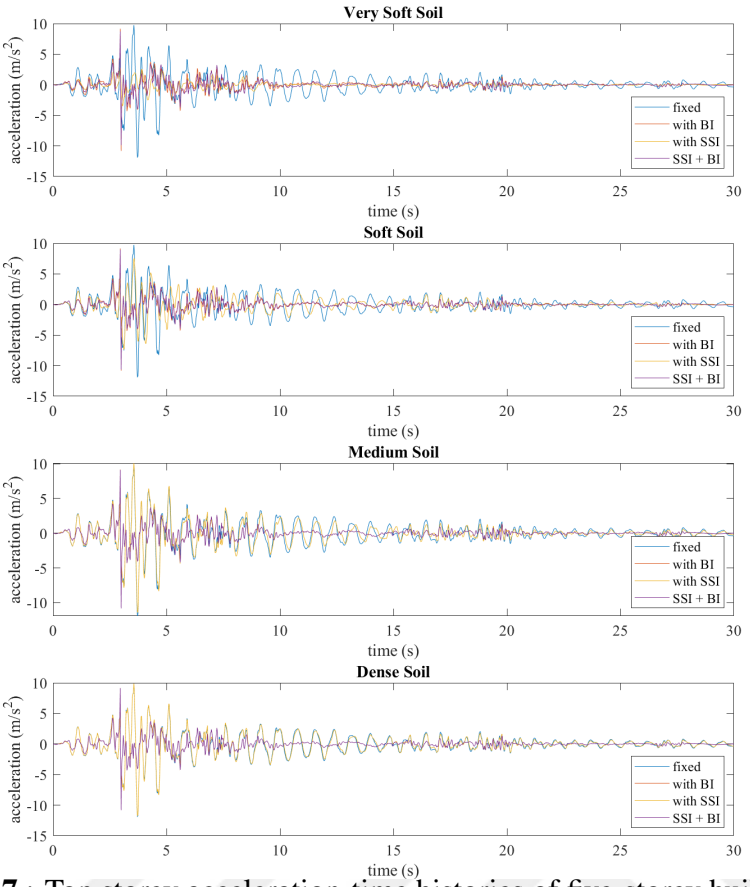

Figure 4.37 : Top storey acceleration-time histories of five-storey building(Cape Mendocino, 1992, near fault).

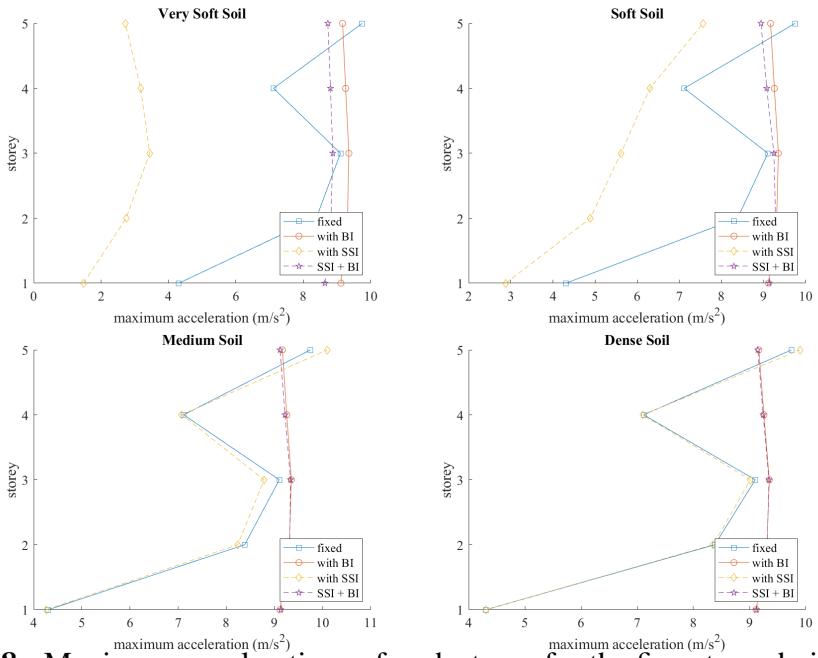

Figure 4.38 : Maximum accelerations of each storey for the five-storey building(Cape Mendocino, 1992, near fault).

Figure 4.37 shows comparative acceleration-time histories of the five-storey building for each soil type. Figure 4.38 shows maximum acceleration values for each storey.

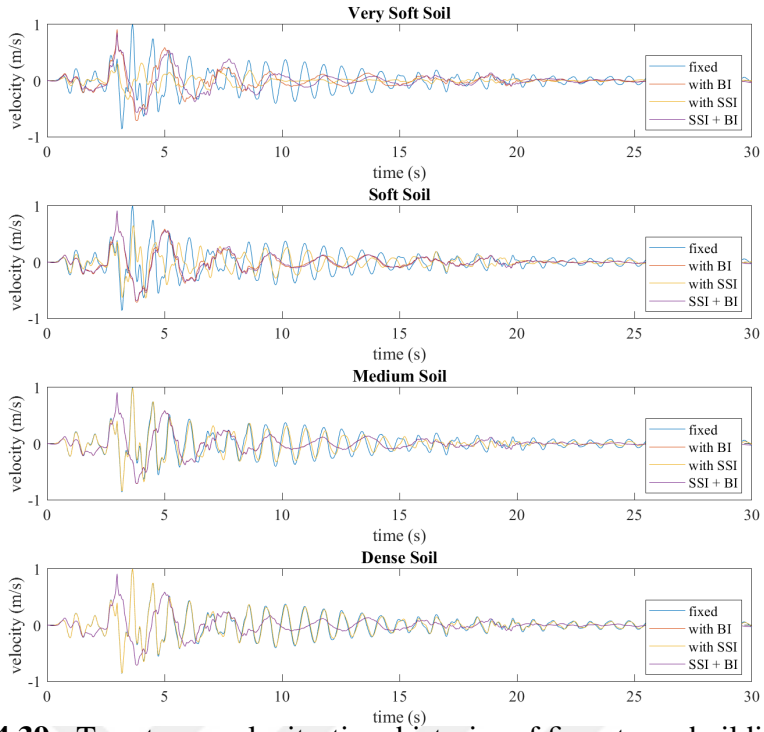

Figure 4.39 : Top storey velocity-time histories of five-storey building(Cape Mendocino, 1992, near fault).

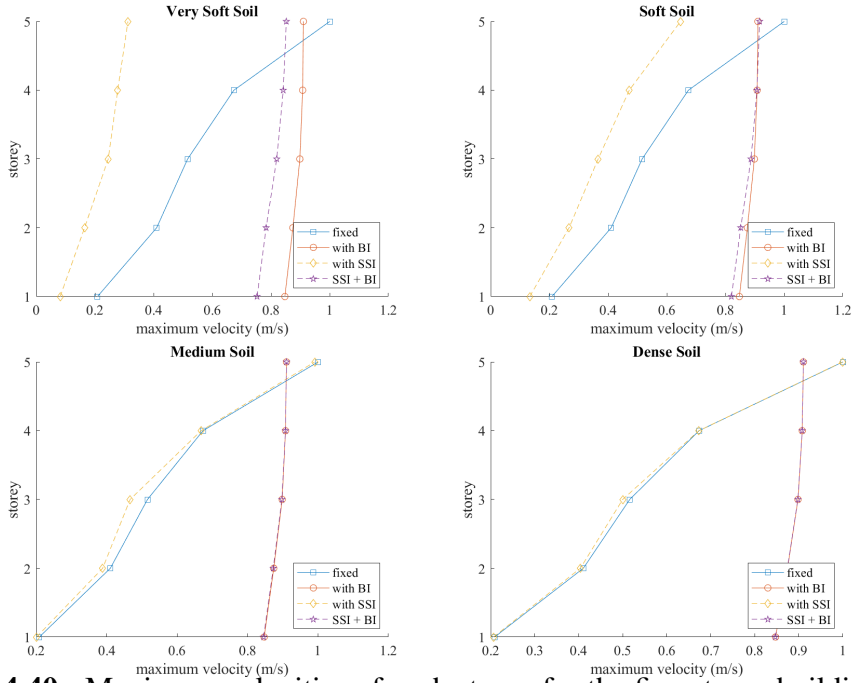

Figure 4.40 : Maximum velocities of each storey for the five-storey building(Cape Mendocino, 1992, near fault).

Figure 4.39 shows comparative velocity-time histories of the five-storey building for each soil type. Figure 4.40 shows maximum velocity values for each storey.

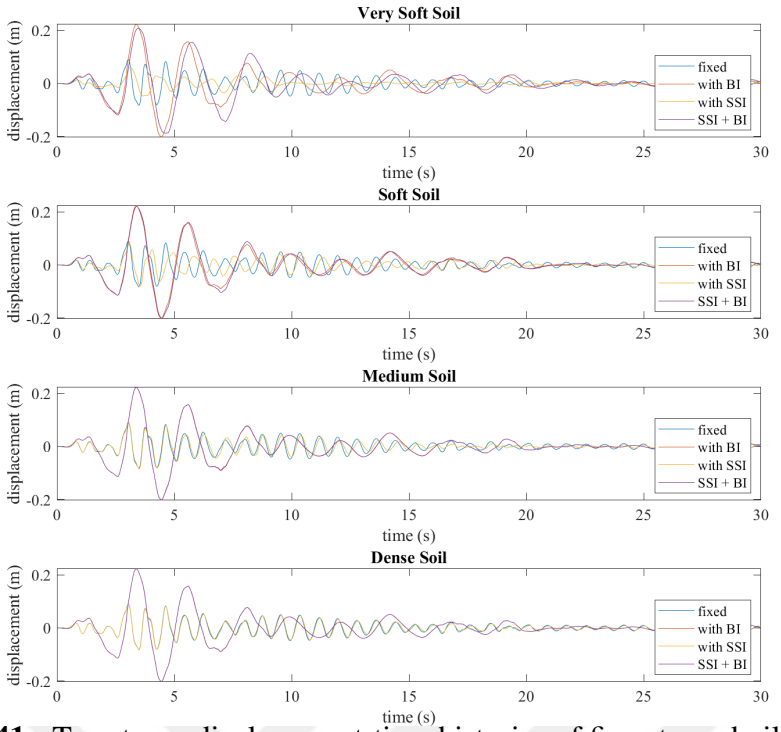

Figure 4.41 : Top storey displacement-time histories of five-storey building(Cape Mendocino, 1992, near fault).

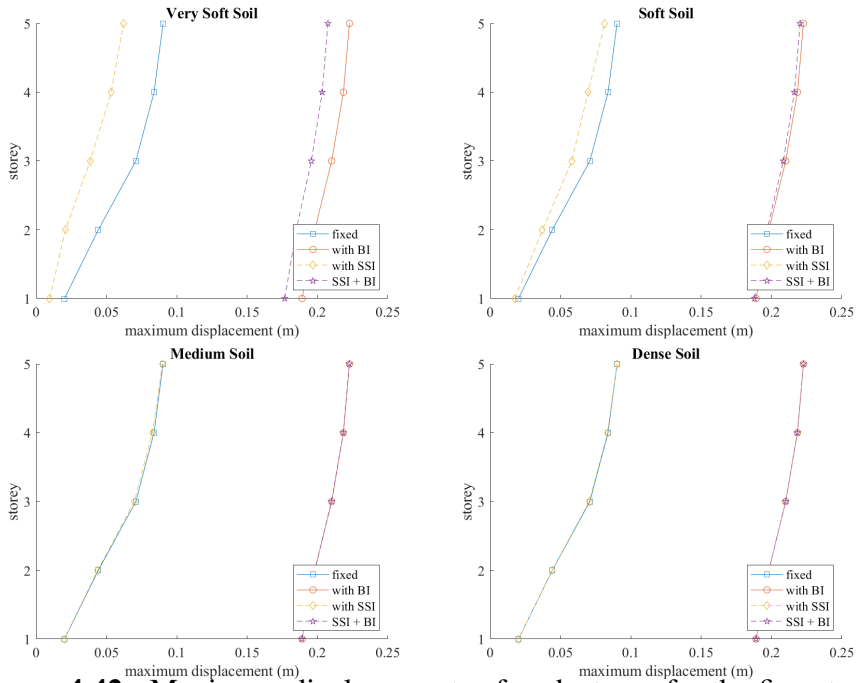

Figure 4.42 : Maximum displacements of each storey for the five-storey building(Cape Mendocino, 1992, near fault).

Figure 4.41 shows comparative displacement-time histories of the five-storey building for each soil type. Figure 4.42 shows maximum displacement values for each storey.

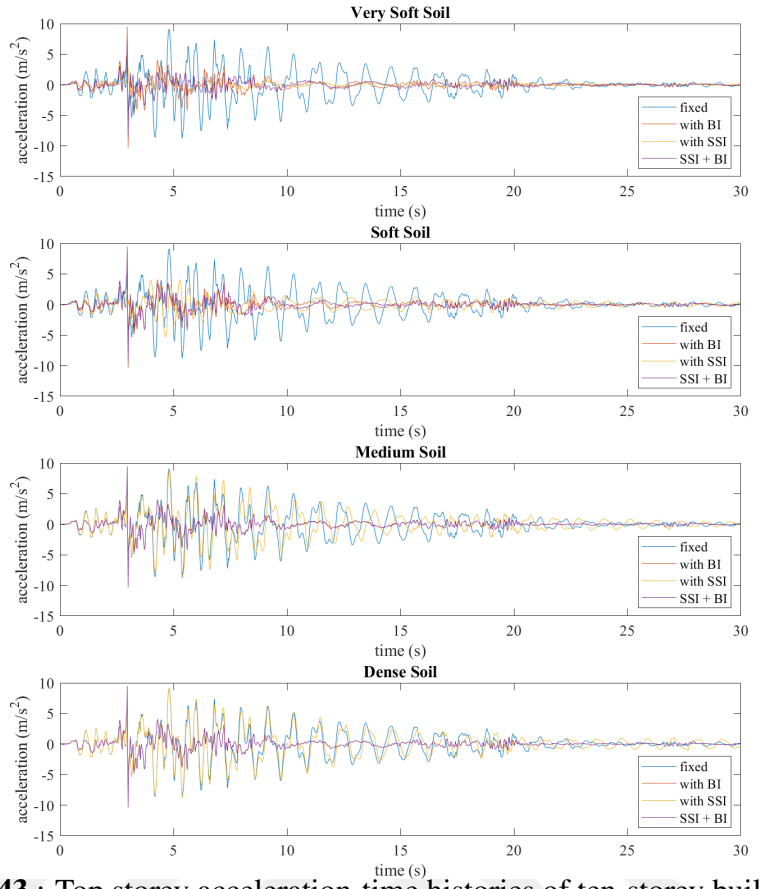

Figure 4.43 : Top storey acceleration-time histories of ten-storey building(Cape Mendocino, 1992, near fault).

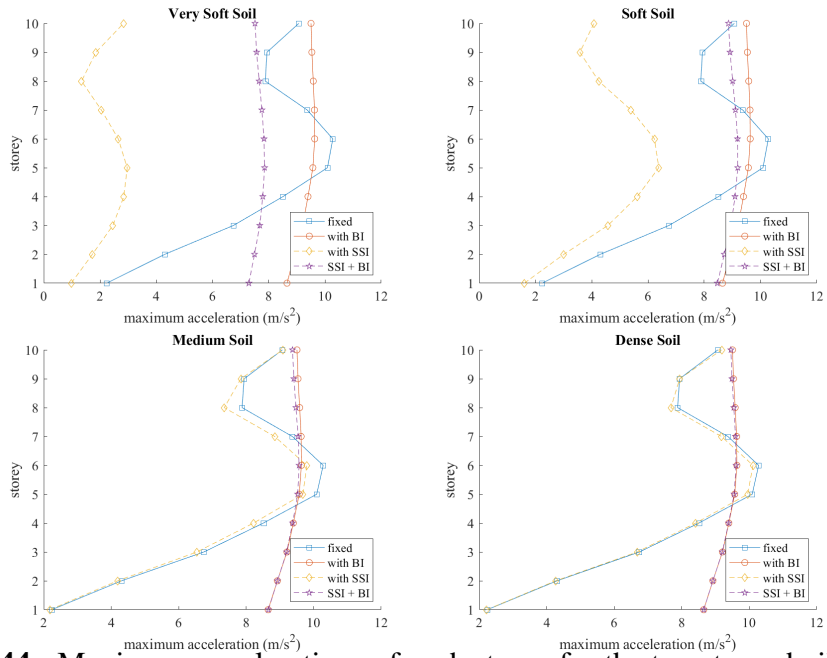

Figure 4.44 : Maximum accelerations of each storey for the ten-storey building(Cape Mendocino, 1992, near fault).

Figure 4.43 shows comparative acceleration-time histories of the five-storey building for each soil type. Figure 4.44 shows maximum acceleration values for each storey.

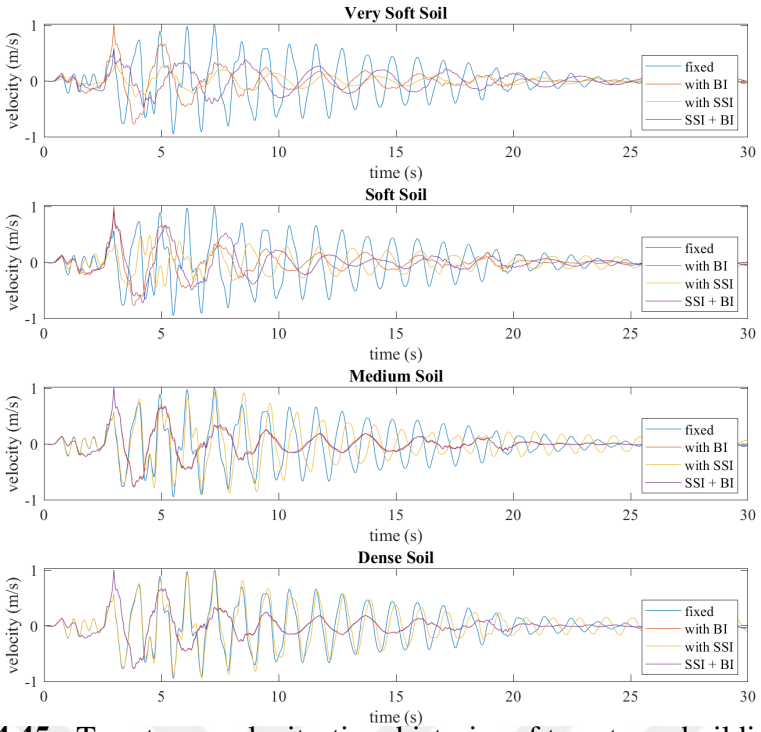

Figure 4.45 : Top storey velocity-time histories of ten-storey building(Cape Mendocino, 1992, near fault).

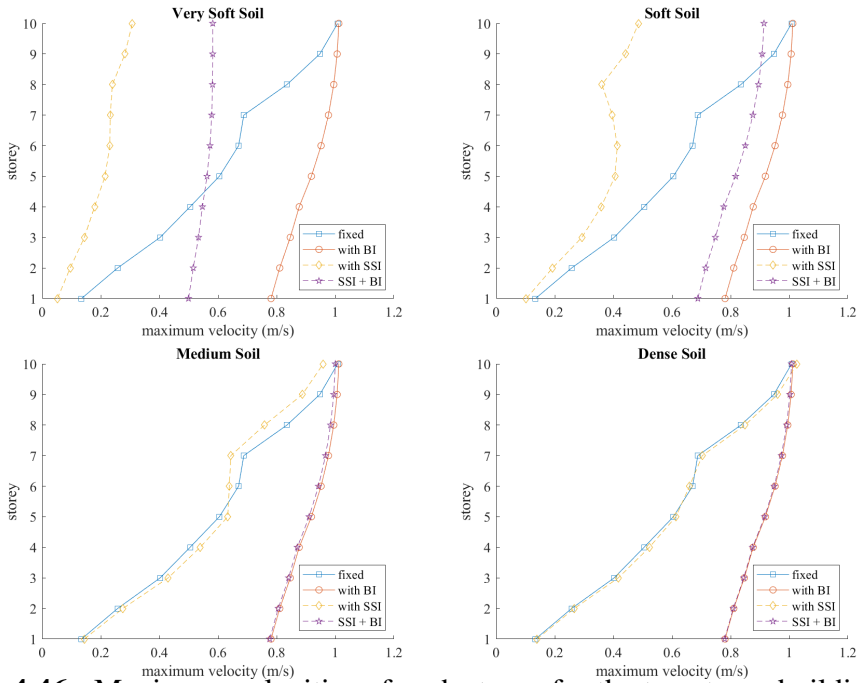

Figure 4.46 : Maximum velocities of each storey for the ten-storey building(Cape Mendocino, 1992, near fault).

Figure 4.45 shows comparative velocity-time histories of the ten-storey building for each soil type. Figure 4.46 shows maximum velocity values for each storey.

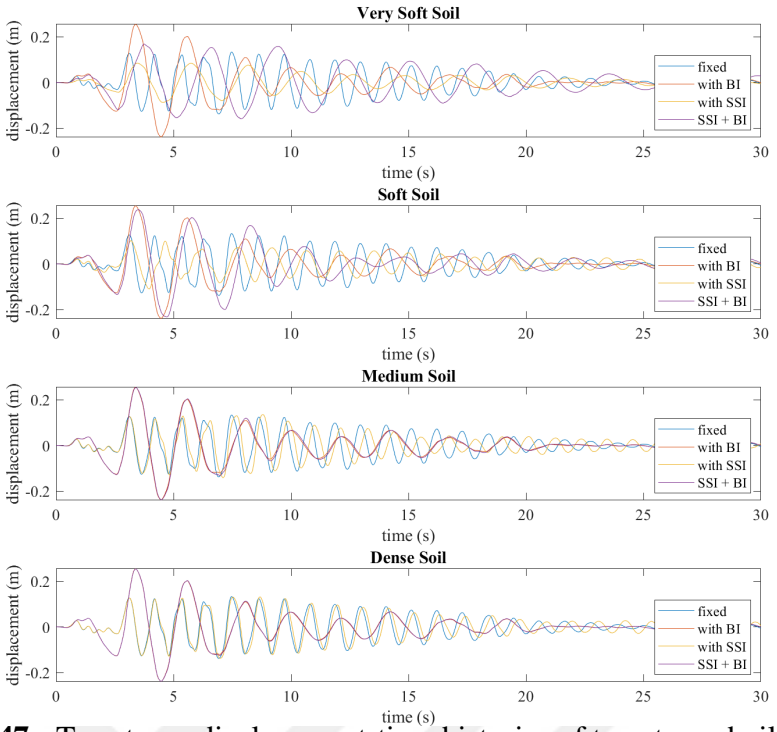

Figure 4.47 : Top storey displacement-time histories of ten-storey building(Cape Mendocino, 1992, near fault).

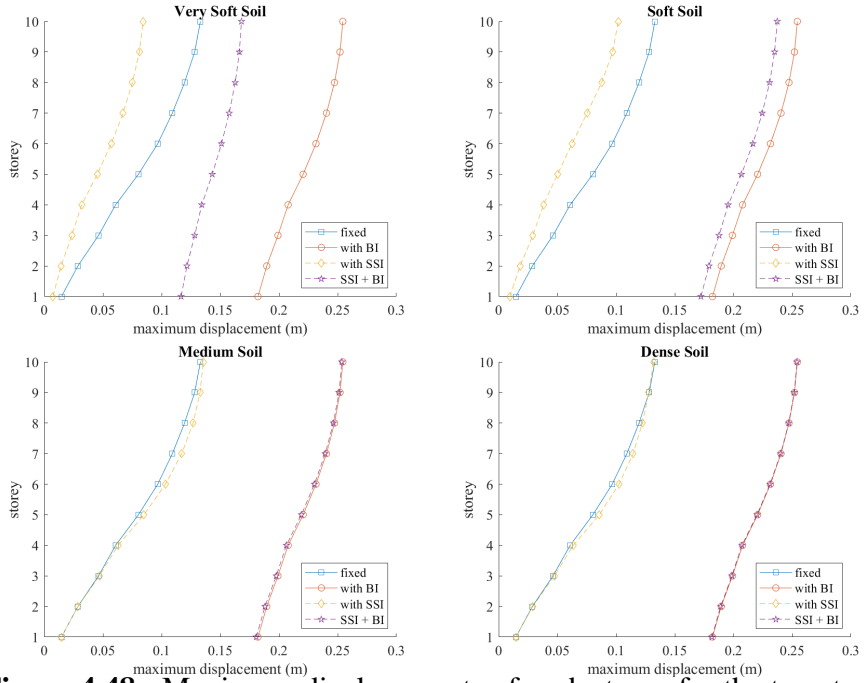

Figure 4.48 : Maximum displacements of each storey for the ten-storey building(Cape Mendocino, 1992, near fault).

Figure 4.47 shows comparative displacement-time histories of the ten-storey building for each soil type. Figure 4.48 shows maximum displacement values for each storey.

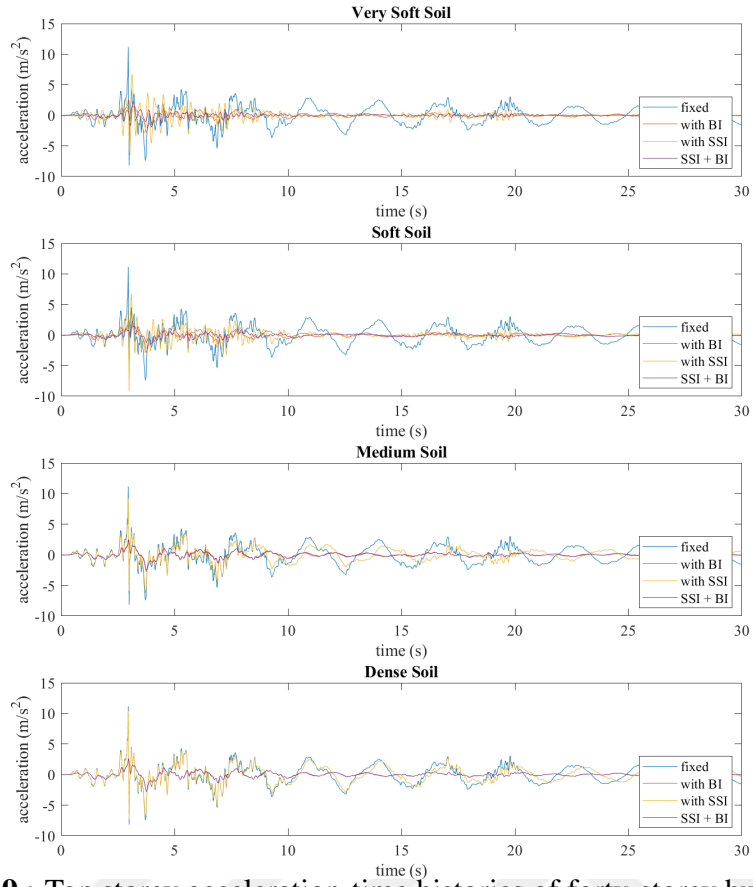

Figure 4.49 : Top storey acceleration-time histories of forty-storey building(Cape Mendocino, 1992, near fault).

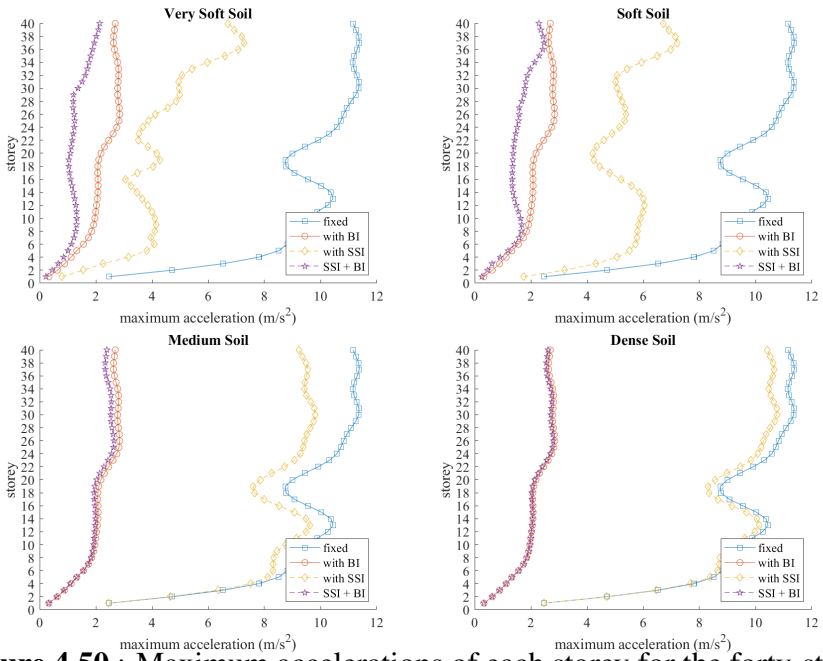

Figure 4.50 : Maximum accelerations of each storey for the forty-storey building(Cape Mendocino, 1992, near fault).

Figure 4.49 shows comparative acceleration-time histories of the forty-storey building for each soil type. Figure 4.50 shows maximum acceleration values for each storey.

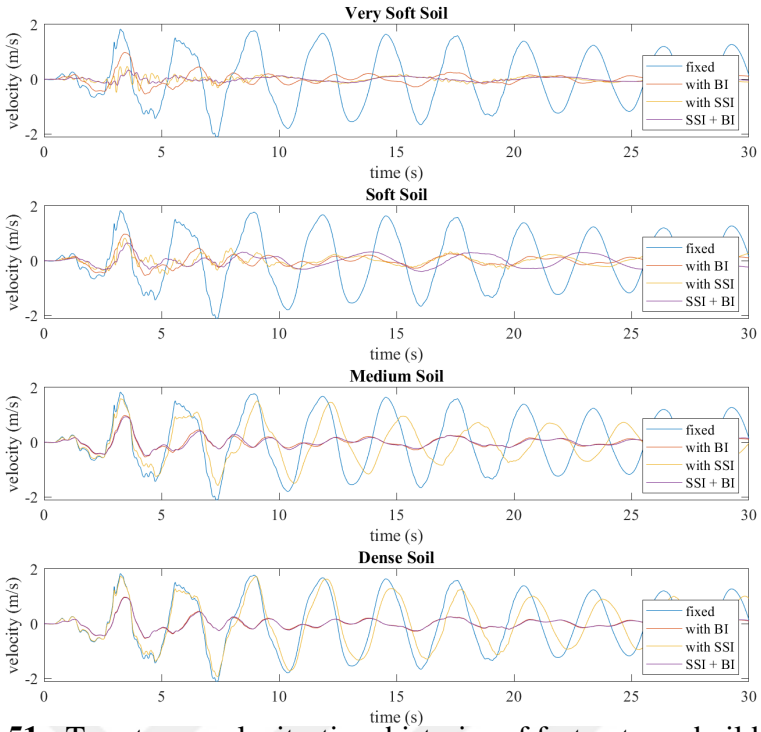

Figure 4.51 : Top storey velocity-time histories of forty-storey building(Cape Mendocino, 1992, near fault).

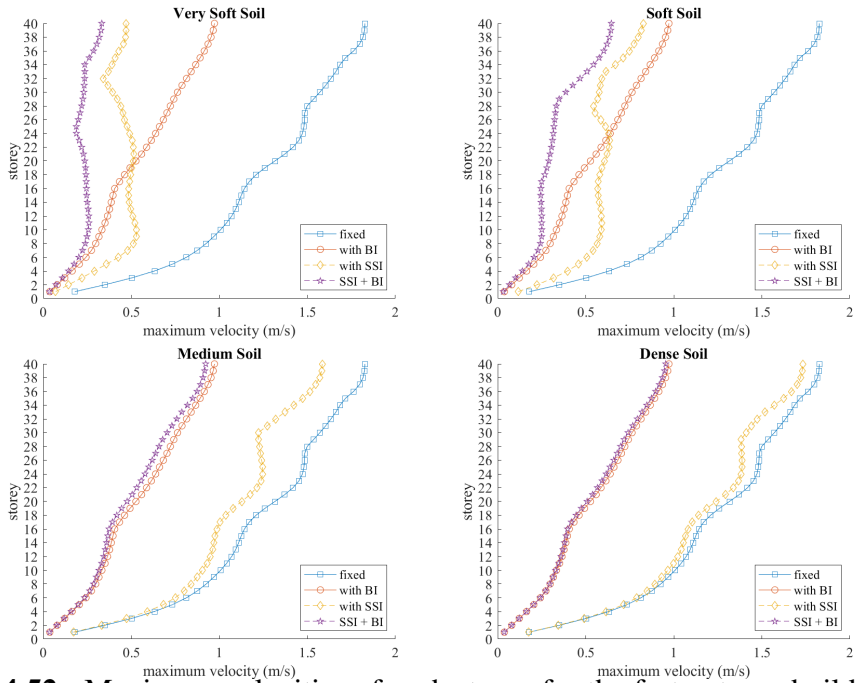

Figure 4.52 : Maximum velocities of each storey for the forty-storey building(Cape Mendocino, 1992, near fault).

Figure 4.51 shows comparative velocity-time histories of the forty-storey building for each soil type. Figure 4.52 shows maximum velocity values for each storey.

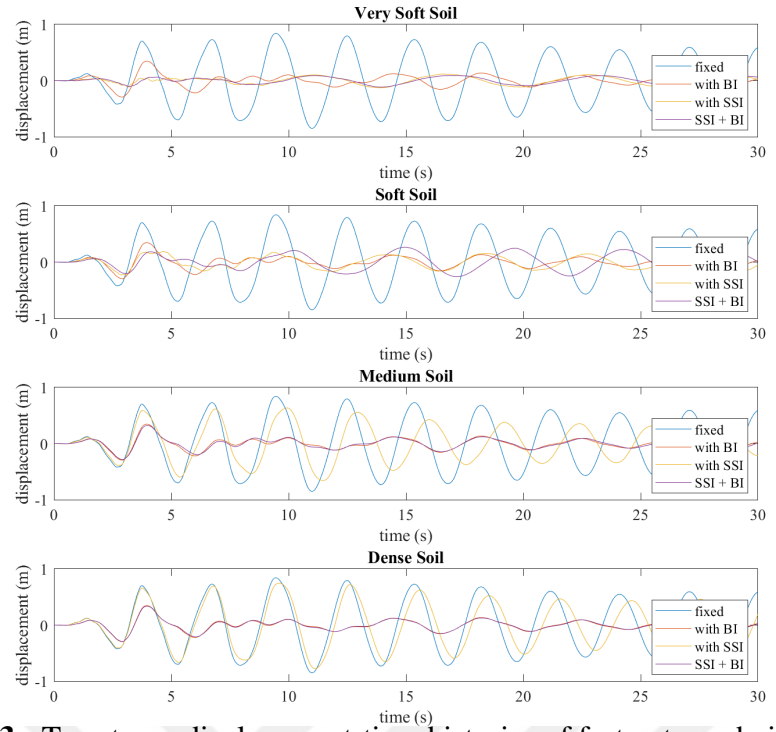

Figure 4.53 : Top storey displacement-time histories of forty-storey building(Cape Mendocino, 1992, near fault).

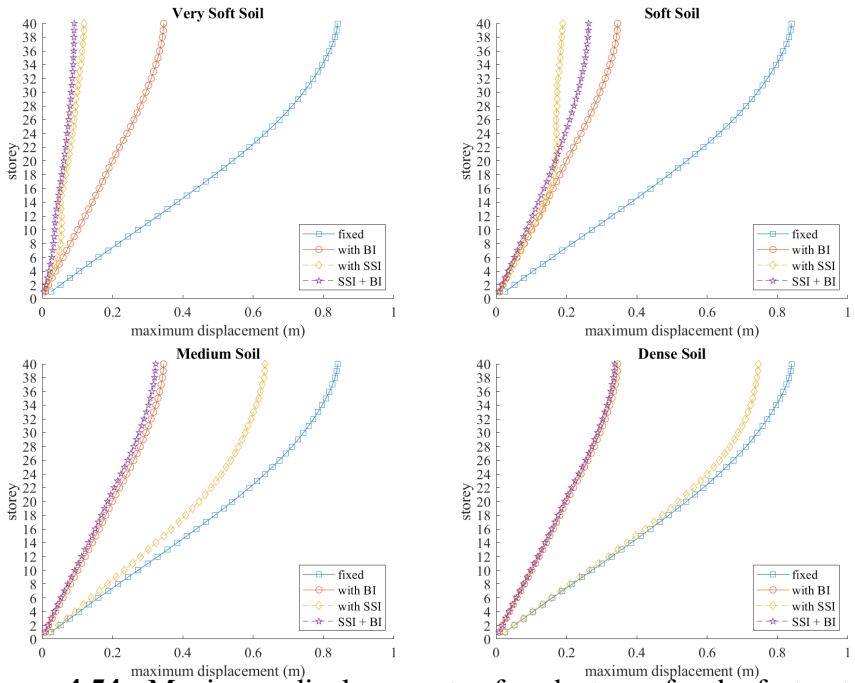

Figure 4.54 : Maximum displacements of each storey for the forty-storey building(Cape Mendocino, 1992, near fault).

Figure 4.53 shows comparative displacement-time histories of the forty-storey building for each soil type. Figure 4.54 shows maximum displacement values for each storey.

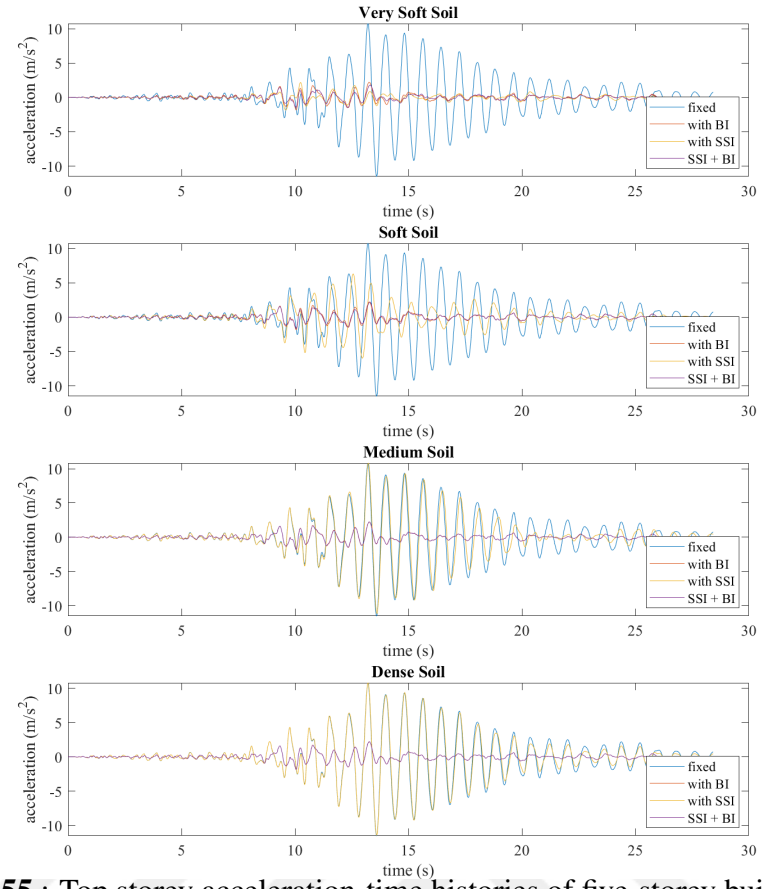

Figure 4.55 : Top storey acceleration-time histories of five-storey building(Cape Mendocino, 1992, far fault).

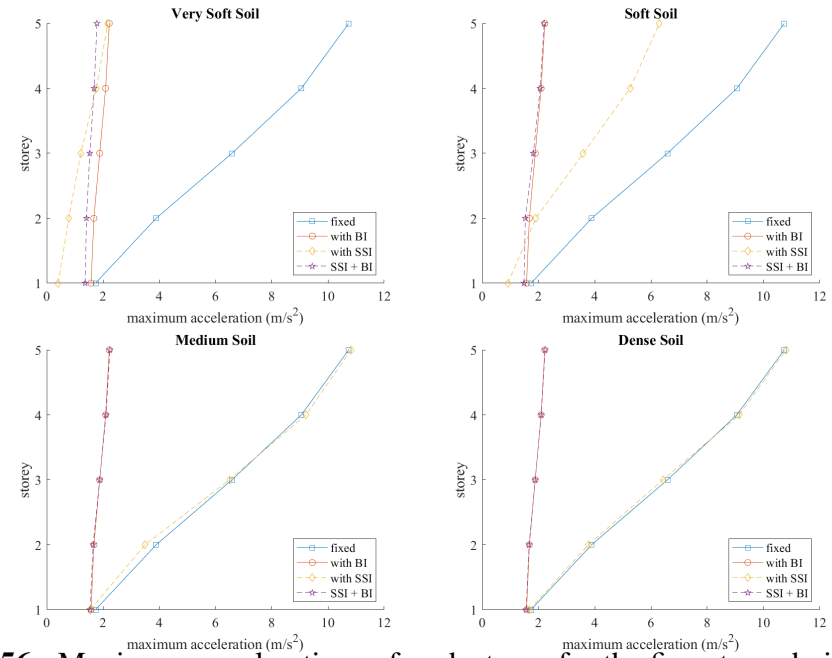

Figure 4.56 : Maximum accelerations of each storey for the five-storey building(Cape Mendocino, 1992, far fault).

Figure 4.55 shows comparative acceleration-time histories of the five-storey building for each soil type. Figure 4.56 shows maximum acceleration values for each storey.

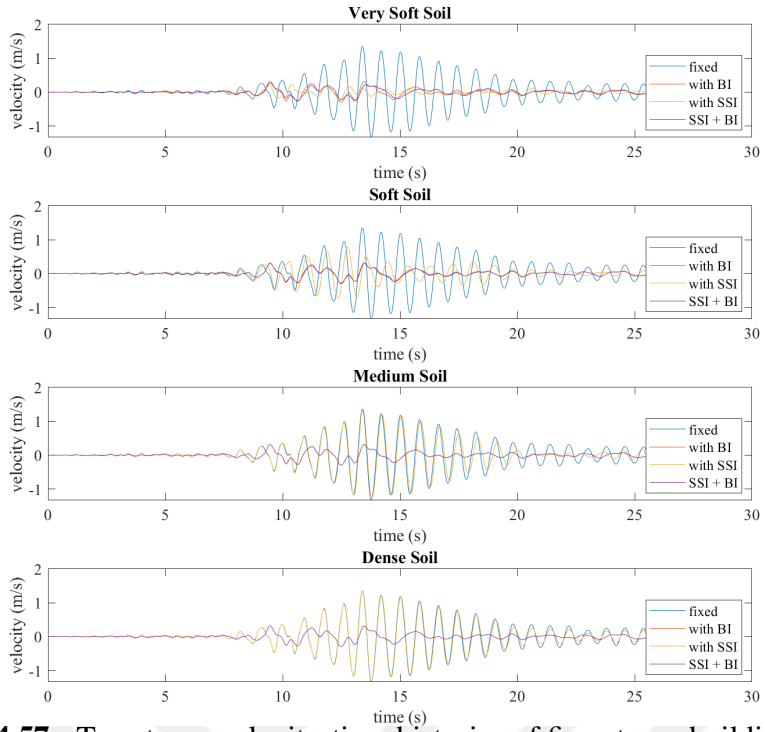

Figure 4.57 : Top storey velocity-time histories of five-storey building(Cape Mendocino, 1992, far fault).

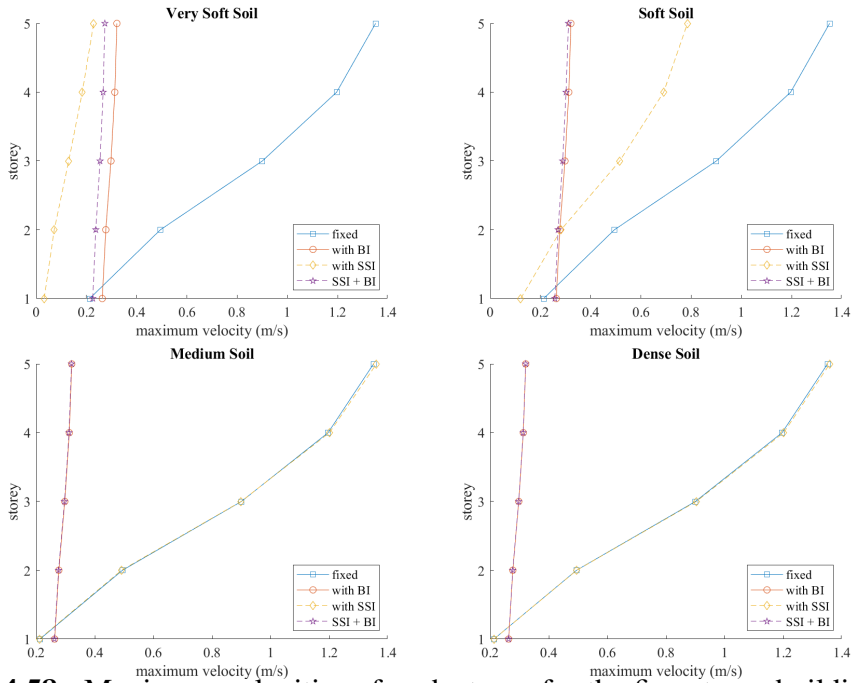

Figure 4.58 : Maximum velocities of each storey for the five-storey building(Cape Mendocino, 1992, far fault).

Figure 4.57 shows comparative velocity-time histories of the five-storey building for each soil type. Figure 4.58 shows maximum velocity values for each storey.

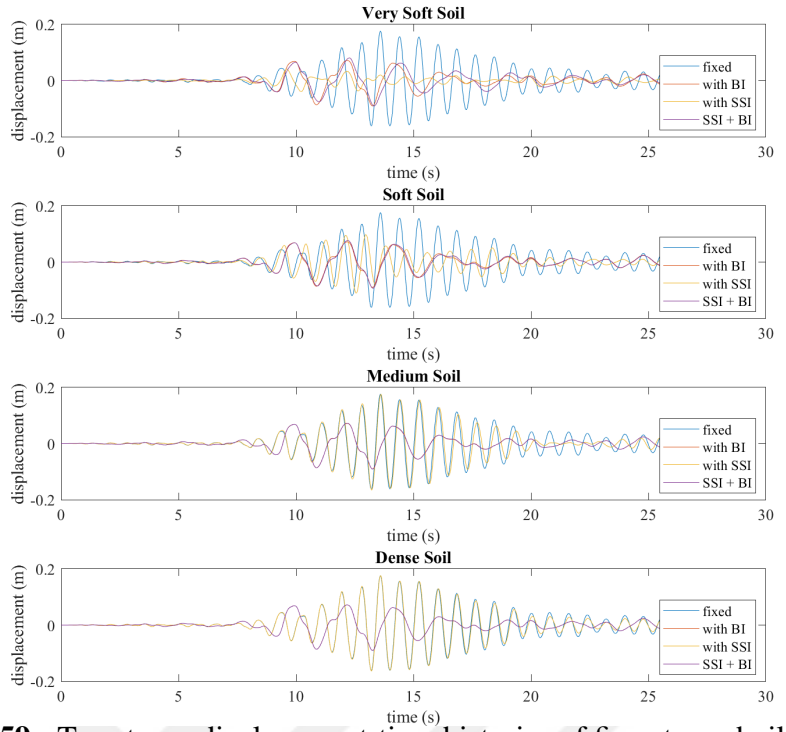

Figure 4.59 : Top storey displacement-time histories of five-storey building(Cape Mendocino, 1992, far fault).

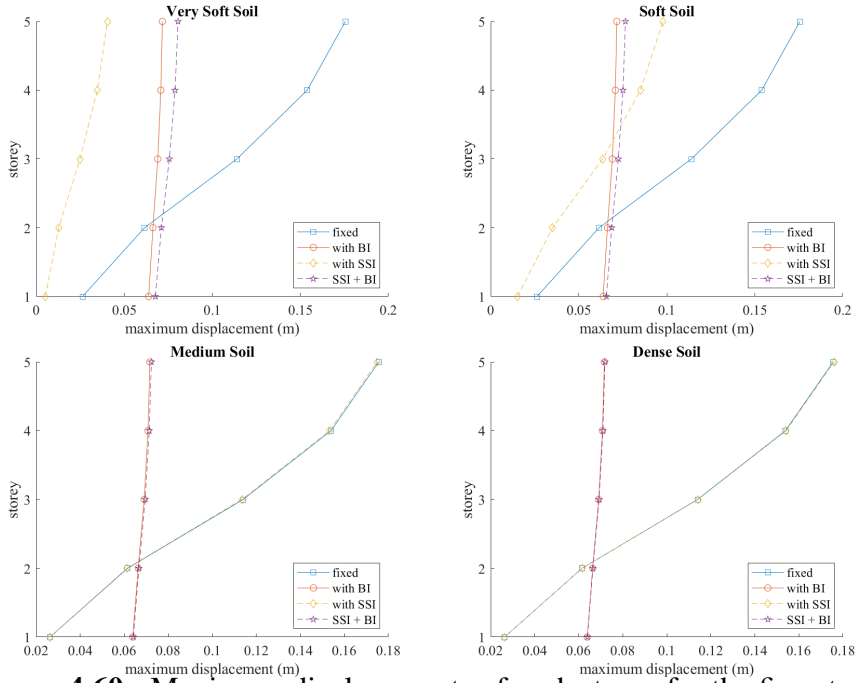

Figure 4.60 : Maximum displacements of each storey for the five-storey building(Cape Mendocino, 1992, far fault).

Figure 4.59 shows comparative displacement-time histories of the five-storey building for each soil type. Figure 4.60 shows maximum displacement values for each storey.

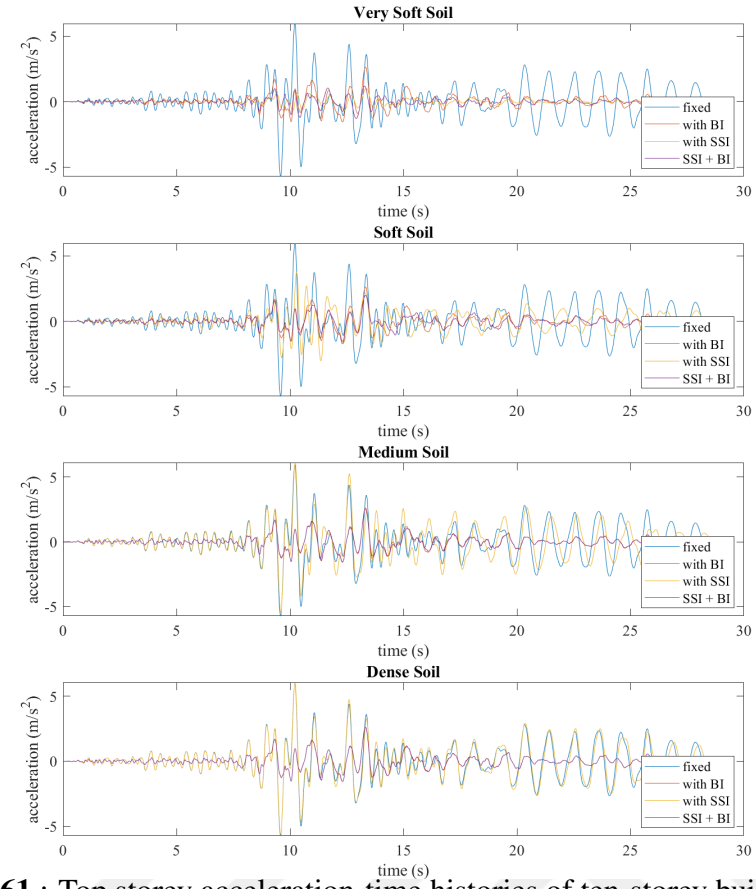

Figure 4.61 : Top storey acceleration-time histories of ten-storey building(Cape Mendocino, 1992, far fault).

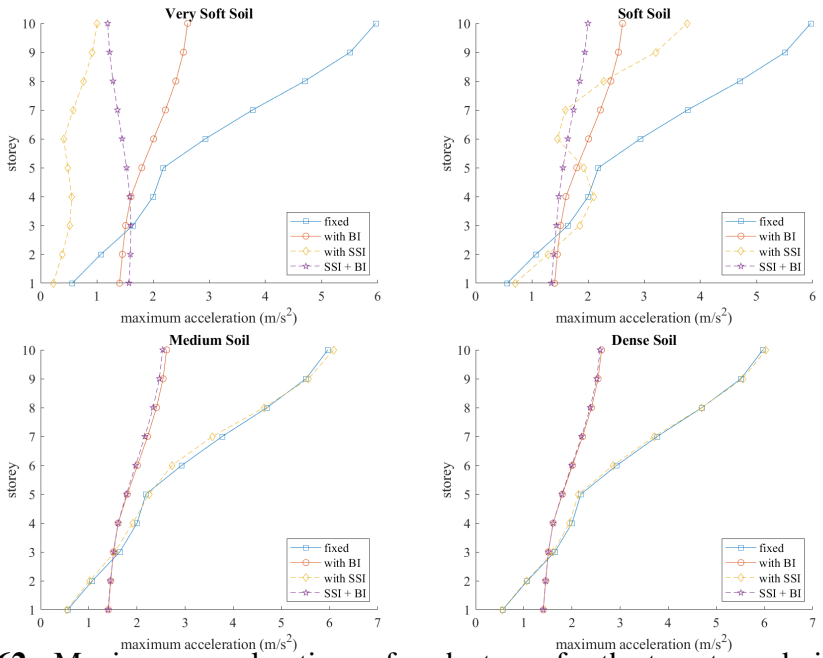

Figure 4.62 : Maximum accelerations of each storey for the ten-storey building(Cape Mendocino, 1992, far fault).

Figure 4.61 shows comparative acceleration-time histories of the ten-storey building for each soil type. Figure 4.62 shows maximum acceleration values for each storey.

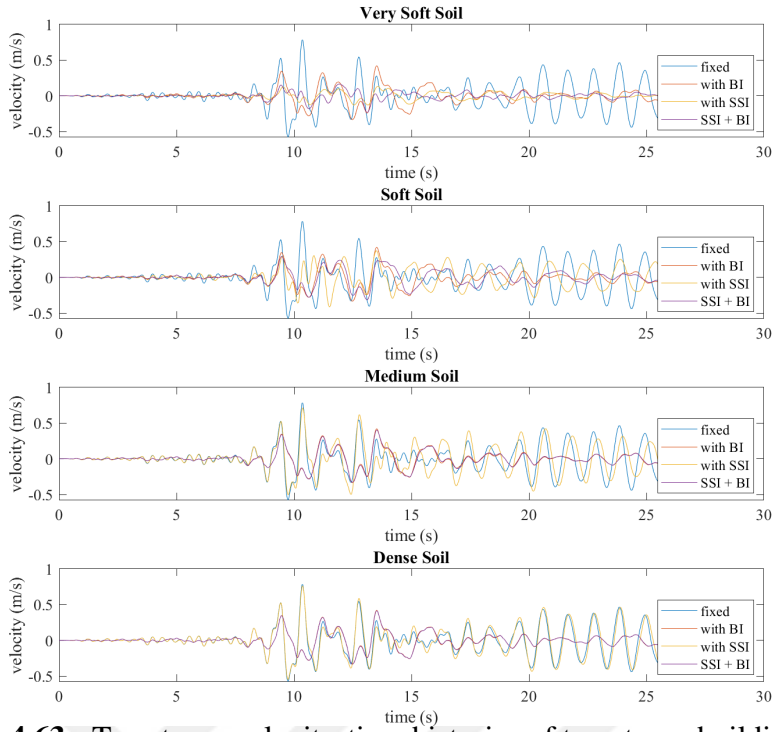

Figure 4.63 : Top storey velocity-time histories of ten-storey building(Cape Mendocino, 1992, far fault).

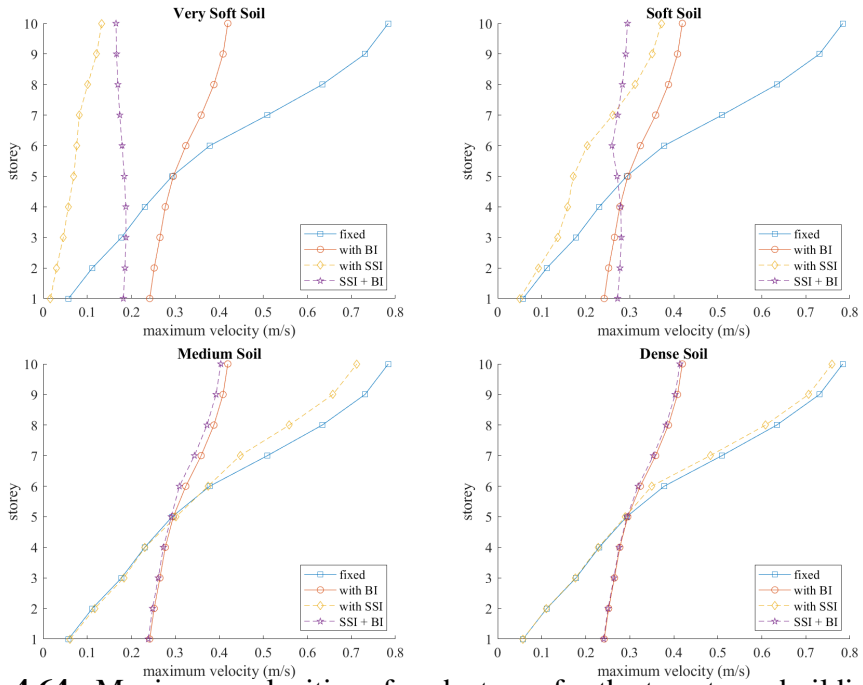

Figure 4.64 : Maximum velocities of each storey for the ten-storey building(Cape Mendocino, 1992, far fault).

Figure 4.63 shows comparative velocity-time histories of the ten-storey building for each soil type. Figure 4.64 shows maximum velocity values for each storey.

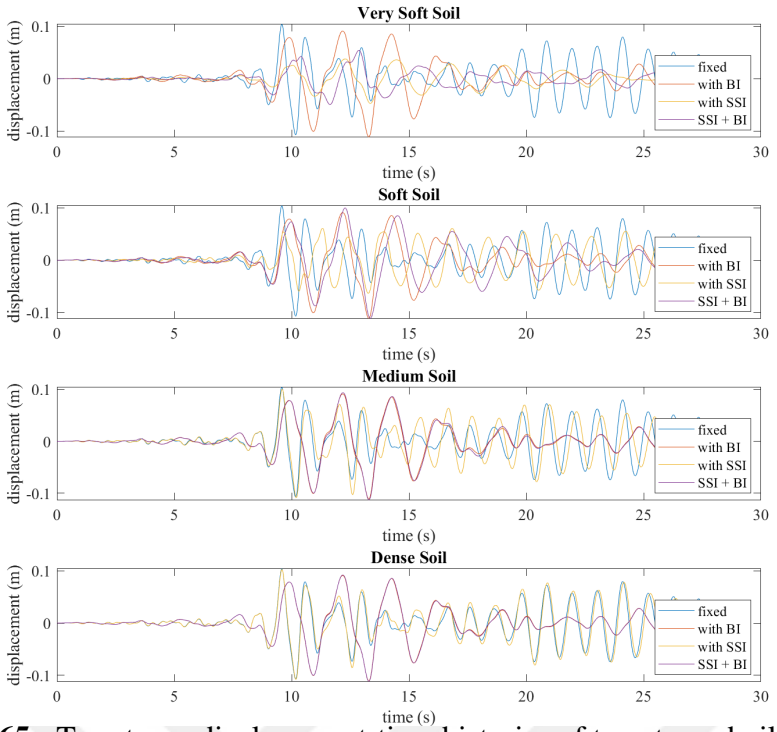

Figure 4.65 : Top storey displacement-time histories of ten-storey building(Cape Mendocino, 1992, far fault).

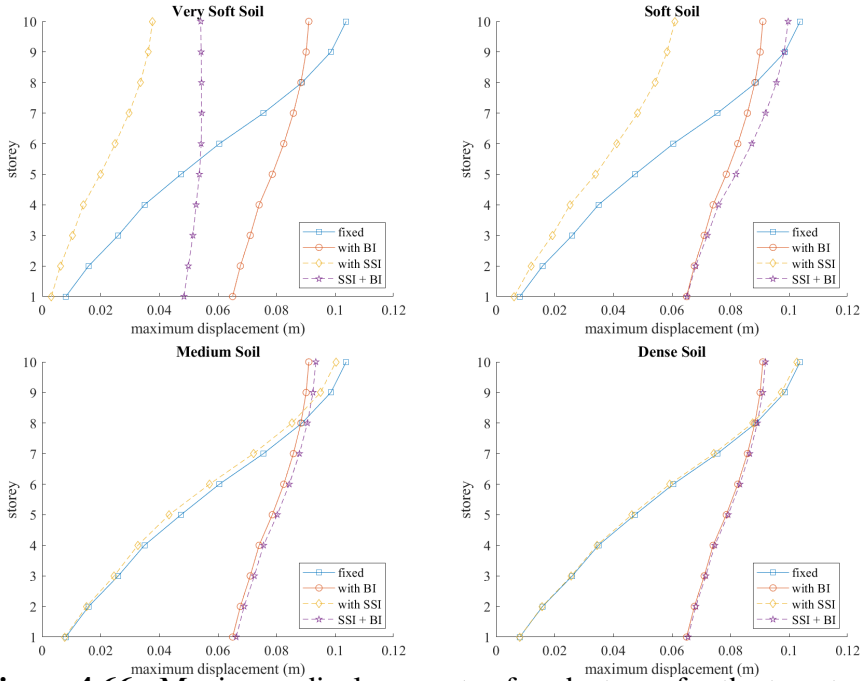

Figure 4.66 : Maximum displacements of each storey for the ten-storey building(Cape Mendocino, 1992, far fault).

Figure 4.65 shows comparative displacement-time histories of the ten-storey building for each soil type. Figure 4.66 shows maximum displacement values for each storey.

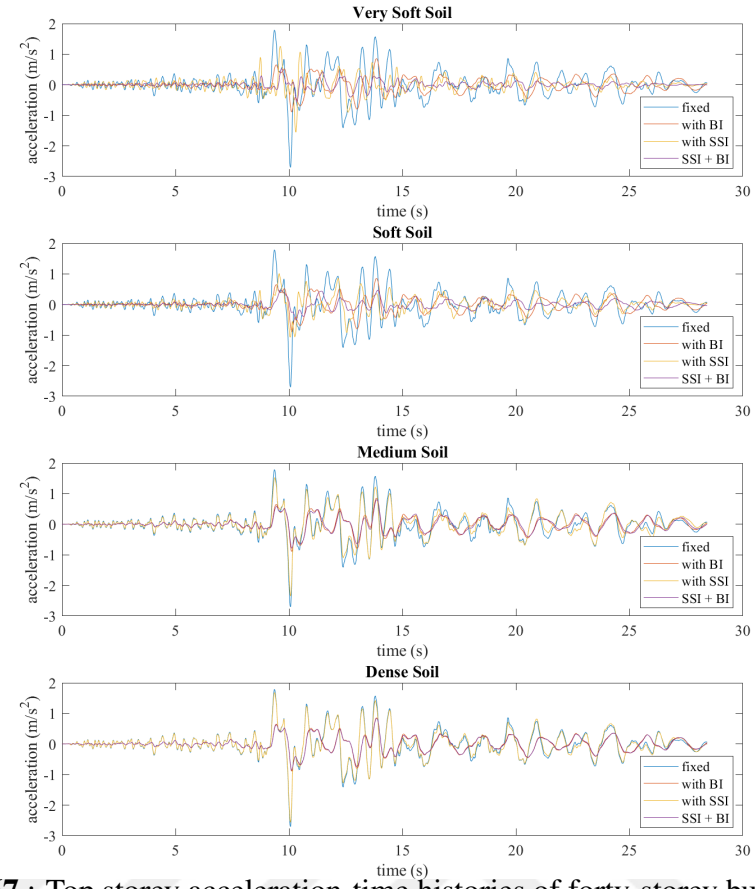

Figure 4.67 : Top storey acceleration-time histories of forty-storey building(Cape Mendocino, 1992, far fault).

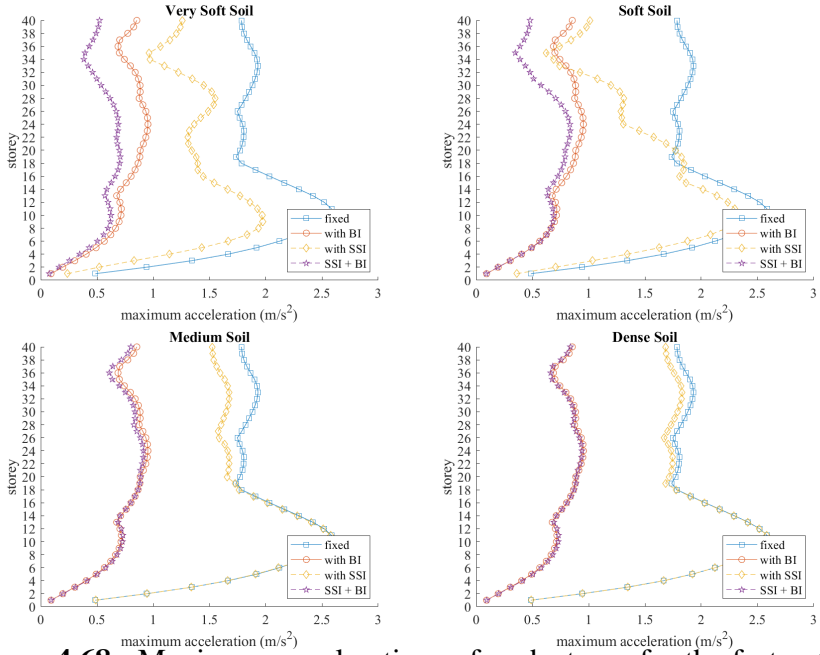

Figure 4.68 : Maximum accelerations of each storey for the forty-storey building(Cape Mendocino, 1992, far fault).

Figure 4.67 shows comparative acceleration-time histories of the forty-storey building for each soil type. Figure 4.68 shows maximum acceleration values for each storey.

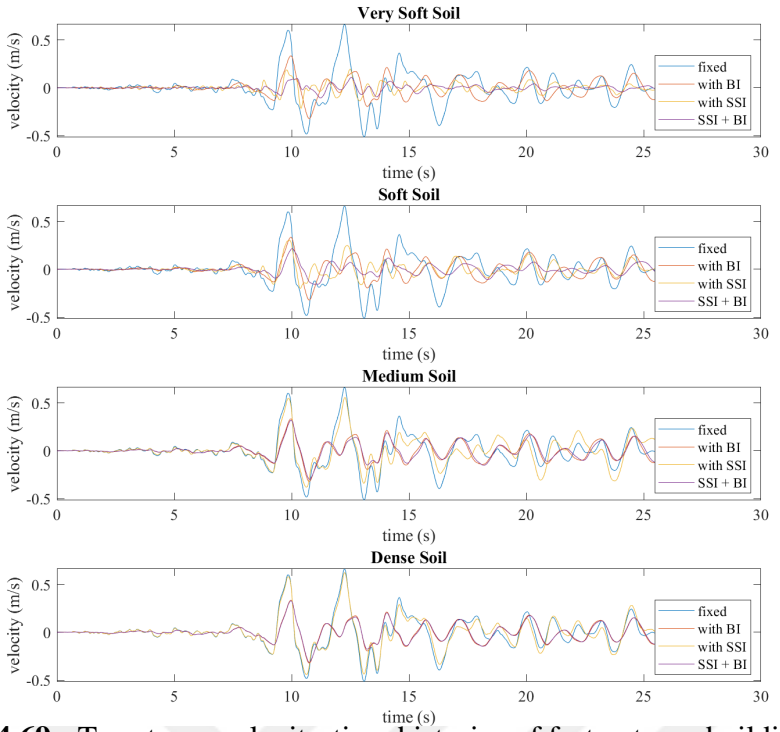

Figure 4.69 : Top storey velocity-time histories of forty-storey building(Cape Mendocino, 1992, far fault).

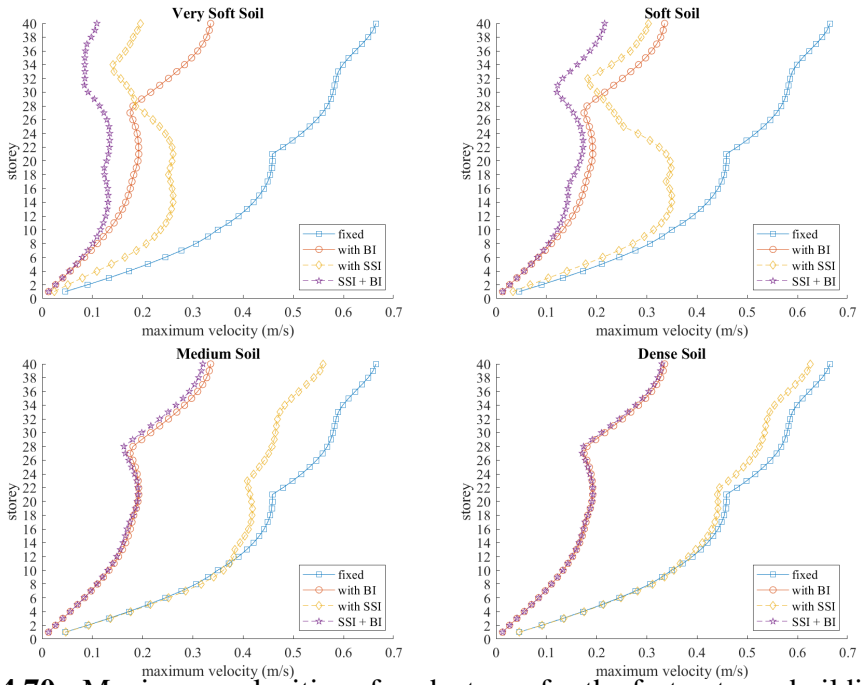

Figure 4.70 : Maximum velocities of each storey for the forty-storey building(Cape Mendocino, 1992, far fault).

Figure 4.69 shows comparative velocity-time histories of the forty-storey building for each soil type. Figure 4.70 shows maximum velocity values for each storey.

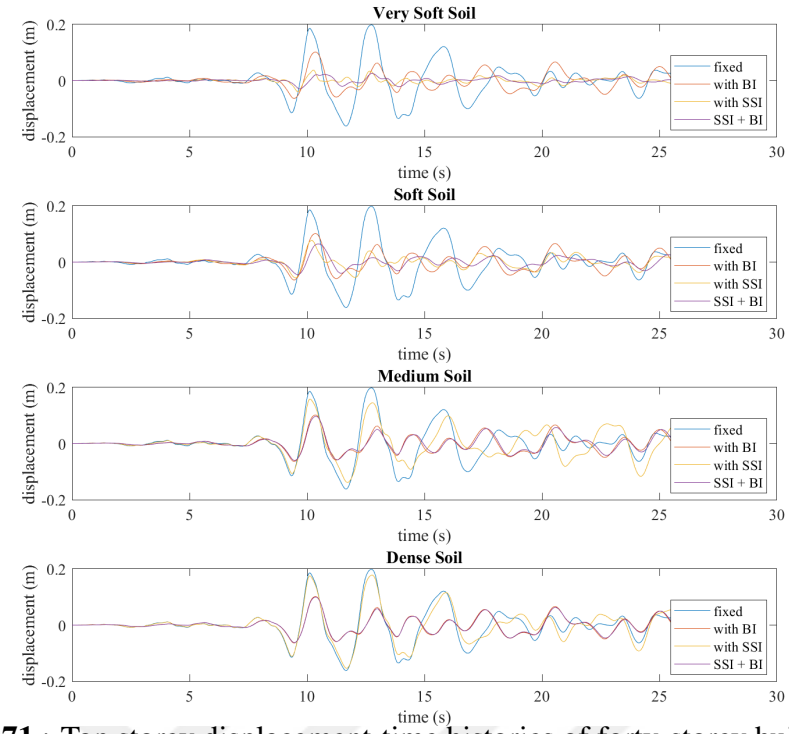

Figure 4.71 : Top storey displacement-time histories of forty-storey building(Cape Mendocino, 1992, far fault).

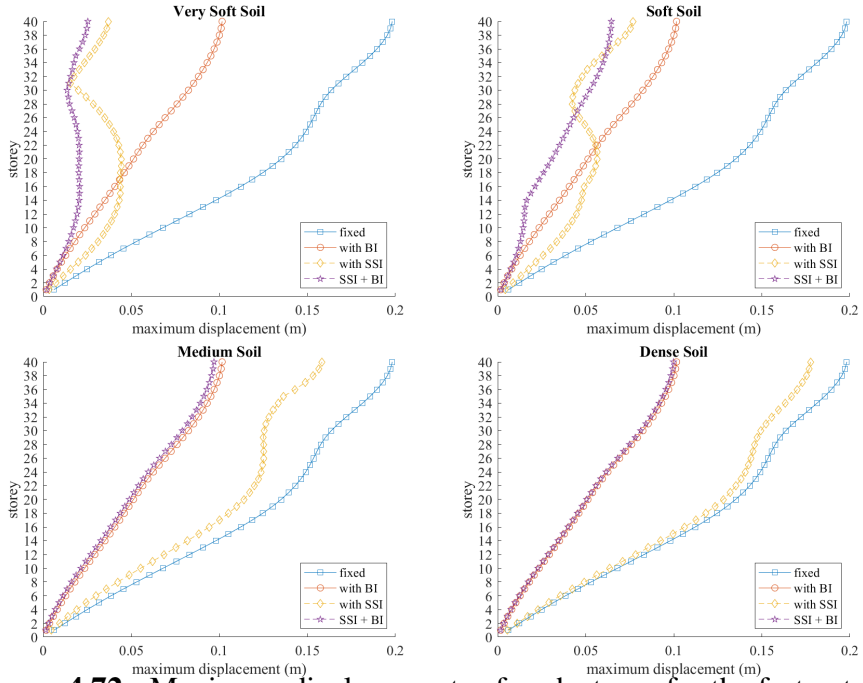

Figure 4.72 : Maximum displacements of each storey for the forty-storey building(Cape Mendocino, 1992, far fault).

Figure 4.71 shows comparative displacement-time histories of the forty-storey building for each soil type. Figure 4.72 shows maximum displacement values for each storey.

The 1999 Kocaeli earthquake results are shown in figures 4.73 to 4.108. The acceleration results show us that for five to forty storey buildings implementing base isolation to the structure reduces responses significantly for all soil conditions. It can also be mentioned that SSI reduces the acceleration values, but these effects are only pronounced in softer soil conditions. In very soft soil conditions, SSI effects can be observed clearly, but moving towards denser soil, effects disappear and structures behave like they are fixed based. These effects can be seen by comparing figures 4.74, 4.80, 4.86, 4.92, 4.98 and 4.104.

Looking at the velocity results for five, ten and forty storey buildings results are almost identical with acceleration results; base isolation reduces responses significantly. It can also be said that SSI reduces the velocity values, but again, these effects are only related to softer soil conditions. In very soft soil conditions, SSI effects can be observed clearly, but moving towards denser soil, effects disappear and structures behave like they are fixed based. These findings are derived from figures 4.76, 4.82, 4.88, 4.94, 4.100 and 4.106.

Considering the displacement results for five, ten and forty storey buildings; although base isolated displacements might be higher than fixed cases, large displacements occur at base isolation layer, providing low inter-storey displacements and structures behave linearly. It can also be stated that SSI reduces the displacement values, like in previous results, these effects are only occurring in softer soil conditions. In very soft soil conditions, SSI effects can be observed clearly, but moving towards denser soil, these impacts fade and structures behave like they are fixed based. These effects can be seen by comparing figures 4.78, 4.84, 4.90, 4.96, 4.102 and 4.108.

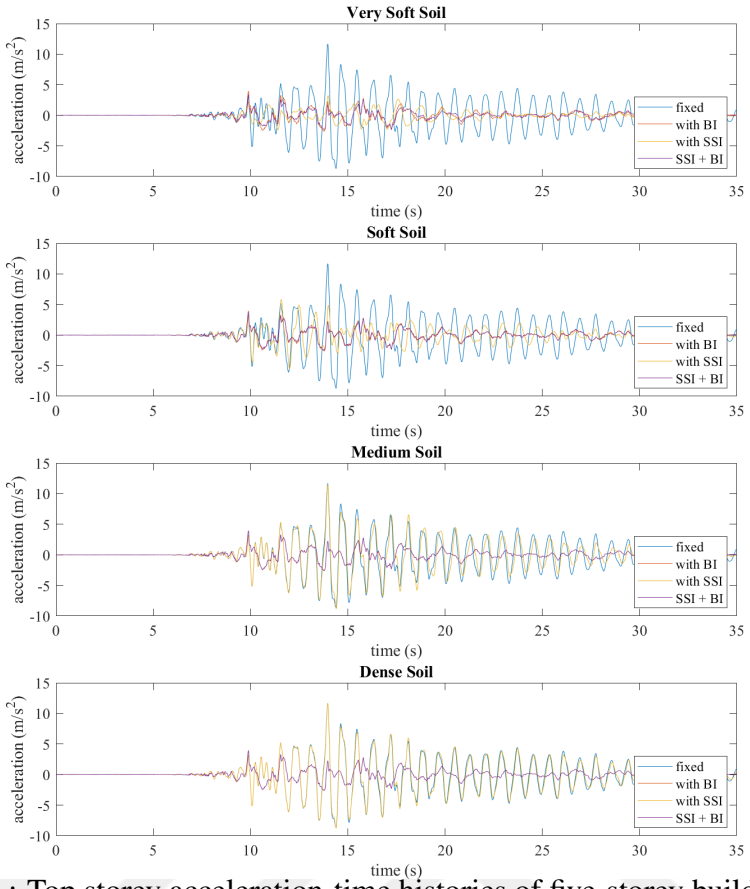

Figure 4.73 : Top storey acceleration-time histories of five-storey building(Kocaeli, 1999, near fault).

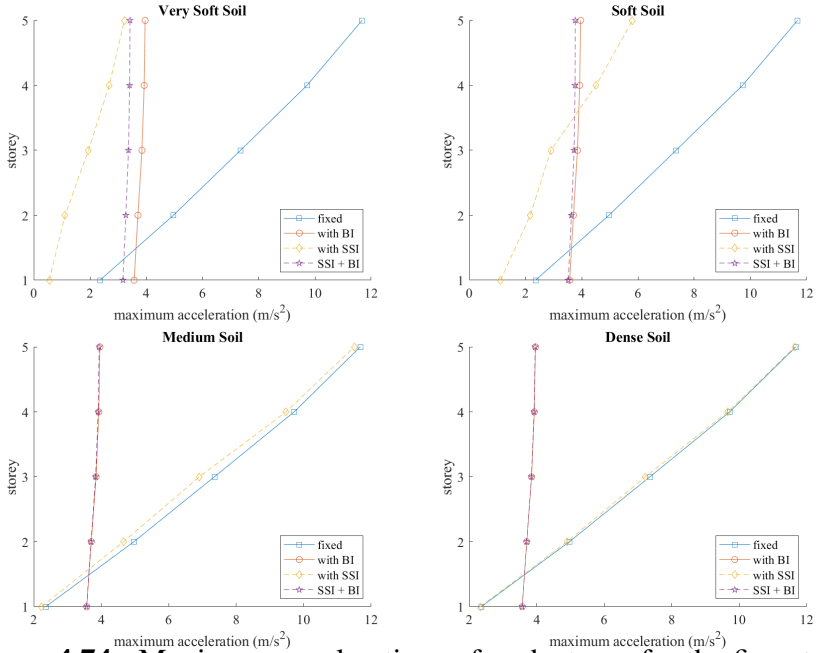

Figure 4.74 : Maximum accelerations of each storey for the five-storey building(Kocaeli, 1999, near fault).

Figure 4.73 shows comparative acceleration-time histories of the five-storey building for each soil type. Figure 4.74 shows maximum acceleration values for each storey.

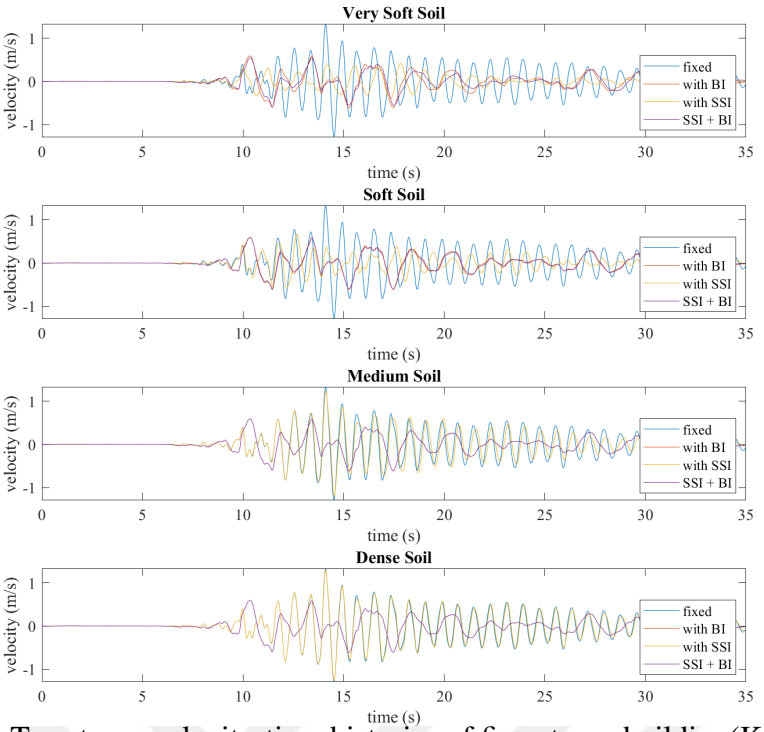

Figure 4.75 : Top storey velocity-time histories of five-storey building(Kocaeli, 1999, near fault).

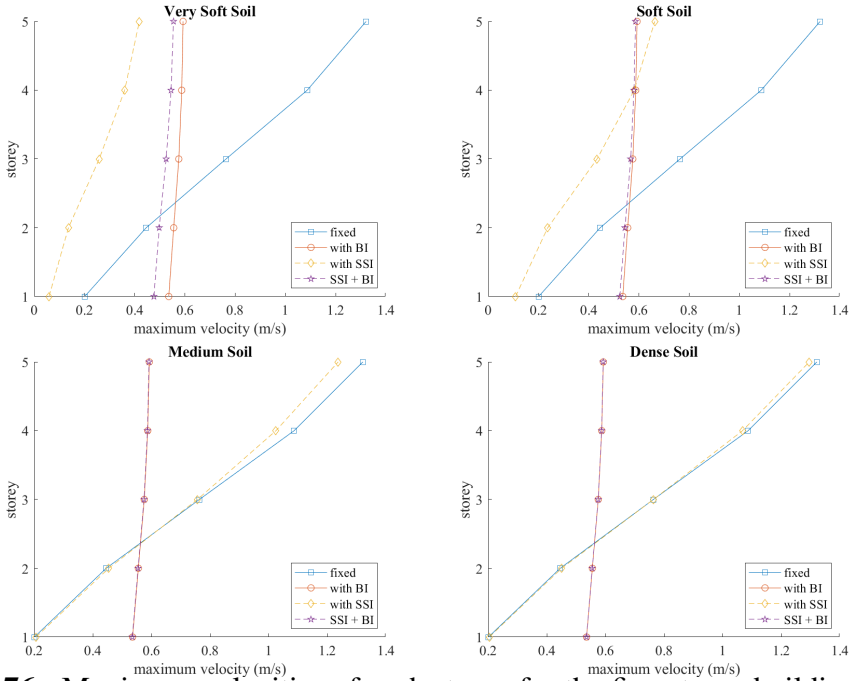

Figure 4.76 : Maximum velocities of each storey for the five-storey building(Kocaeli, 1999, near fault).

Figure 4.75 shows comparative velocity-time histories of the five-storey building for each soil type. Figure 4.76 shows maximum velocity values for each storey.

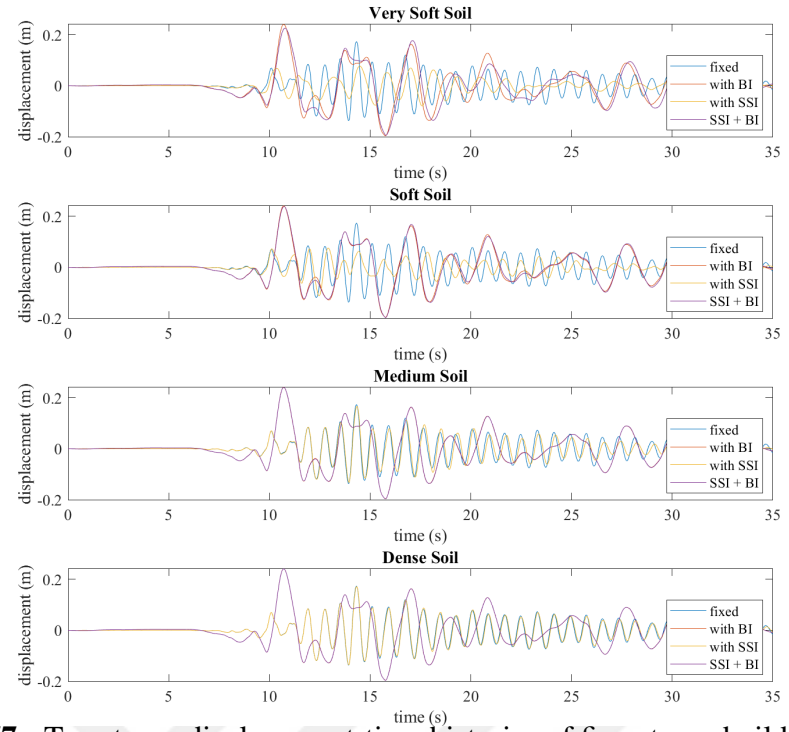

Figure 4.77 : Top storey displacement-time histories of five-storey building(Kocaeli, 1999, near fault).

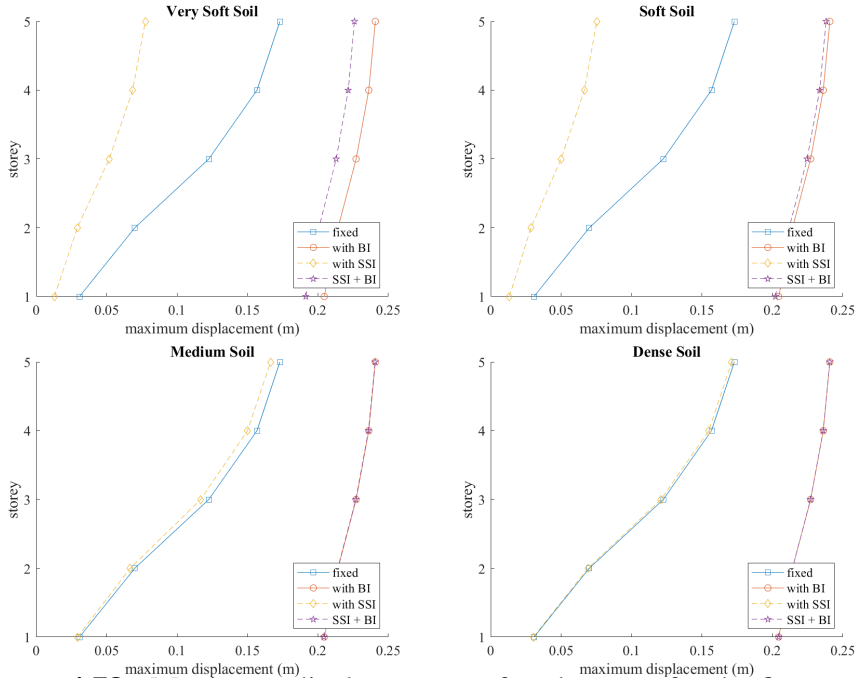

Figure 4.78 : Maximum displacements of each storey for the five-storey building(Kocaeli, 1999, near fault).

Figure 4.77 shows comparative displacement-time histories of the five-storey building for each soil type. Figure 4.78 shows maximum displacement values for each storey.

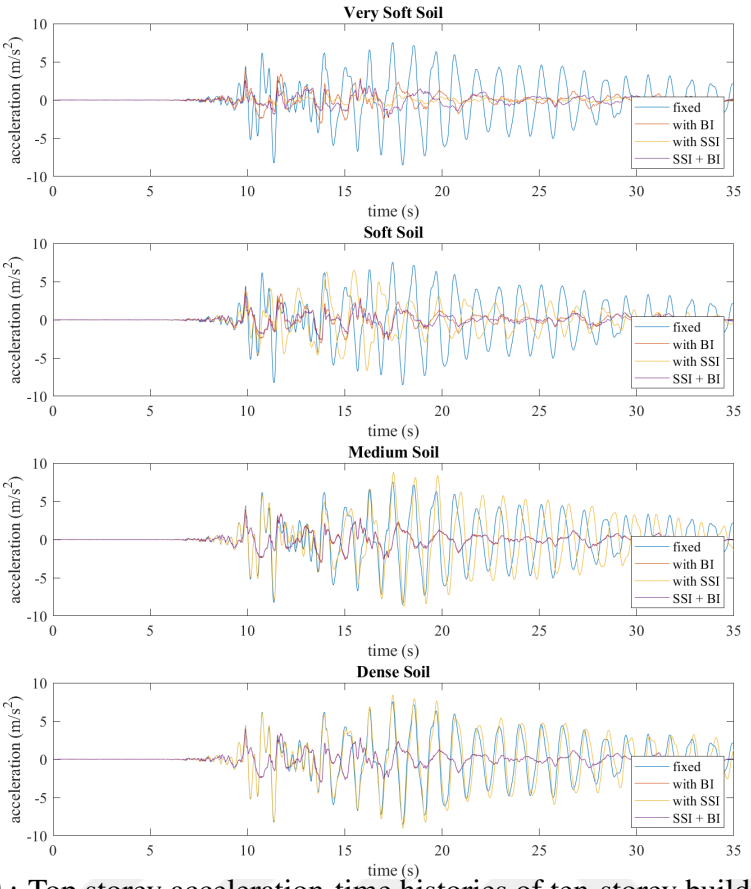

Figure 4.79 : Top storey acceleration-time histories of ten-storey building(Kocaeli, 1999, near fault).

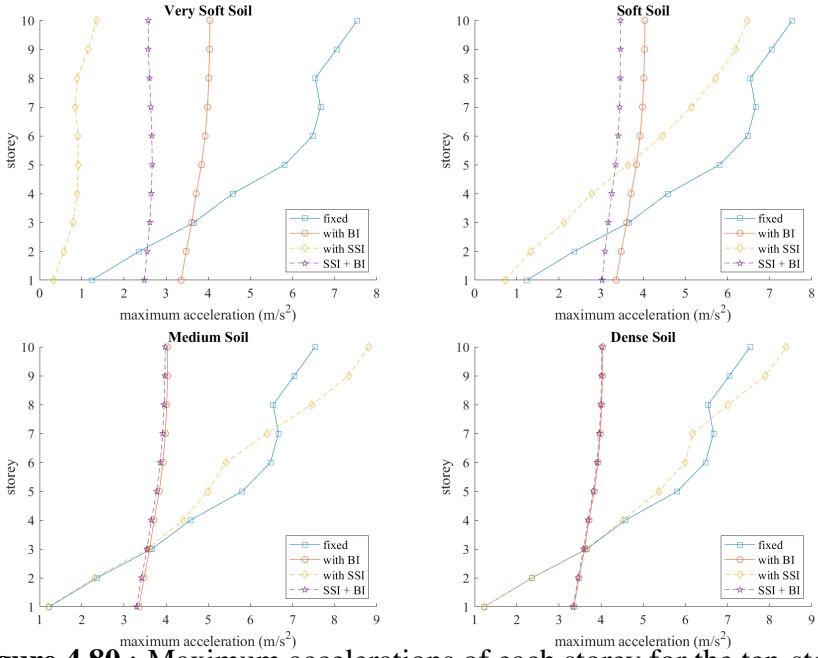

Figure 4.80 : Maximum accelerations of each storey for the ten-storey building(Kocaeli, 1999, near fault).

Figure 4.79 shows comparative acceleration-time histories of the five-storey building for each soil type. Figure 4.80 shows maximum acceleration values for each storey.

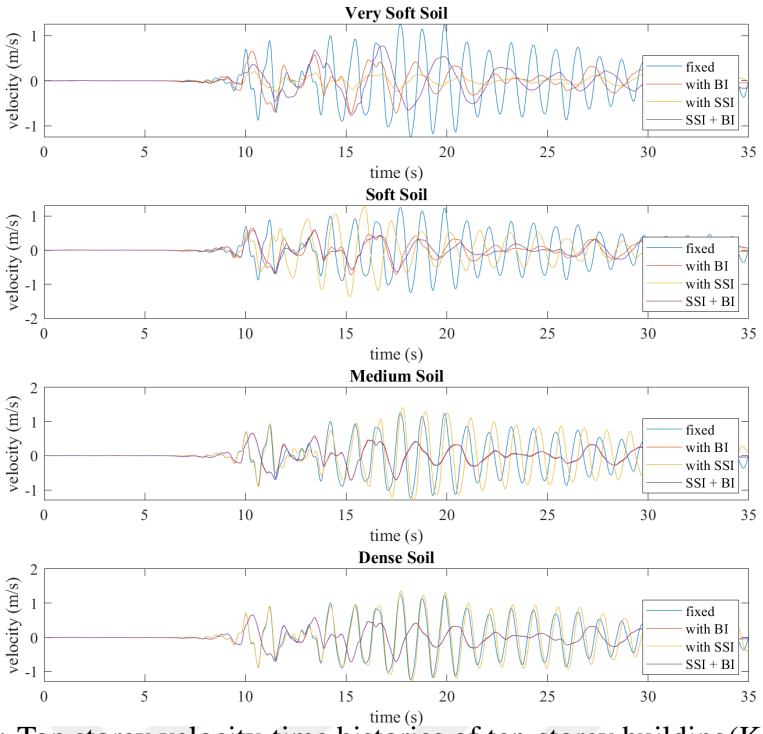

Figure 4.81 : Top storey velocity-time histories of ten-storey building(Kocaeli, 1999, near fault).

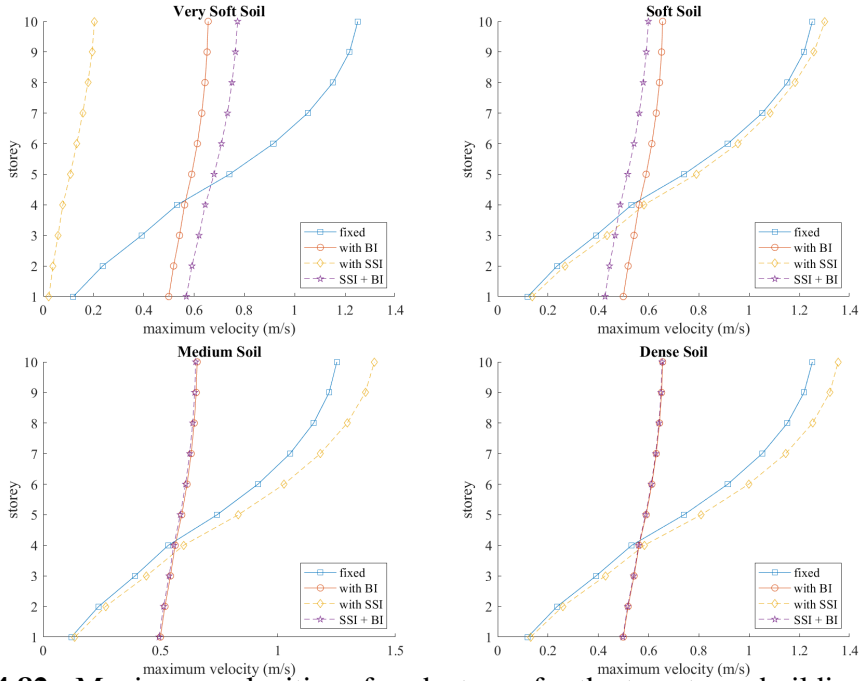

Figure 4.82 : Maximum velocities of each storey for the ten-storey building(Kocaeli, 1999, near fault).

Figure 4.81 shows comparative velocity-time histories of the ten-storey building for each soil type. Figure 4.82 shows maximum velocity values for each storey.

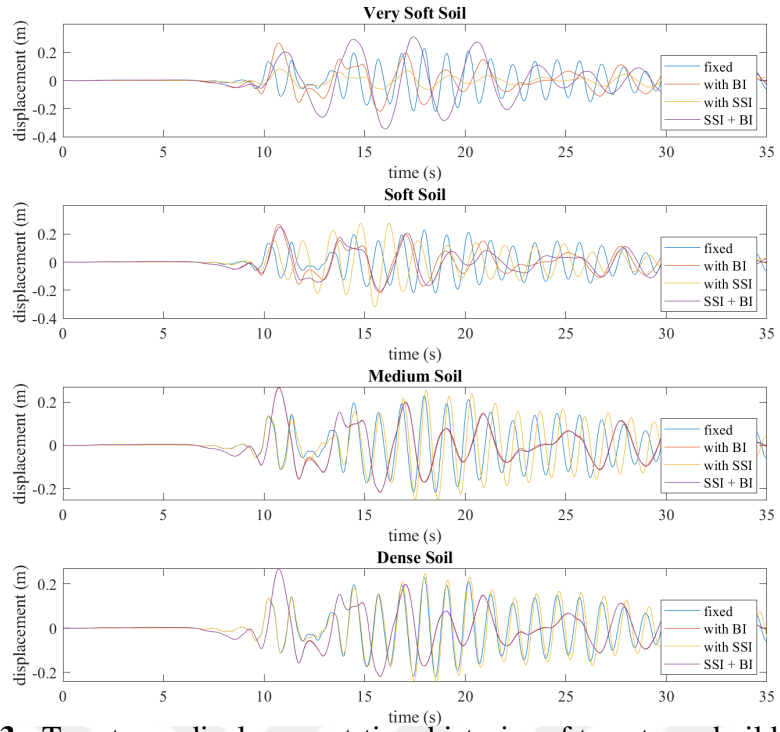

Figure 4.83 : Top storey displacement-time histories of ten-storey building(Kocaeli, 1999, near fault).

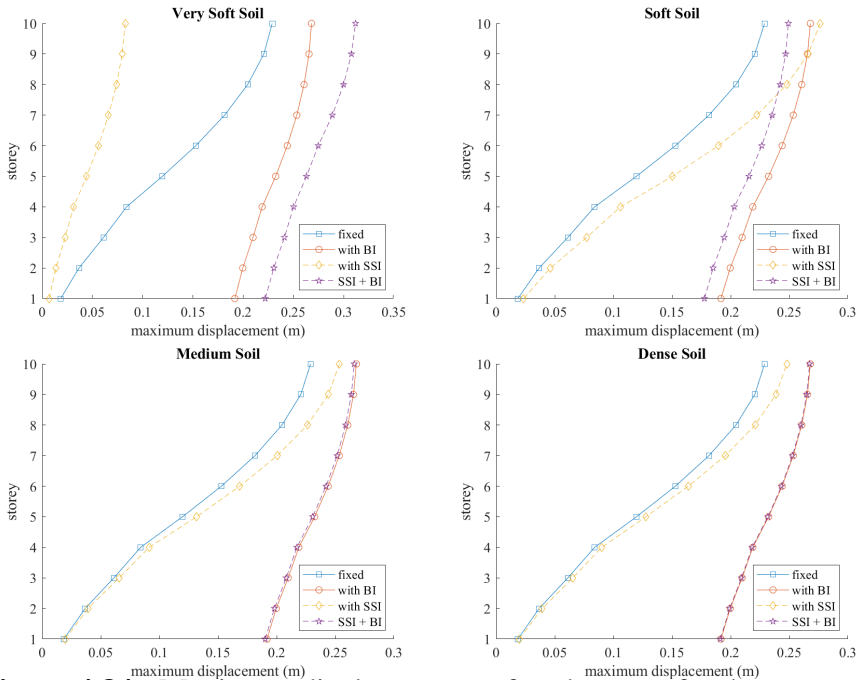

Figure 4.84 : Maximum displacements of each storey for the ten-storey building(Kocaeli, 1999, near fault).

Figure 4.83 shows comparative displacement-time histories of the ten-storey building for each soil type. Figure 4.84 shows maximum displacement values for each storey.

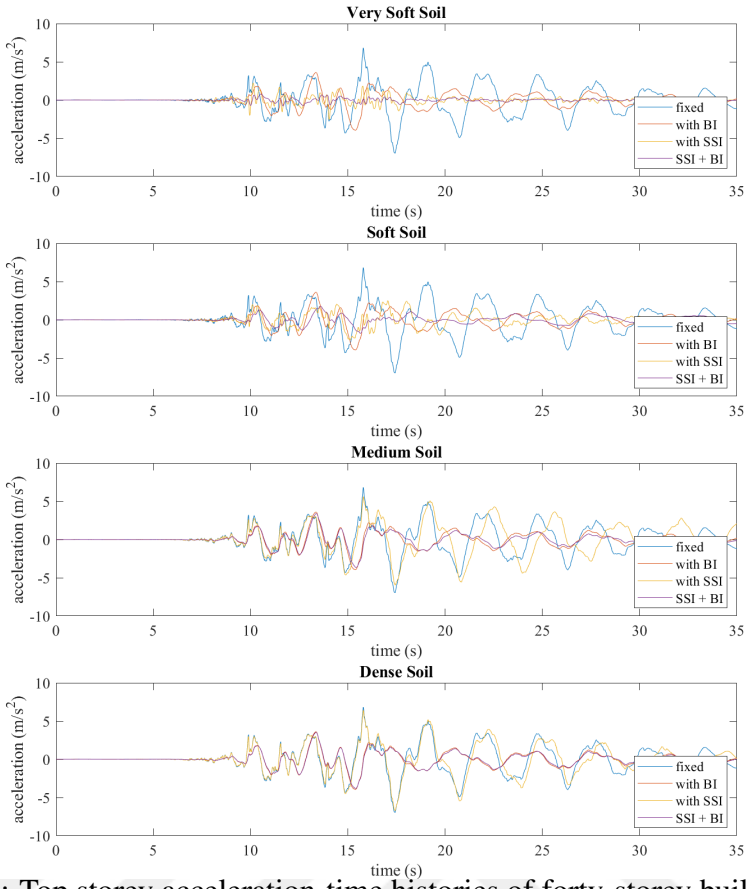

Figure 4.85 : Top storey acceleration-time histories of forty-storey building(Kocaeli, 1999, near fault).

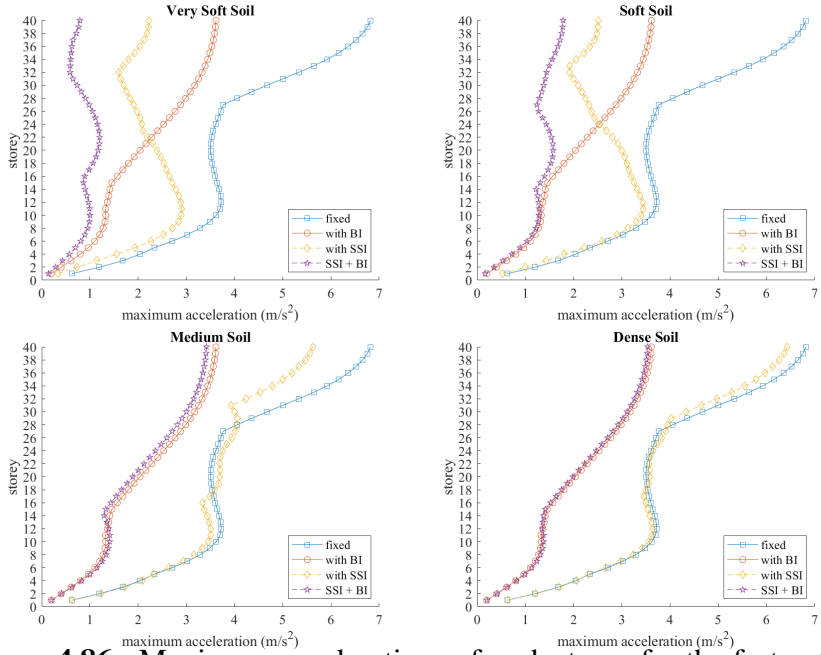

Figure 4.86 : Maximum accelerations of each storey for the forty-storey building(Kocaeli, 1999, near fault).

Figure 4.85 shows comparative acceleration-time histories of the forty-storey building for each soil type. Figure 4.86 shows maximum acceleration values for each storey.

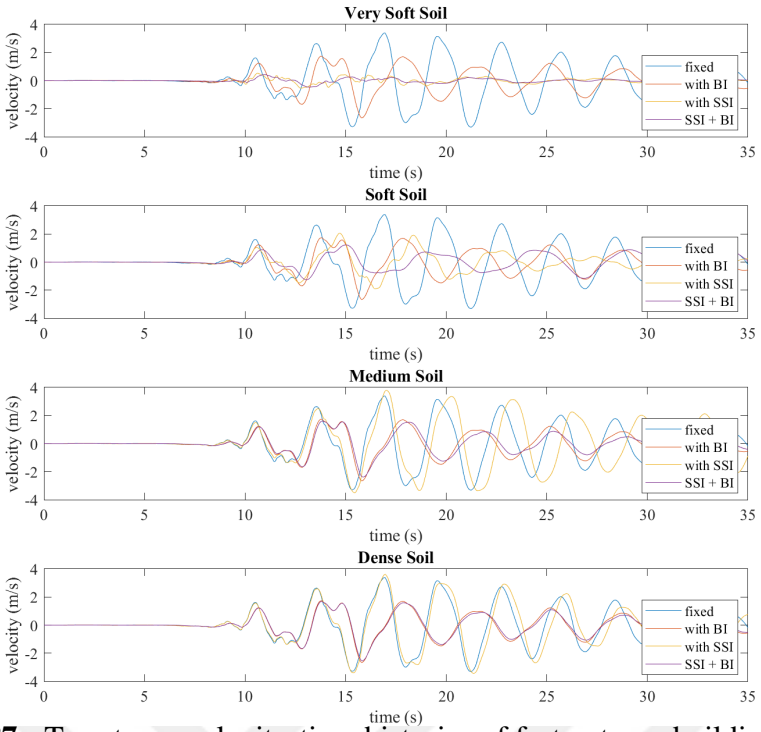

Figure 4.87 : Top storey velocity-time histories of forty-storey building(Kocaeli, 1999, near fault).

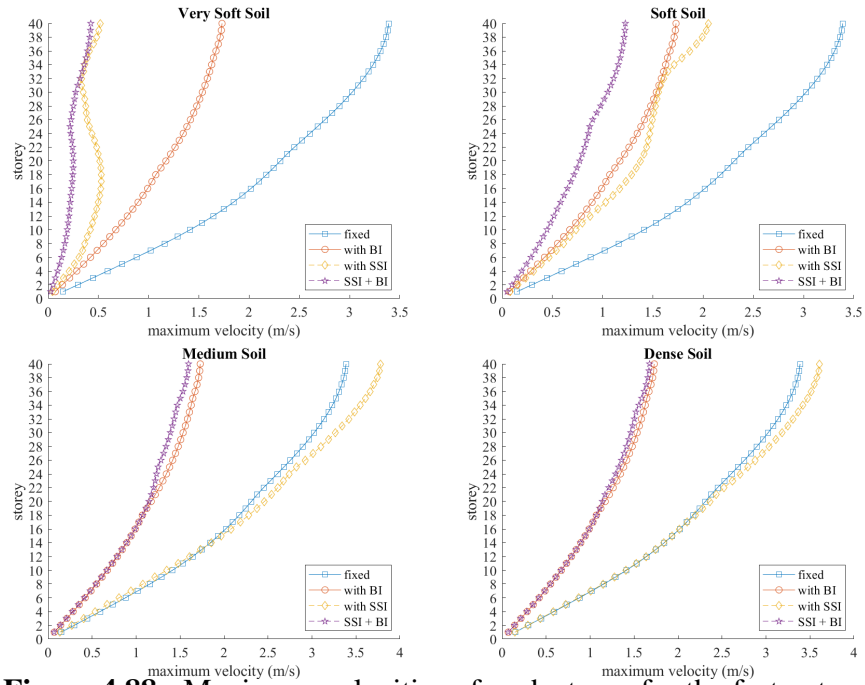

Figure 4.88 : Maximum velocities of each storey for the forty-storey building(Kocaeli, 1999, near fault).

Figure 4.87 shows comparative velocity-time histories of the forty-storey building for each soil type. Figure 4.88 shows maximum velocity values for each storey.

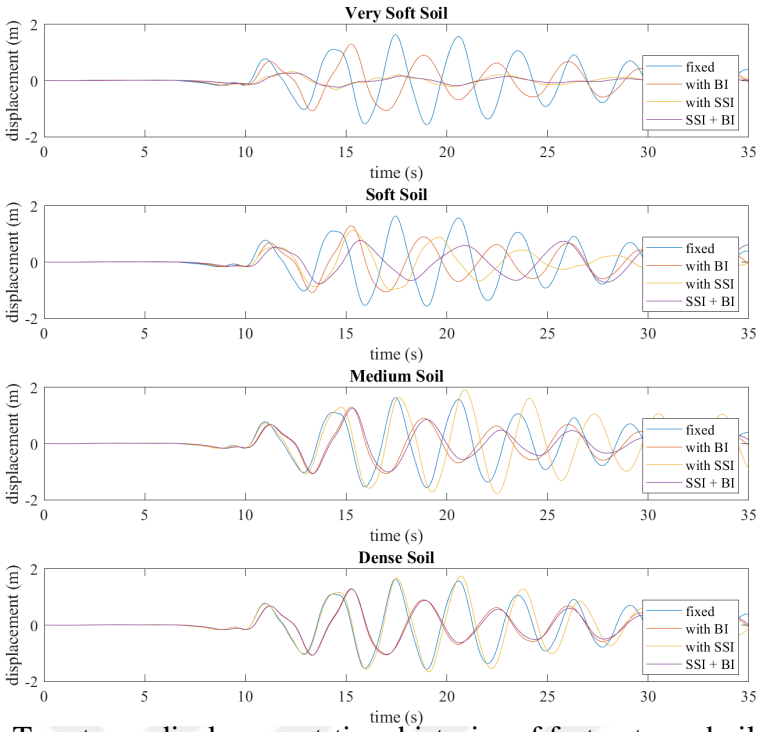

Figure 4.89 : Top storey displacement-time histories of forty-storey building(Kocaeli, 1999, near fault).

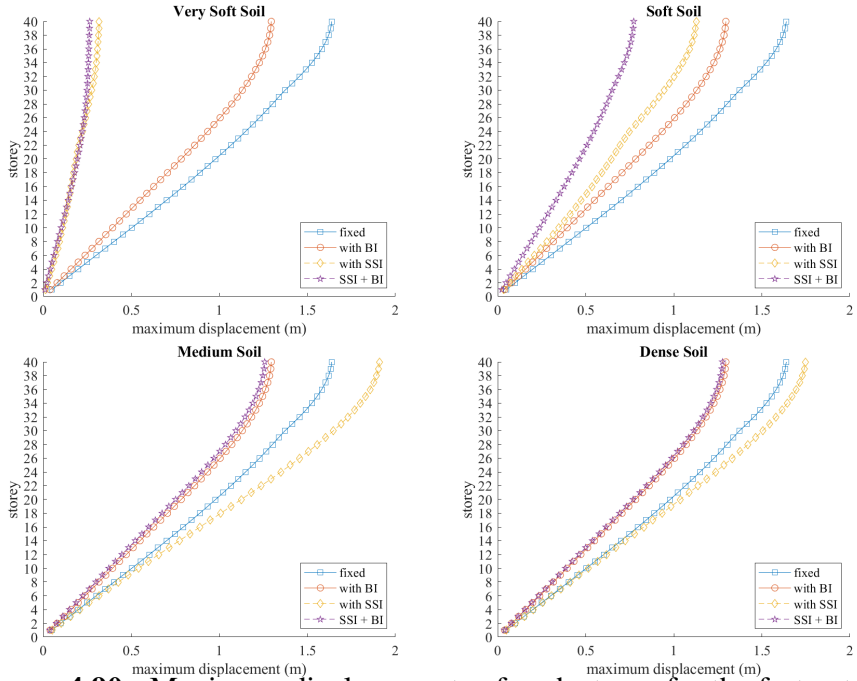

Figure 4.90 : Maximum displacements of each storey for the forty-storey building(Kocaeli, 1999, near fault).

Figure 4.89 shows comparative displacement-time histories of the forty-storey building for each soil type. Figure 4.90 shows maximum displacement values for each storey.

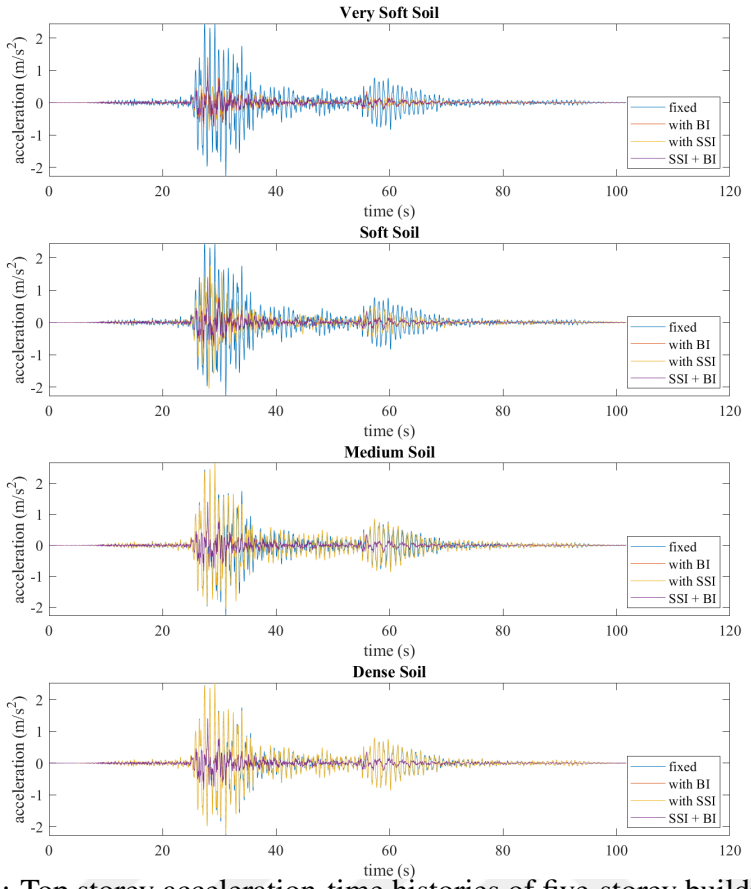

Figure 4.91 : Top storey acceleration-time histories of five-storey building(Kocaeli, 1999, far fault).

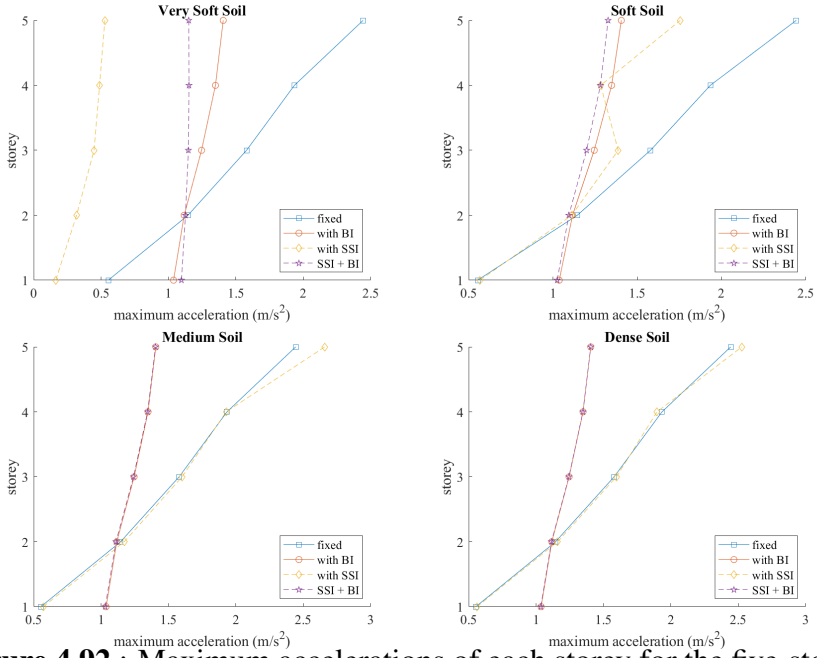

Figure 4.92 : Maximum accelerations of each storey for the five-storey building(Kocaeli, 1999, far fault).

Figure 4.91 shows comparative acceleration-time histories of the five-storey building for each soil type. Figure 4.92 shows maximum acceleration values for each storey.

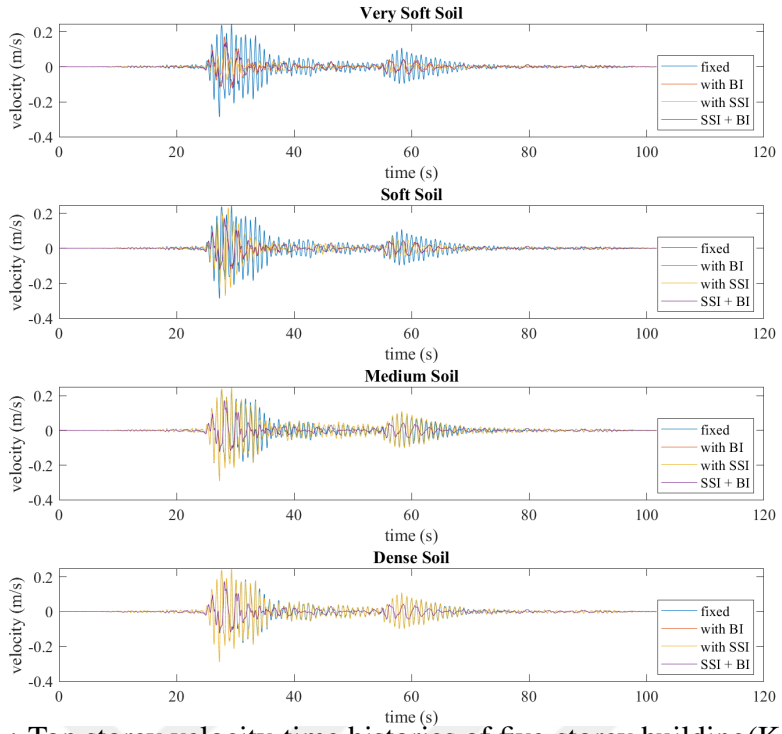

Figure 4.93 : Top storey velocity-time histories of five-storey building(Kocaeli, 1999, far fault).

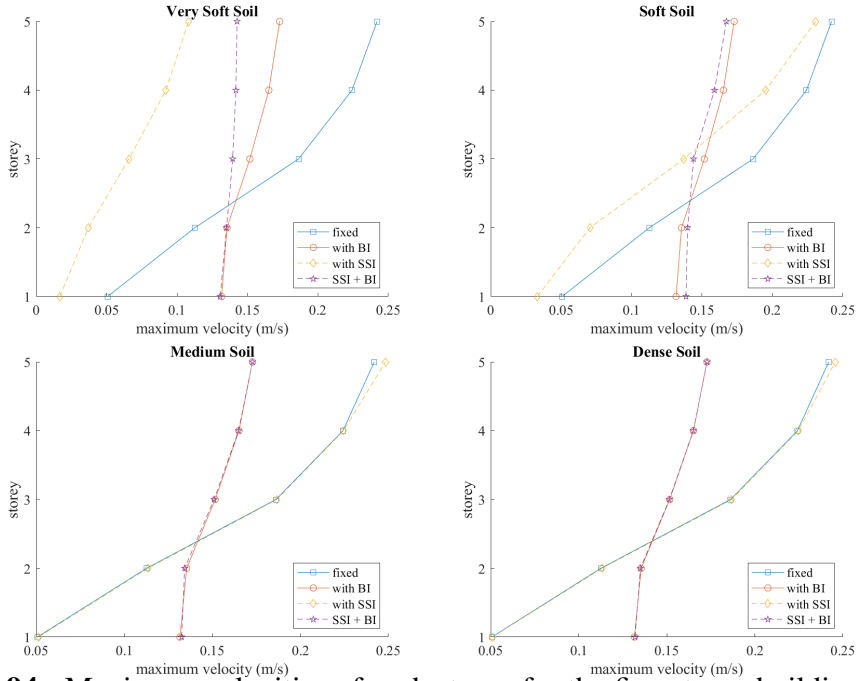

Figure 4.94 : Maximum velocities of each storey for the five-storey building(Kocaeli, 1999, far fault).

Figure 4.93 shows comparative velocity-time histories of the five-storey building for each soil type. Figure 4.94 shows maximum velocity values for each storey.

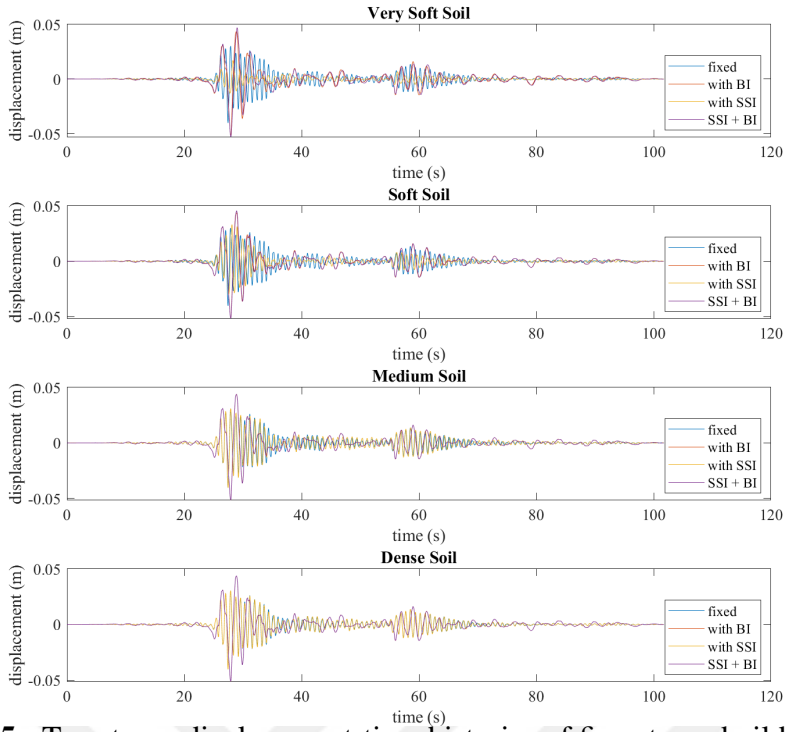

Figure 4.95 : Top storey displacement-time histories of five-storey building(Kocaeli, 1999, far fault).

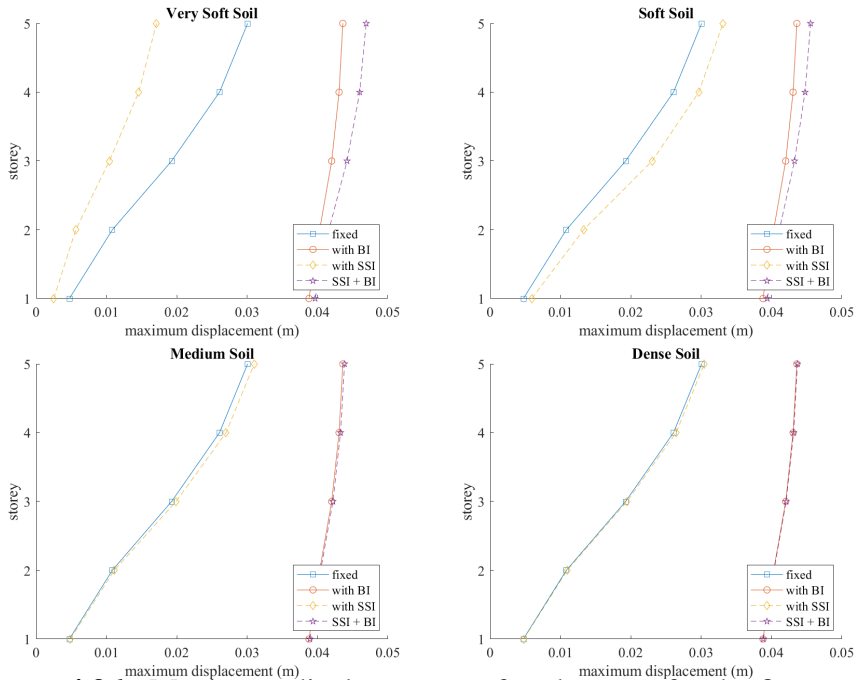

Figure 4.96 : Maximum displacements of each storey for the five-storey building(Kocaeli, 1999, far fault).

Figure 4.95 shows comparative displacement-time histories of the five-storey building for each soil type. Figure 4.96 shows maximum displacement values for each storey.

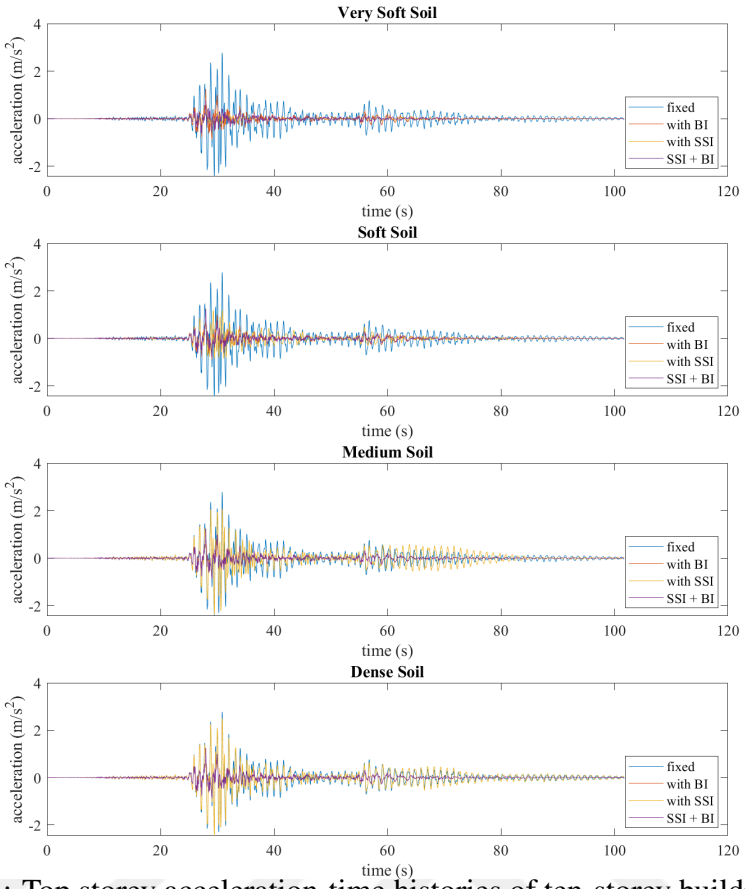

Figure 4.97 : Top storey acceleration-time histories of ten-storey building(Kocaeli, 1999, far fault).

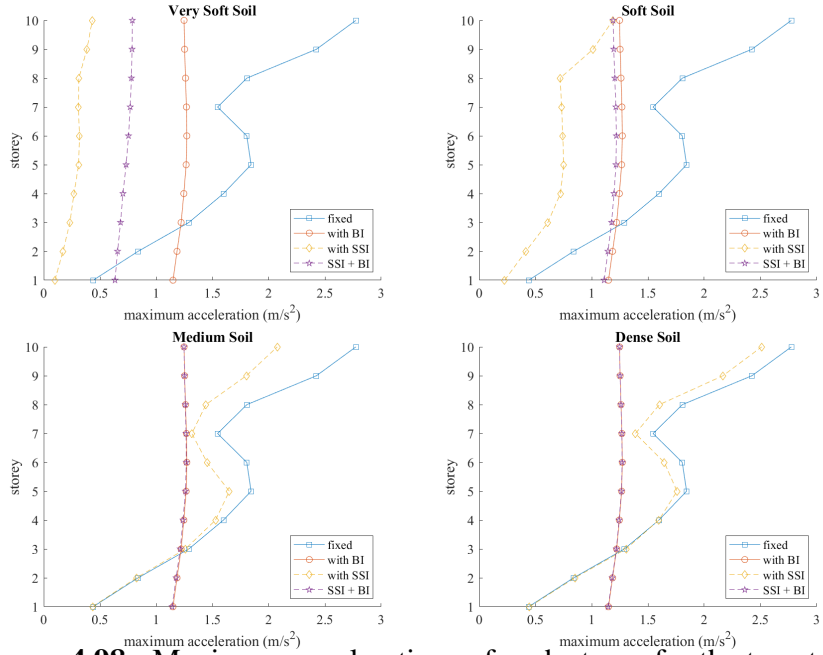

Figure 4.98 : Maximum accelerations of each storey for the ten-storey building(Kocaeli, 1999, far fault).

Figure 4.97 shows comparative acceleration-time histories of the ten-storey building for each soil type. Figure 4.98 shows maximum acceleration values for each storey.

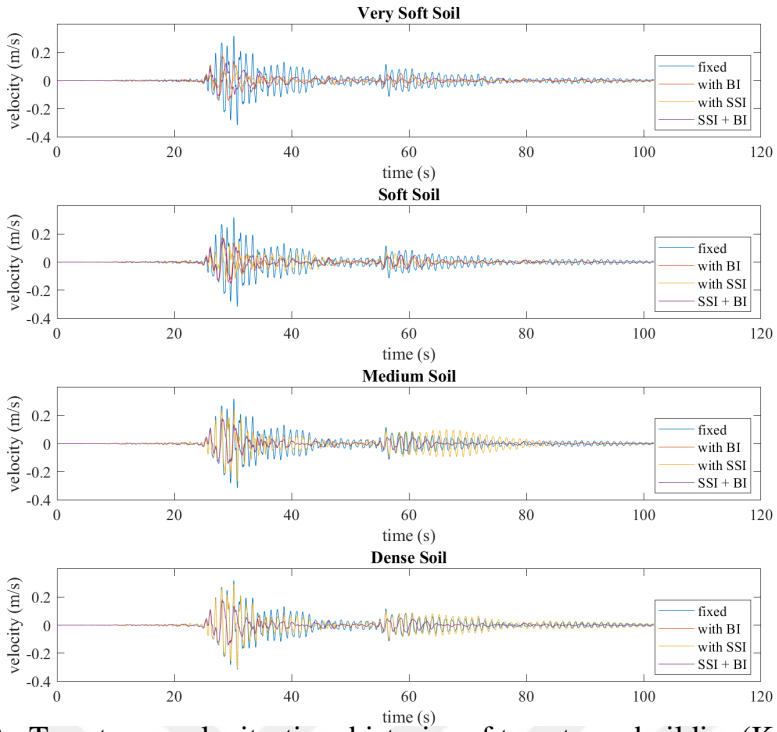

Figure 4.99 : Top storey velocity-time histories of ten-storey building(Kocaeli, 1999, far fault).

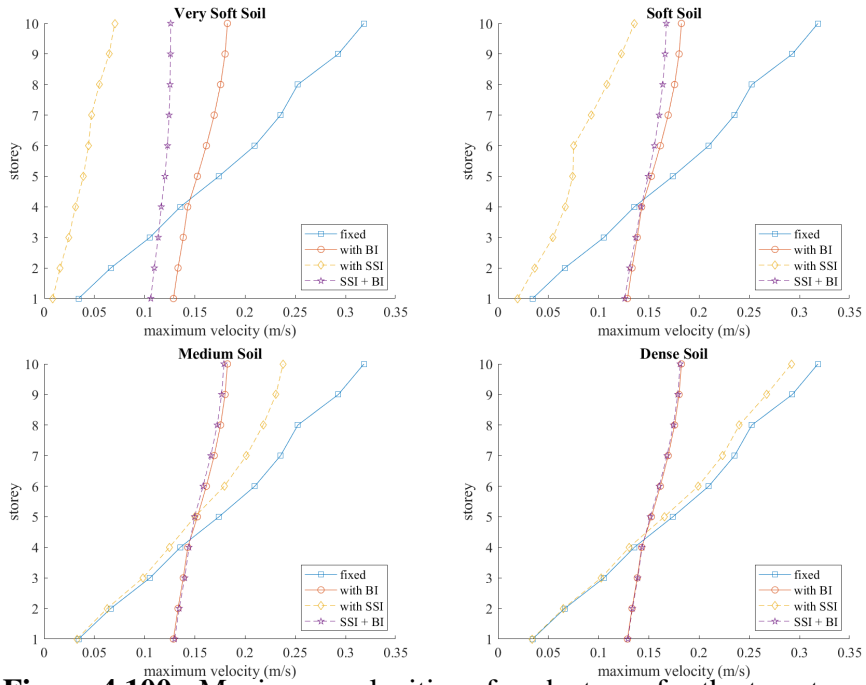

Figure 4.100 : Maximum velocities of each storey for the ten-storey building(Kocaeli, 1999, far fault).

Figure 4.99 shows comparative velocity-time histories of the ten-storey building for each soil type. Figure 4.100 shows maximum velocity values for each storey.

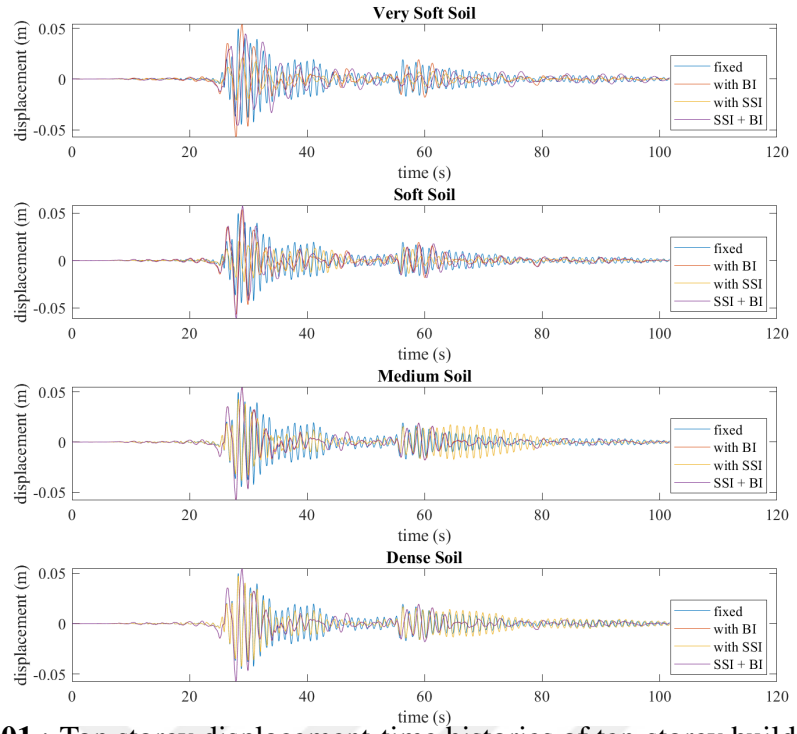

Figure 4.101 : Top storey displacement-time histories of ten-storey building(Kocaeli, 1999, far fault).

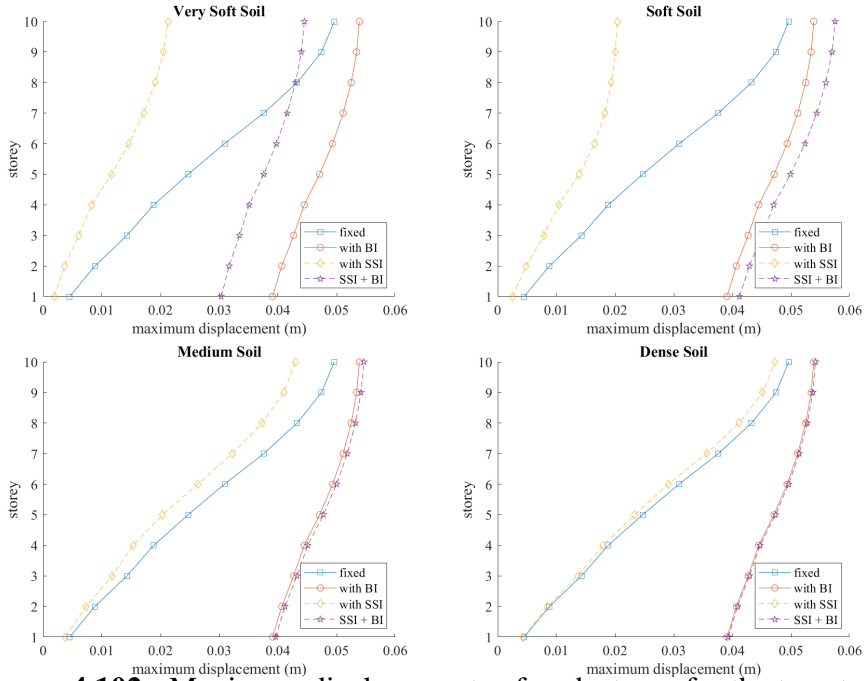

Figure 4.102 : Maximum displacements of each storey for the ten-storey building(Kocaeli, 1999, far fault).

Figure 4.101 shows comparative displacement-time histories of the ten-storey building for each soil type. Figure 4.102 shows maximum displacement values for each storey.

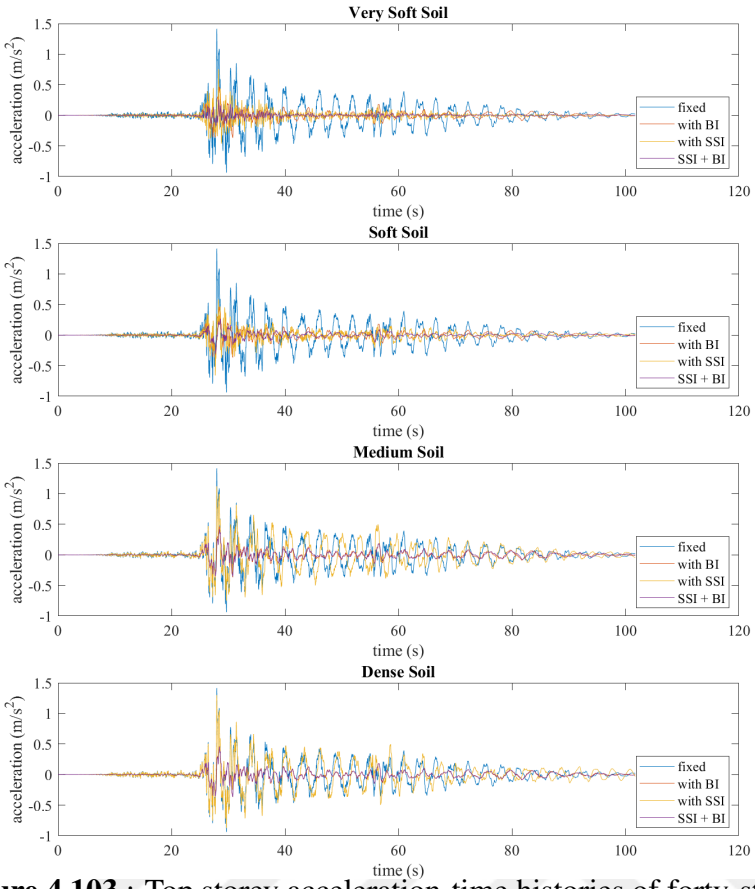

Figure 4.103 : Top storey acceleration-time histories of forty-storey building(Kocaeli, 1999, far fault).

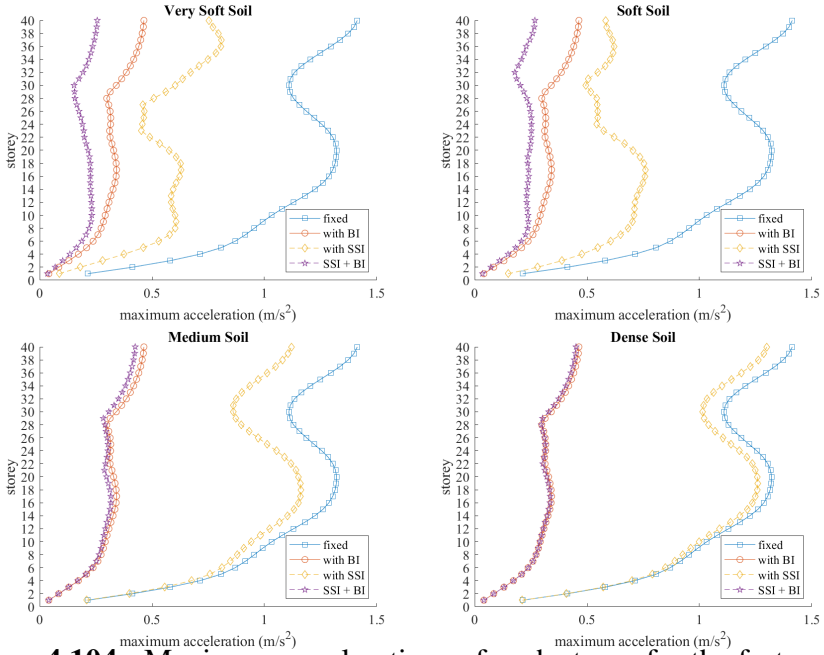

Figure 4.104 : Maximum accelerations of each storey for the forty-storey building(Kocaeli, 1999, far fault).

Figure 4.103 shows comparative acceleration-time histories of the forty-storey building for each soil type. Figure 4.104 shows maximum acceleration values for each storey.

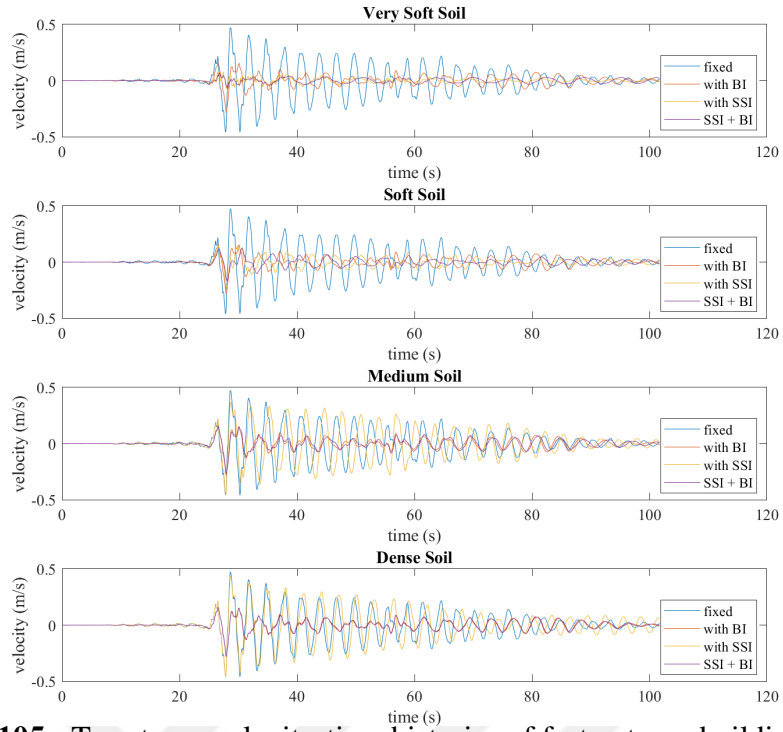

Figure 4.105 : Top storey velocity-time histories of forty-storey building(Kocaeli, 1999, far fault).

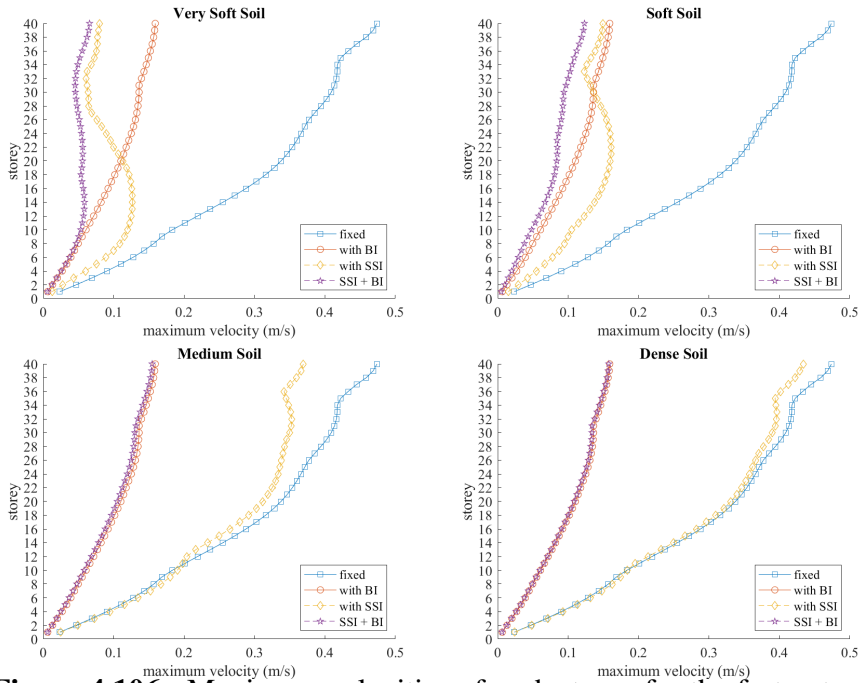

Figure 4.106 : Maximum velocities of each storey for the forty-storey building(Kocaeli, 1999, far fault).

Figure 4.105 shows comparative velocity-time histories of the forty-storey building for each soil type. Figure 4.106 shows maximum velocity values for each storey.

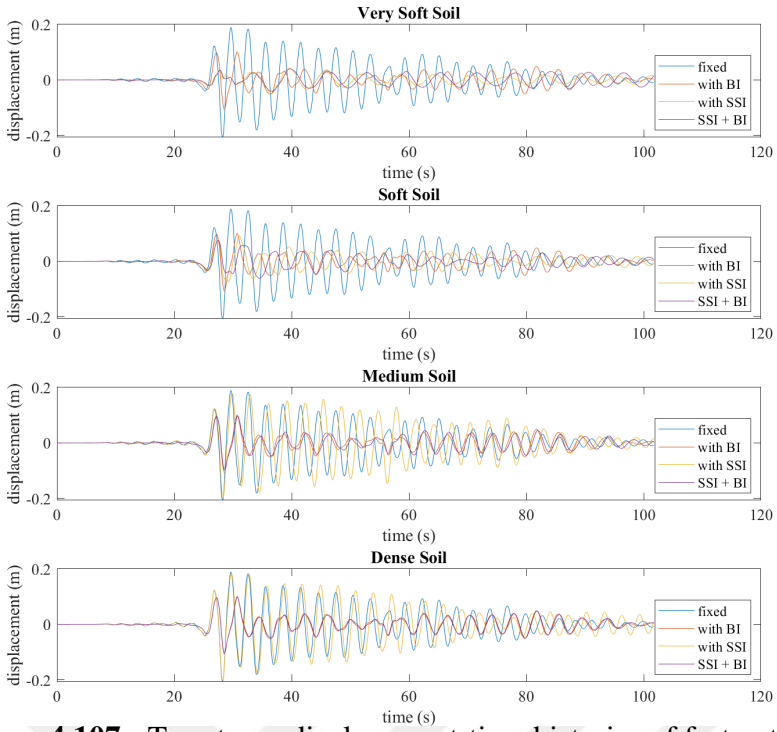

Figure 4.107 : Top storey displacement-time histories of forty-storey building(Kocaeli, 1999, far fault).

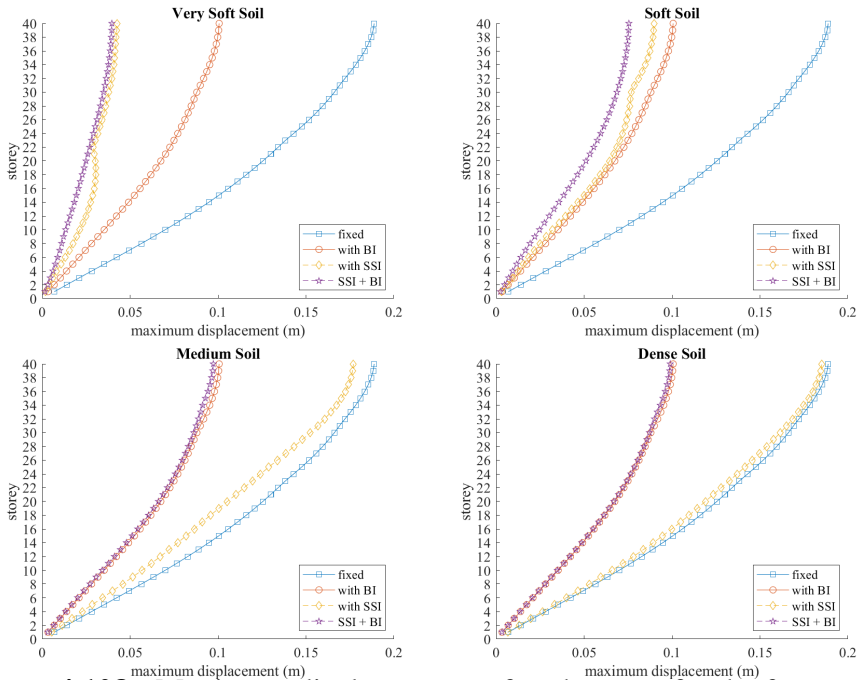

Figure 4.108 : Maximum displacements of each storey for the forty-storey building(Kocaeli, 1999, far fault).

Figure 4.107 shows comparative displacement-time histories of the forty-storey building for each soil type. Figure 4.108 shows maximum displacement values for each storey.

Results for 1990 Manjil Earthquake are presented from figure 4.109 to figure 4.144. If we consider the acceleration results for five, ten and forty storey buildings; in consistent with the results obtained from previous earthquakes presented in this section, implementing base isolation reduces responses significantly in all cases. SSI can be considered as a factor in the reduction of the acceleration values, in softer soil conditions. In very soft soil conditions, SSI effects can be observed clearly, but moving towards denser soil, effects disappear and structures behave like they are fixed based. These effects can be seen by comparing figures 4.110, 4.116, 4.122, 4.128, 4.134 and 4.140.

Comparing the velocity results with the acceleration ones, they are almost identical; base isolation reduces responses considerably. The same observations that are mentioned for previous earthquakes studied in this section, are obtained for 1990 Manjil earthquake as well.

From the observation of the displacements obtained from 1990 Manjil Earthquake, for five to forty storey buildings we can conclude that base isolated structures might have larger displacement than fixed base conventional structures, however the displacement of the base isolation is large and the inter-storey drifts are smaller. Again maximum SSI impact occurs in very soft soil condition while in dense soil becomes nearly similar to the fixed base.

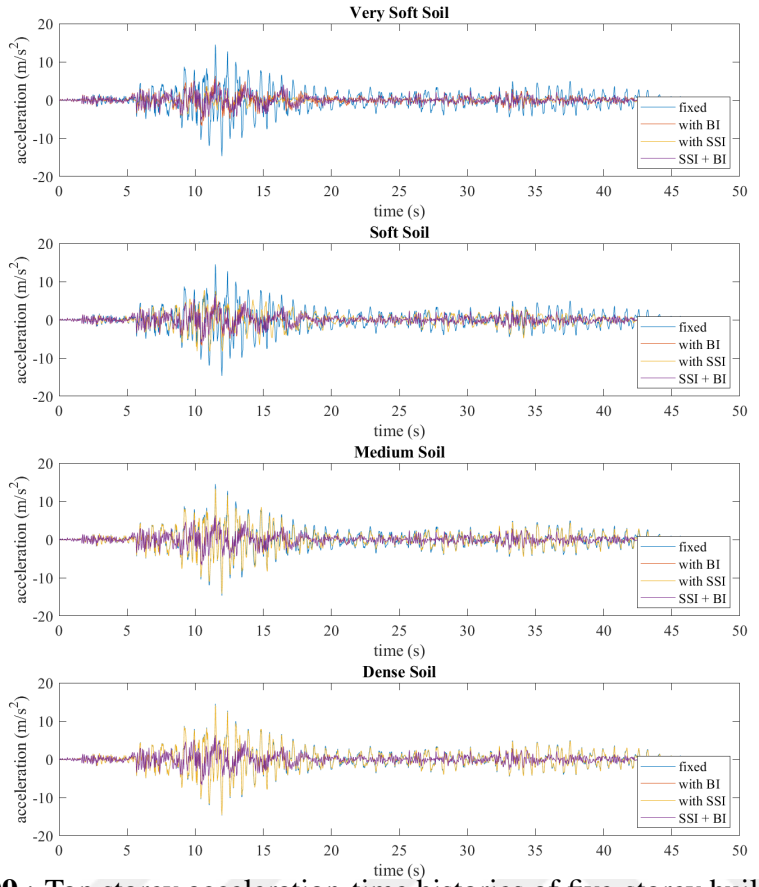

Figure 4.109 : Top storey acceleration-time histories of five-storey building(Manjil, 1990, near fault).

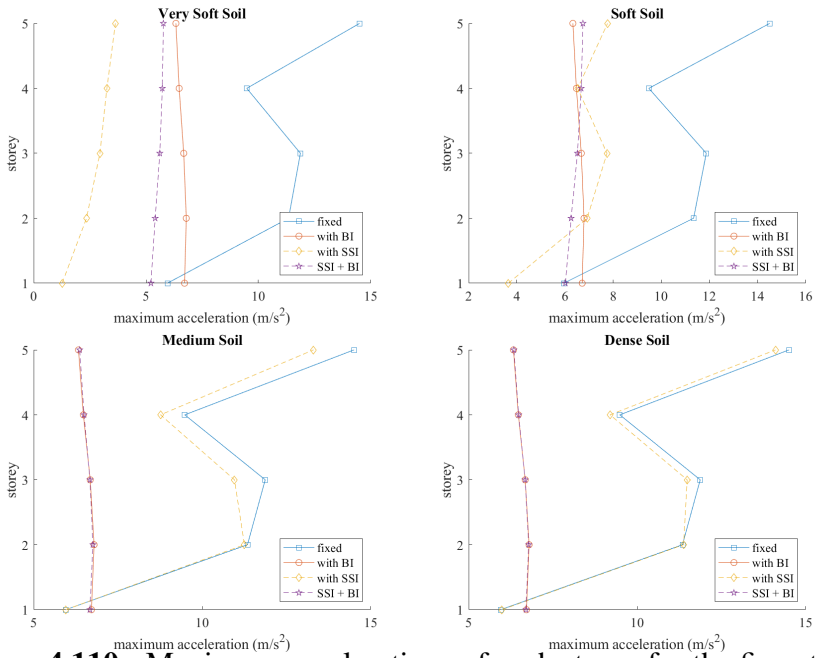

Figure 4.110 : Maximum accelerations of each storey for the five-storey building(Manjil, 1990, near fault).

Figure 4.109 shows comparative acceleration-time histories of the five-storey building for each soil type. Figure 4.110 shows maximum acceleration values for each storey.

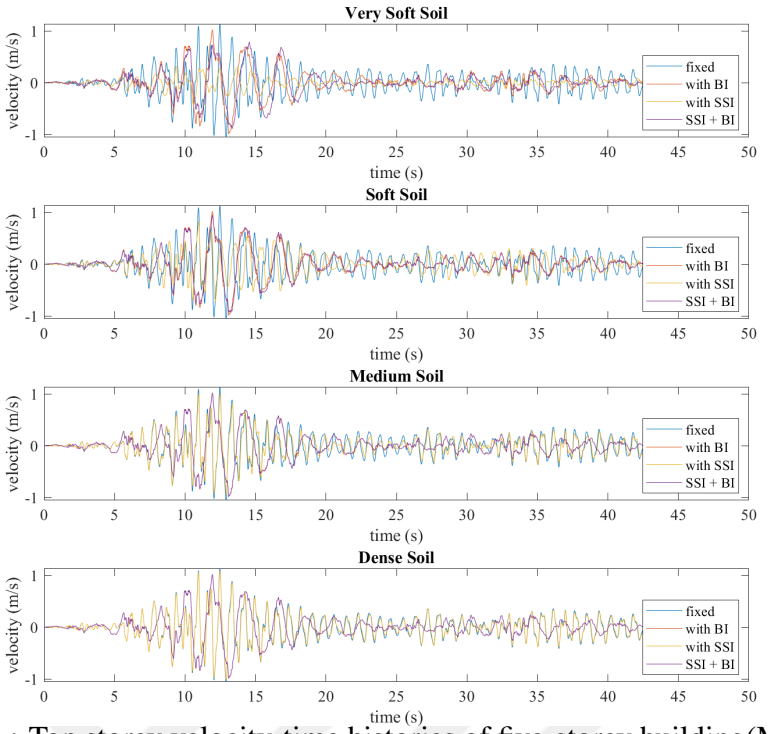

Figure 4.111 : Top storey velocity-time histories of five-storey building(Manjil, 1990, near fault).

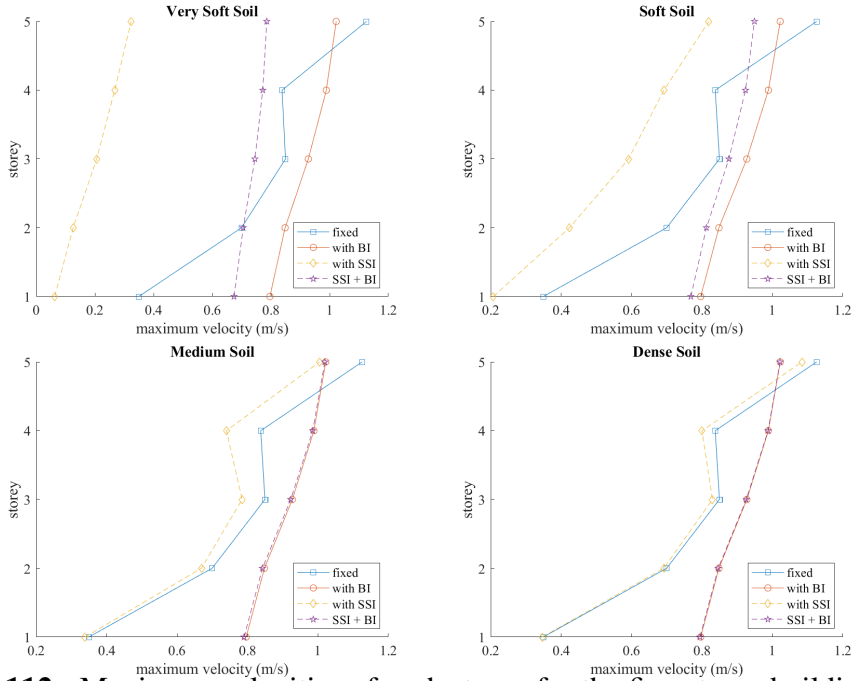

Figure 4.112 : Maximum velocities of each storey for the five-storey building(Manjil, 1990, near fault).

Figure 4.111 shows comparative velocity-time histories of the five-storey building for each soil type. Figure 4.112 shows maximum velocity values for each storey.

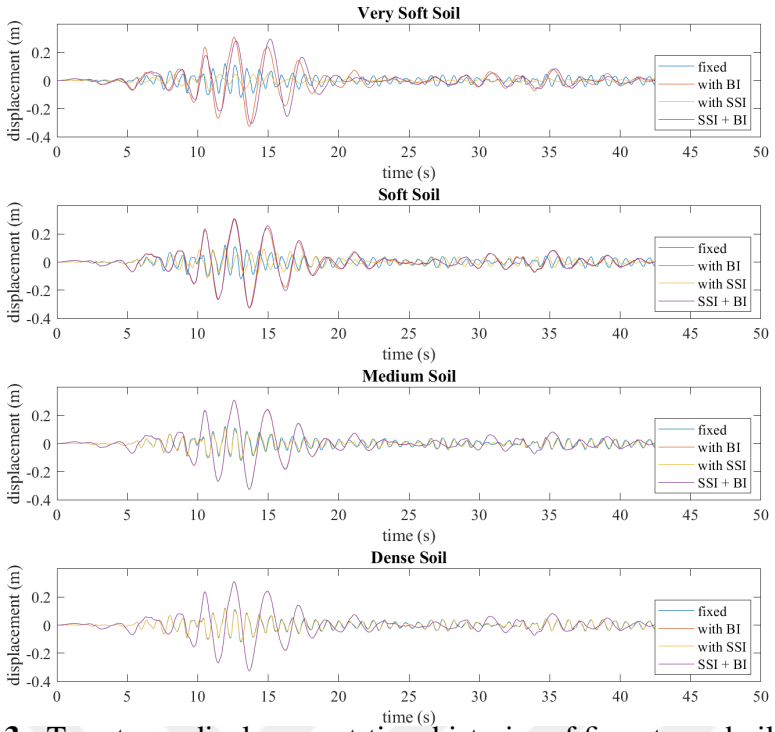

Figure 4.113 : Top storey displacement-time histories of five-storey building(Manjil, 1990, near fault).

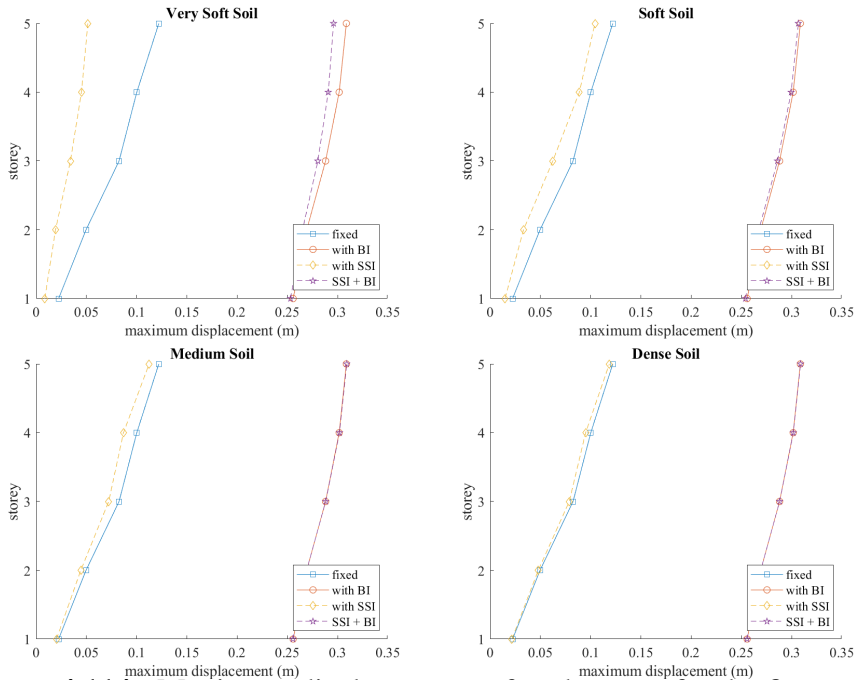

Figure 4.114 : Maximum displacements of each storey for the five-storey building(Manjil, 1990, near fault).

Figure 4.113 shows comparative displacement-time histories of the five-storey building for each soil type. Figure 4.114 shows maximum displacement values for each storey.

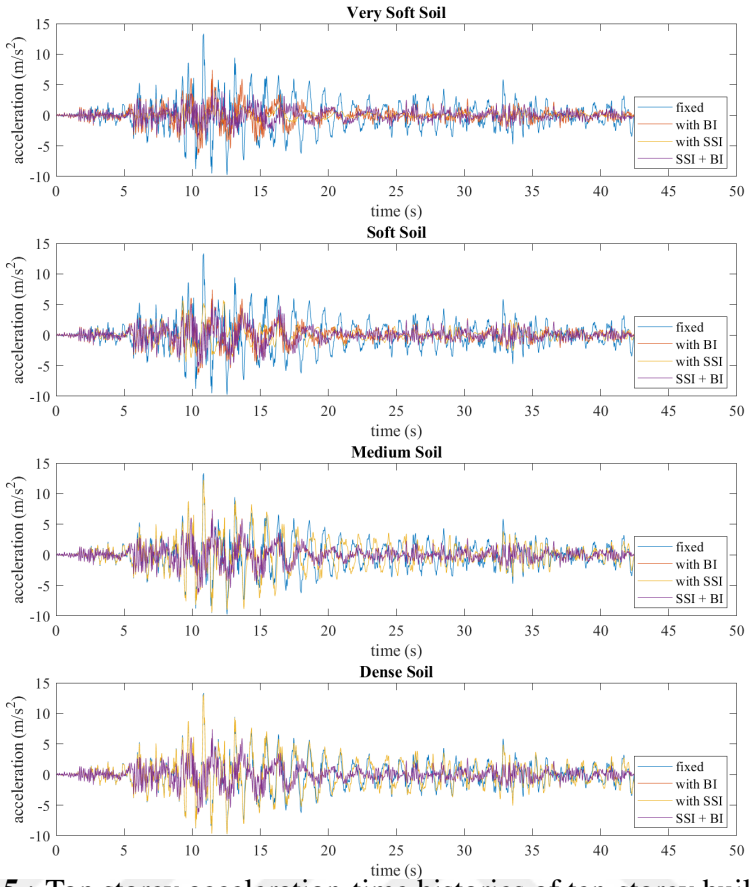

Figure 4.115 : Top storey acceleration-time histories of ten-storey building(Manjil, 1990, near fault).

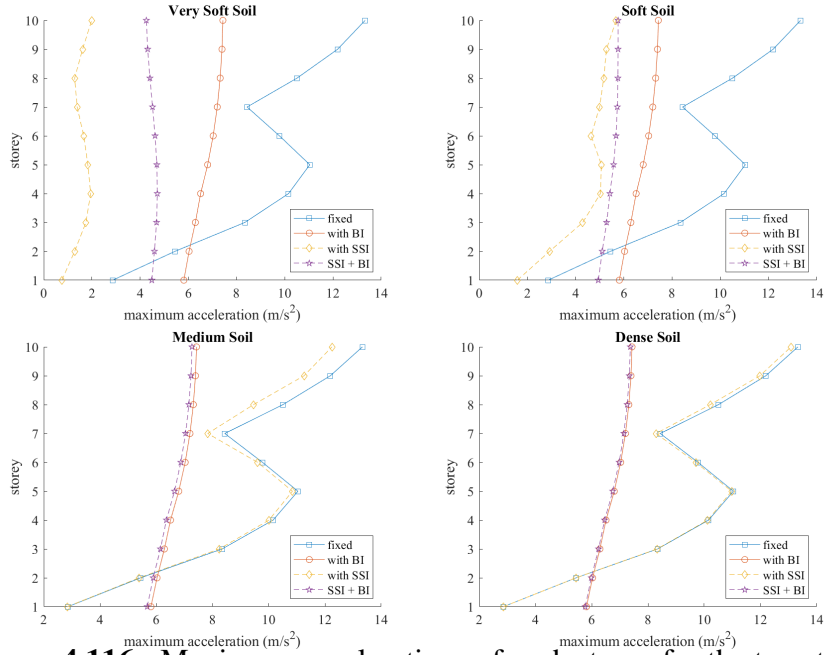

Figure 4.116 : Maximum accelerations of each storey for the ten-storey building(Manjil, 1990, near fault).

Figure 4.115 shows comparative acceleration-time histories of the five-storey building for each soil type. Figure 4.116 shows maximum acceleration values for each storey.

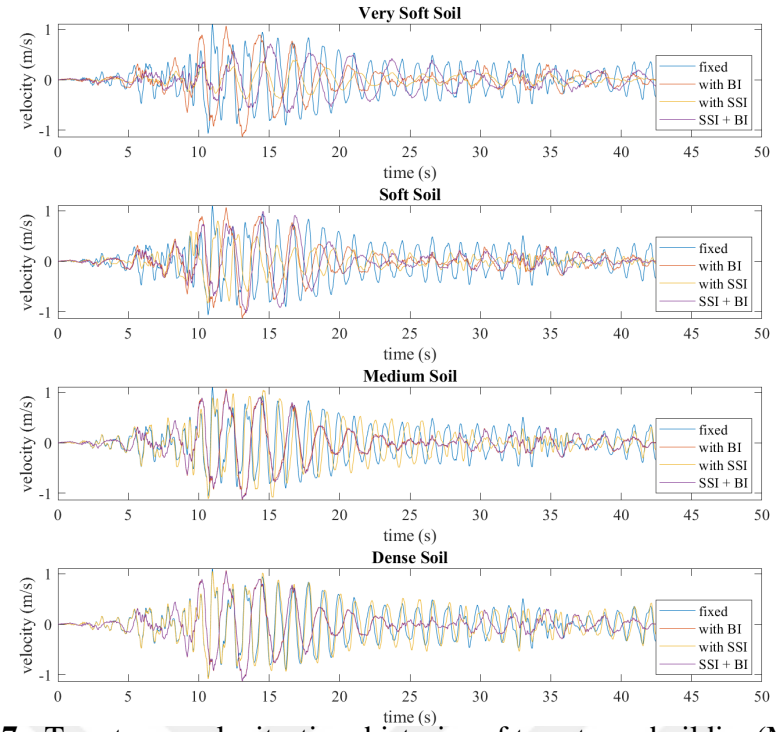

Figure 4.117 : Top storey velocity-time histories of ten-storey building(Manjil, 1990, near fault).

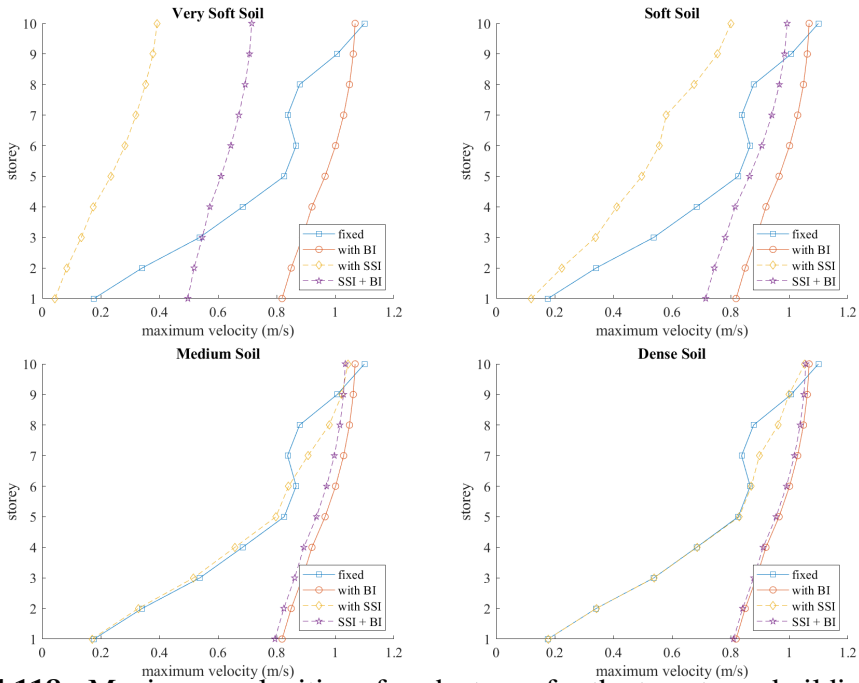

Figure 4.118 : Maximum velocities of each storey for the ten-storey building(Manjil, 1990, near fault).

Figure 4.117 shows comparative velocity-time histories of the ten-storey building for each soil type. Figure 4.118 shows maximum velocity values for each storey.

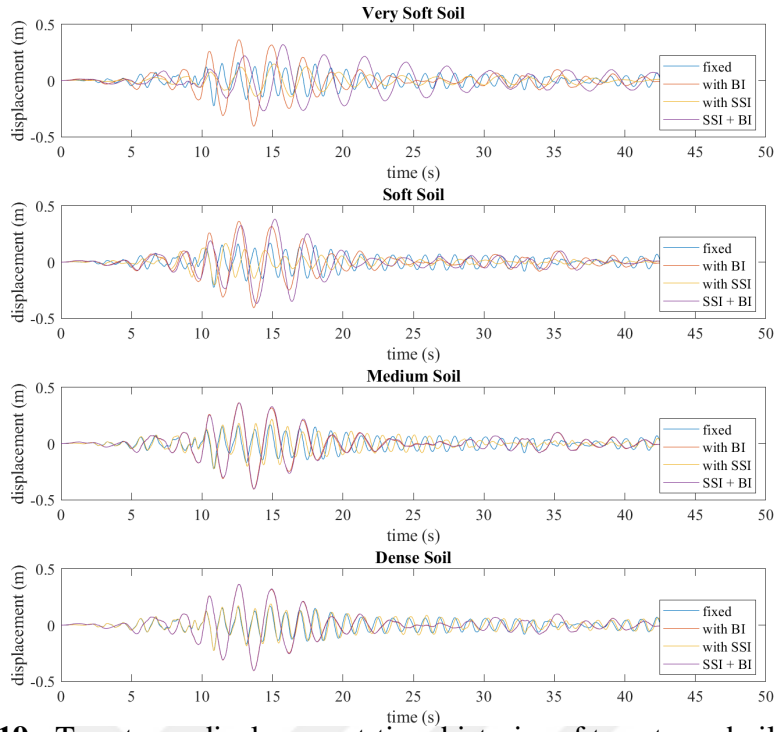

Figure 4.119 : Top storey displacement-time histories of ten-storey building(Manjil, 1990, near fault).

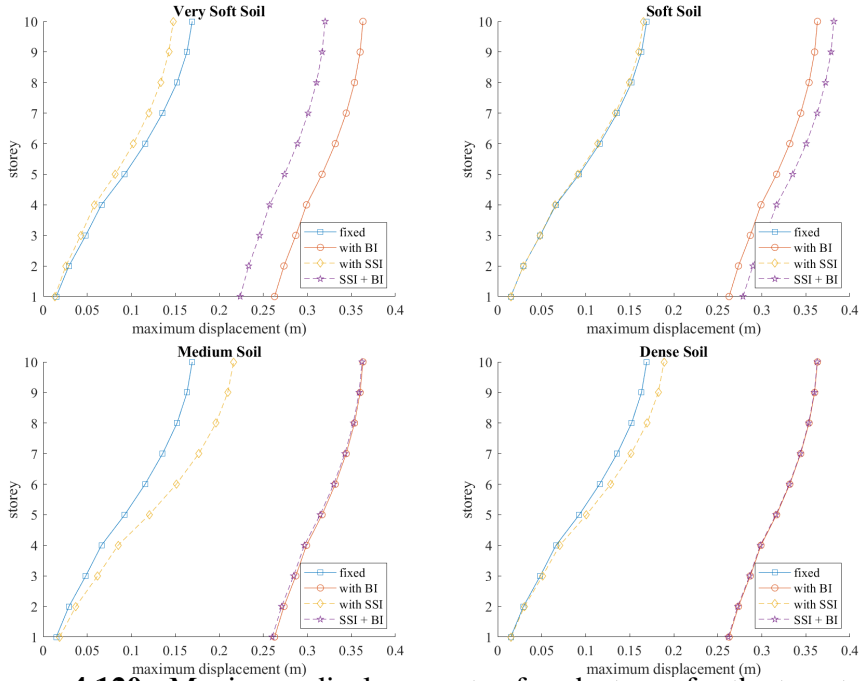

Figure 4.120 : Maximum displacements of each storey for the ten-storey building(Manjil, 1990, near fault).

Figure 4.119 shows comparative displacement-time histories of the ten-storey building for each soil type. Figure 4.120 shows maximum displacement values for each storey.

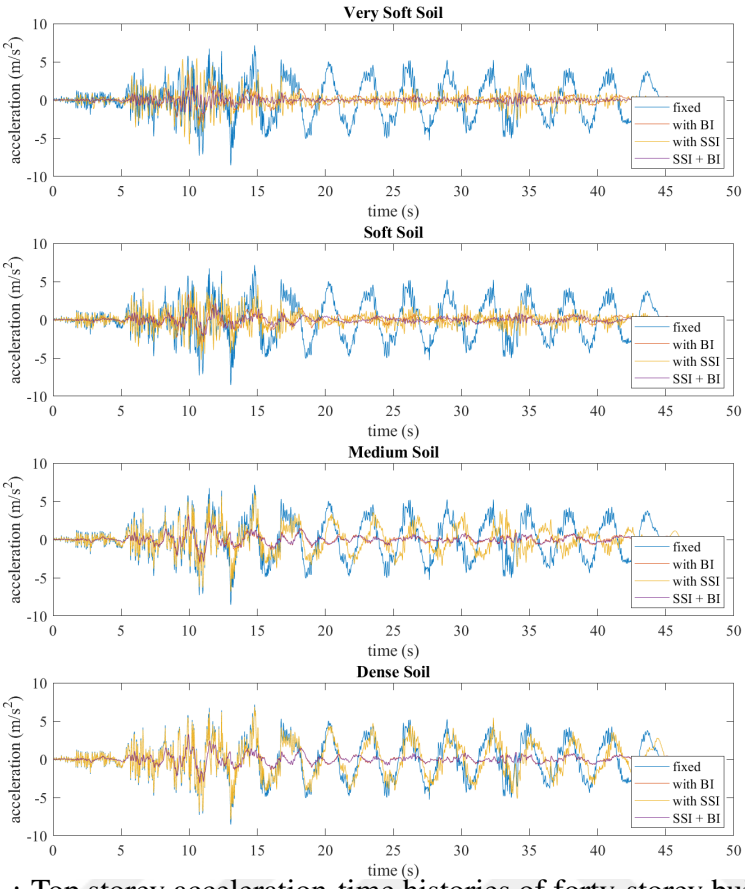

Figure 4.121 : Top storey acceleration-time histories of forty-storey building(Manjil, 1990, near fault).

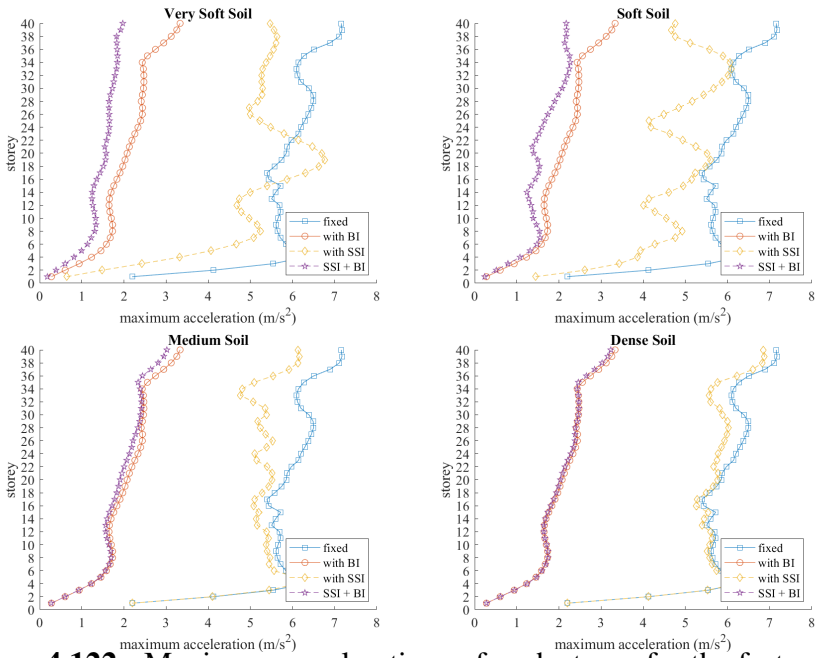

Figure 4.122 : Maximum accelerations of each storey for the forty-storey building(Manjil, 1990, near fault).

Figure 4.121 shows comparative acceleration-time histories of the forty-storey building for each soil type. Figure 4.122 shows maximum acceleration values for each storey.

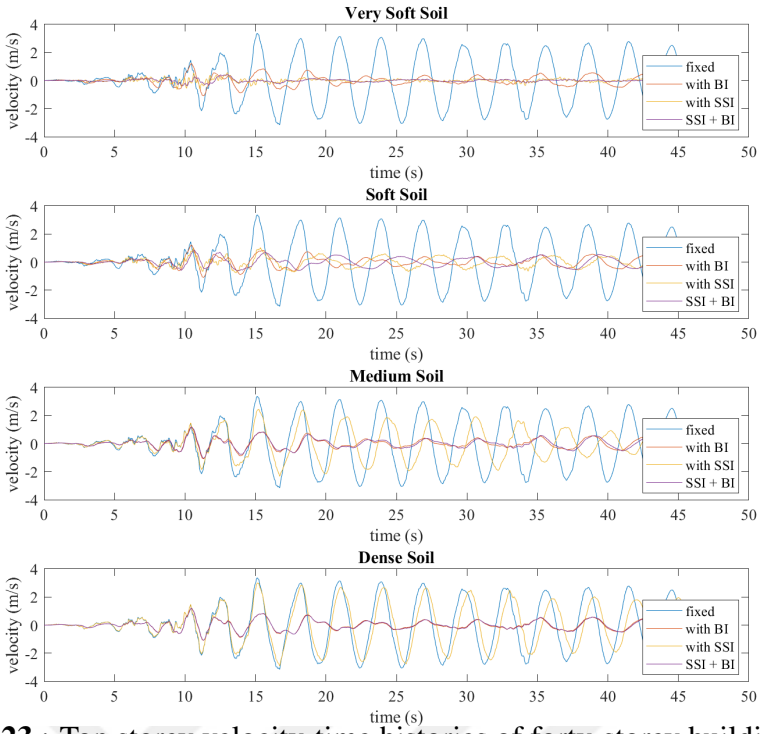

Figure 4.123 : Top storey velocity-time histories of forty-storey building(Manjil, 1990, near fault).

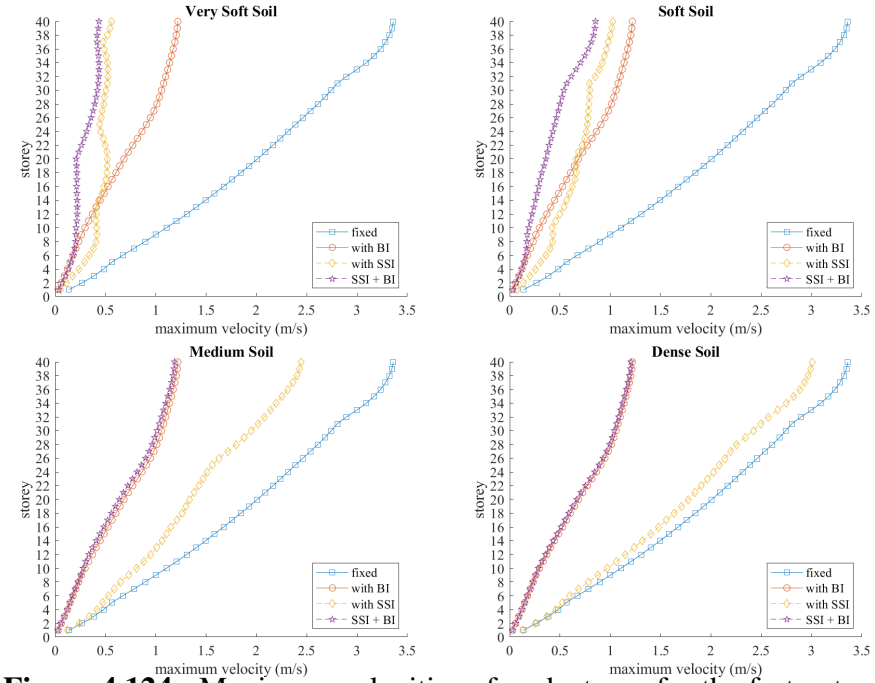

Figure 4.124 : Maximum velocities of each storey for the forty-storey building(Manjil, 1990, near fault).

Figure 4.123 shows comparative velocity-time histories of the forty-storey building for each soil type. Figure 4.124 shows maximum velocity values for each storey.

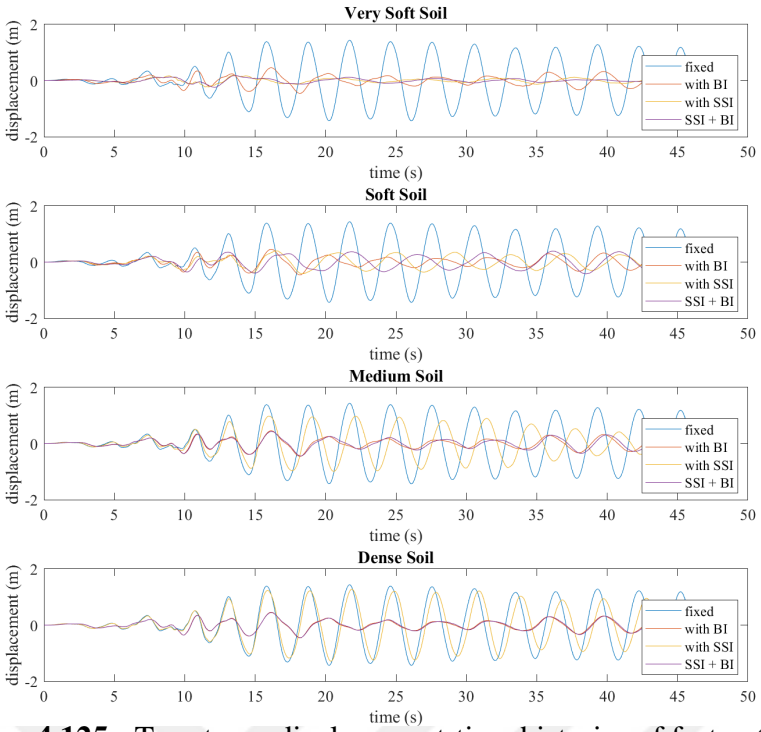

Figure 4.125 : Top storey displacement-time histories of forty-storey building(Manjil, 1990, near fault).

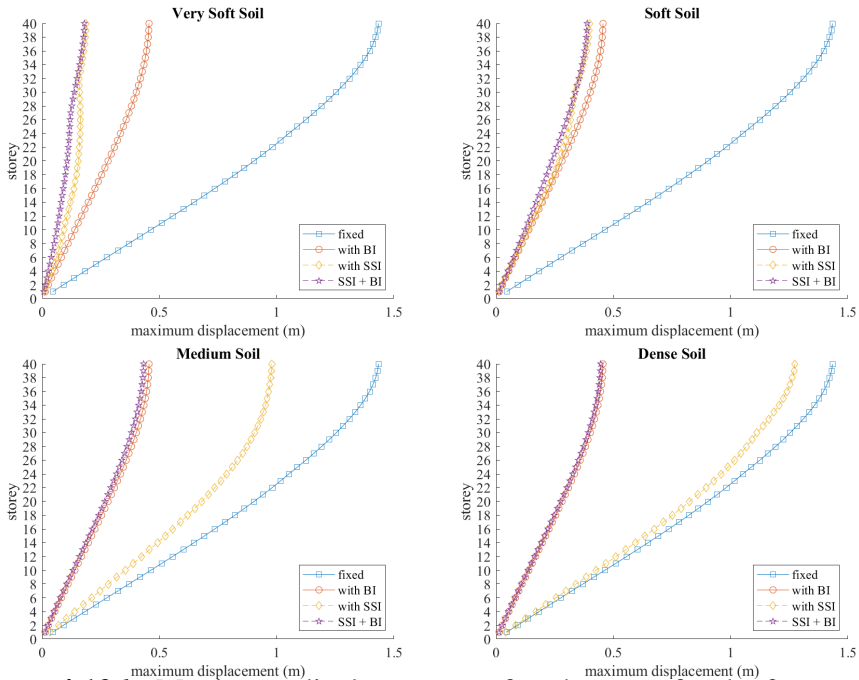

Figure 4.126 : Maximum displacements of each storey for the forty-storey building(Manjil, 1990, near fault).

Figure 4.125 shows comparative displacement-time histories of the forty-storey building for each soil type. Figure 4.126 shows maximum displacement values for each storey.

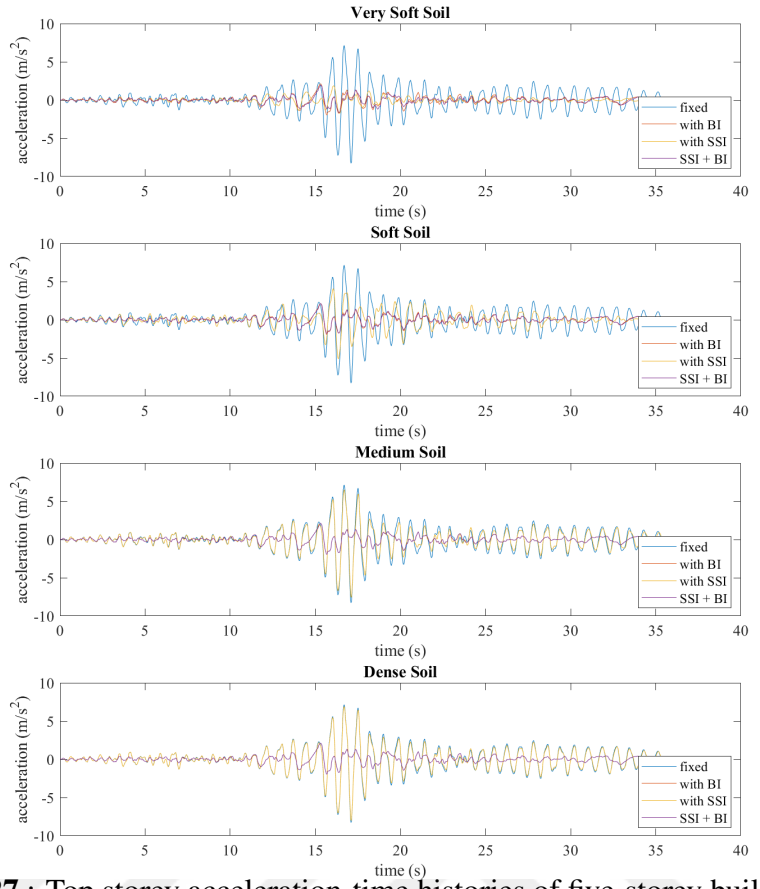

Figure 4.127 : Top storey acceleration-time histories of five-storey building(Manjil, 1990, far fault).

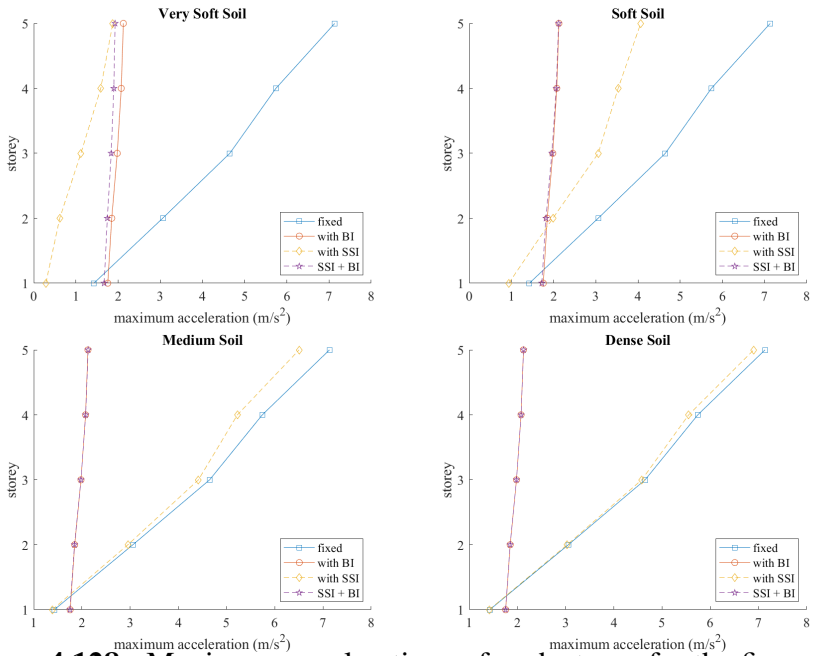

Figure 4.128 : Maximum accelerations of each storey for the five-storey building(Manjil, 1990, far fault).

Figure 4.127 shows comparative acceleration-time histories of the five-storey building for each soil type. Figure 4.128 shows maximum acceleration values for each storey.

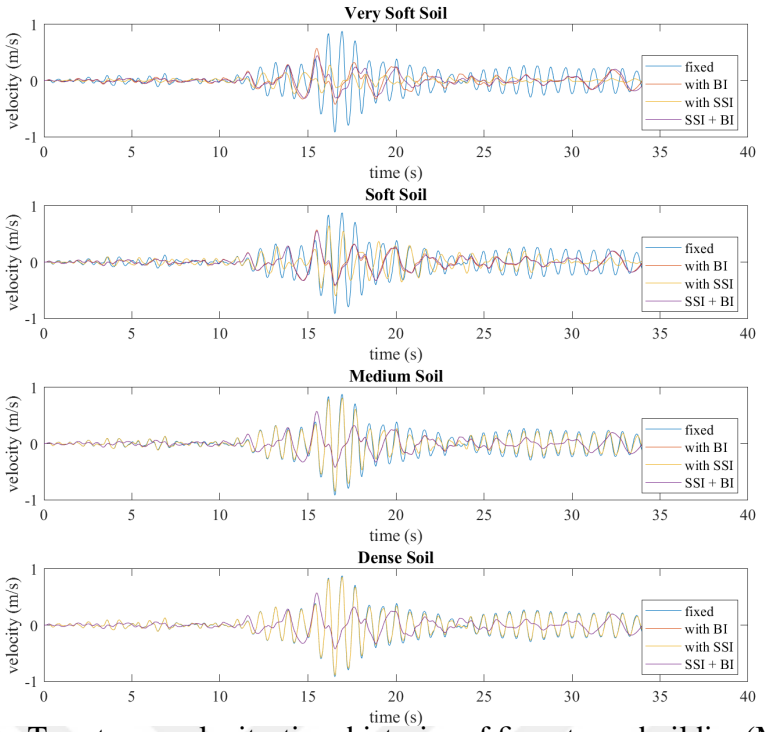

Figure 4.129 : Top storey velocity-time histories of five-storey building(Manjil, 1990, far fault).

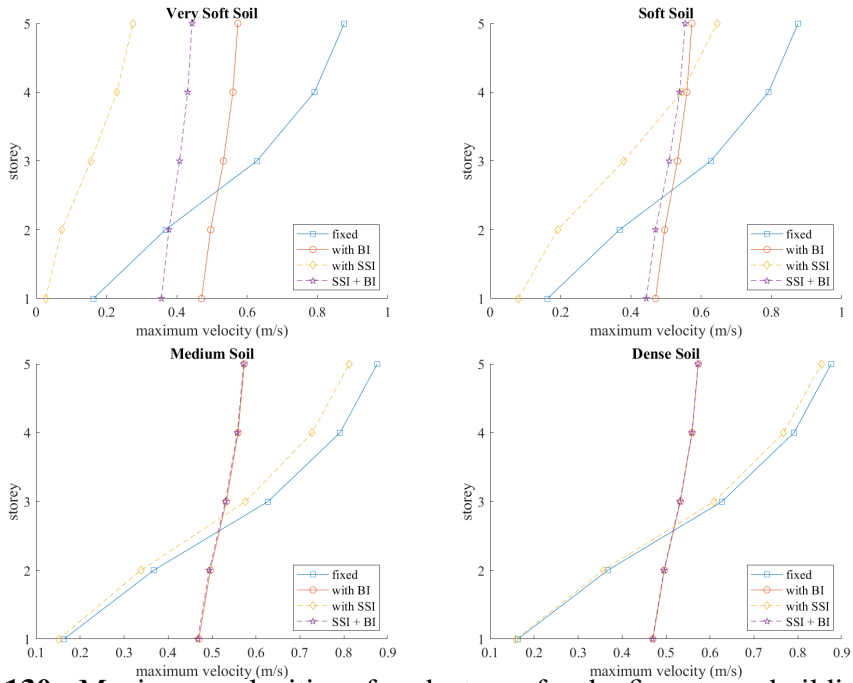

Figure 4.130 : Maximum velocities of each storey for the five-storey building(Manjil, 1990, far fault).

Figure 4.129 shows comparative velocity-time histories of the five-storey building for each soil type. Figure 4.130 shows maximum velocity values for each storey.

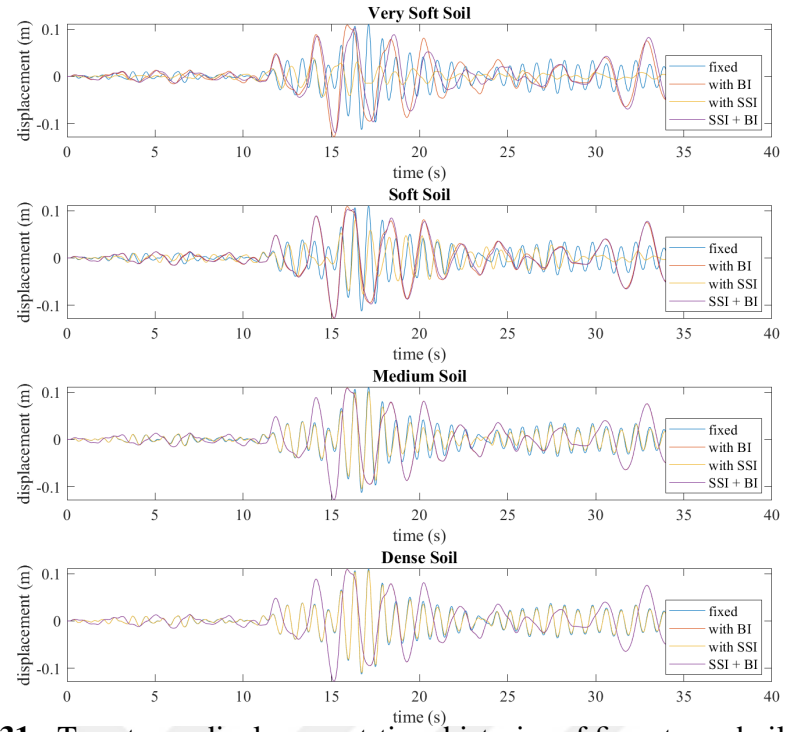

Figure 4.131 : Top storey displacement-time histories of five-storey building(Manjil, 1990, far fault).

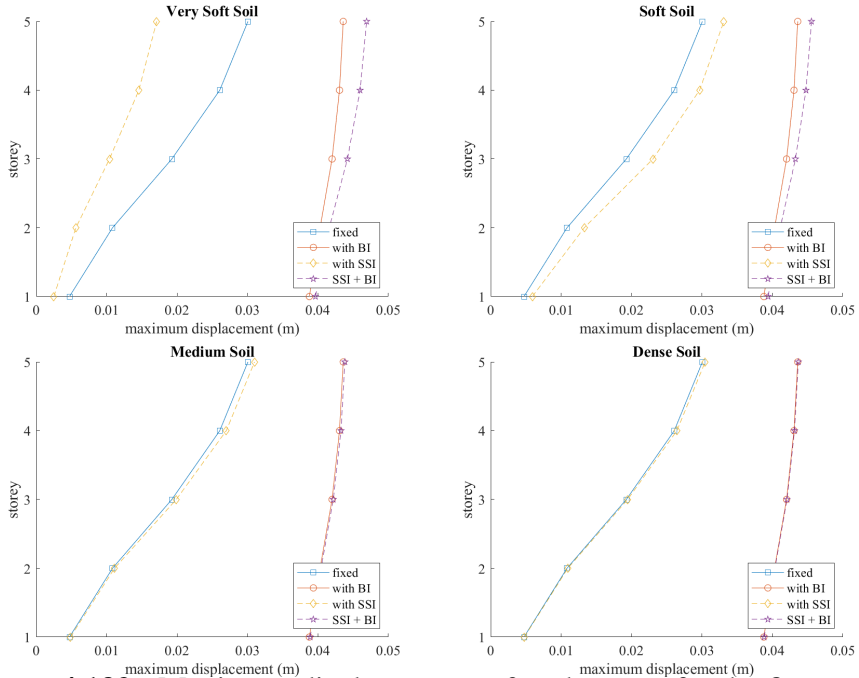

Figure 4.132 : Maximum displacements of each storey for the five-storey building(Manjil, 1990, far fault).

Figure 4.131 shows comparative displacement-time histories of the five-storey building for each soil type. Figure 4.132 shows maximum displacement values for each storey.

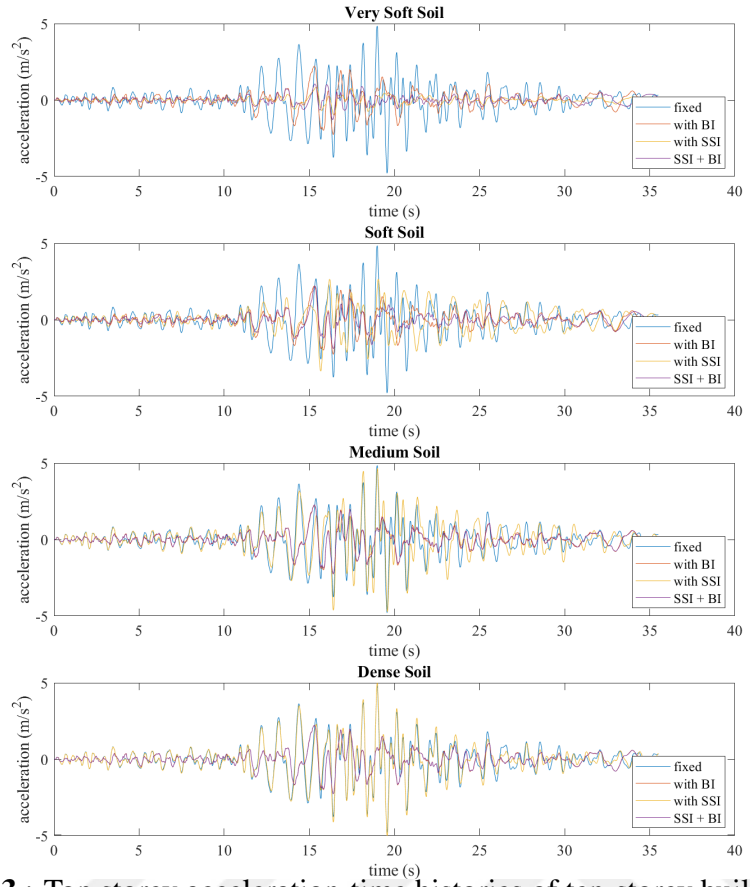

Figure 4.133 : Top storey acceleration-time histories of ten-storey building(Manjil, 1990, far fault).

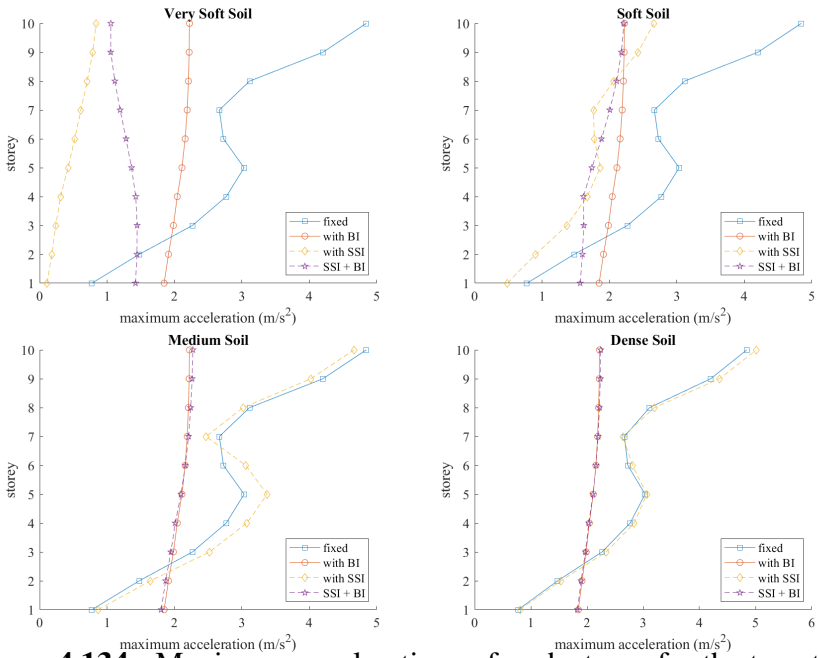

Figure 4.134 : Maximum accelerations of each storey for the ten-storey building(Manjil, 1990, far fault).

Figure 4.133 shows comparative acceleration-time histories of the ten-storey building for each soil type. Figure 4.134 shows maximum acceleration values for each storey.

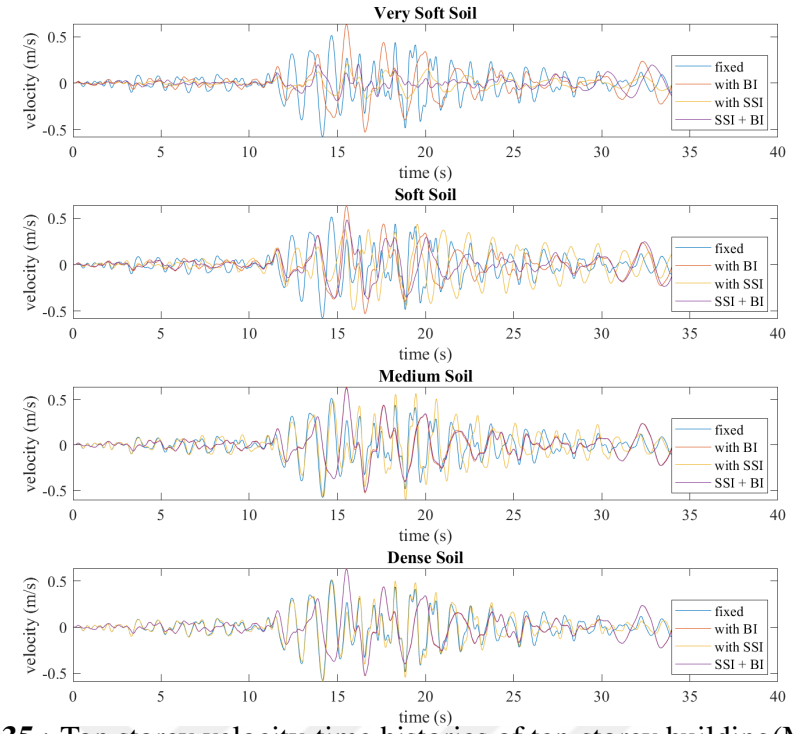

Figure 4.135 : Top storey velocity-time histories of ten-storey building(Manjil, 1990, far fault).

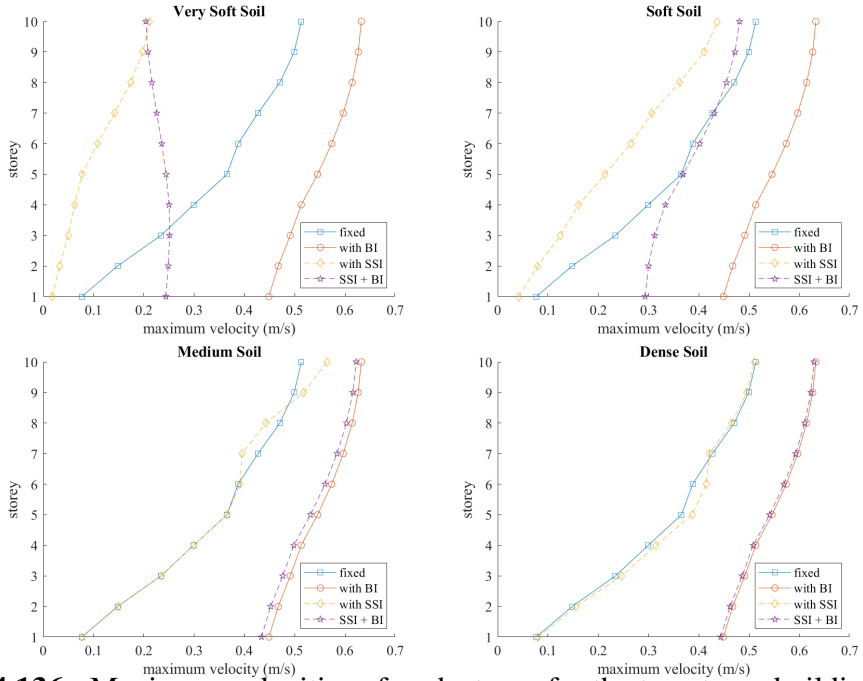

Figure 4.136 : Maximum velocities of each storey for the ten-storey building(Manjil, 1990, far fault).

Figure 4.135 shows comparative velocity-time histories of the ten-storey building for each soil type. Figure 4.136 shows maximum velocity values for each storey.

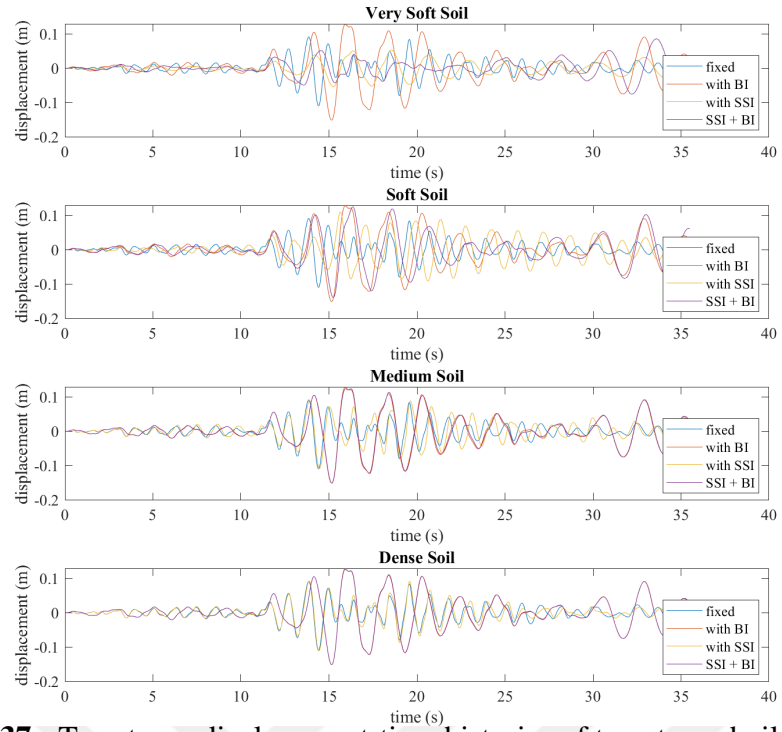

Figure 4.137 : Top storey displacement-time histories of ten-storey building(Manjil, 1990, far fault).

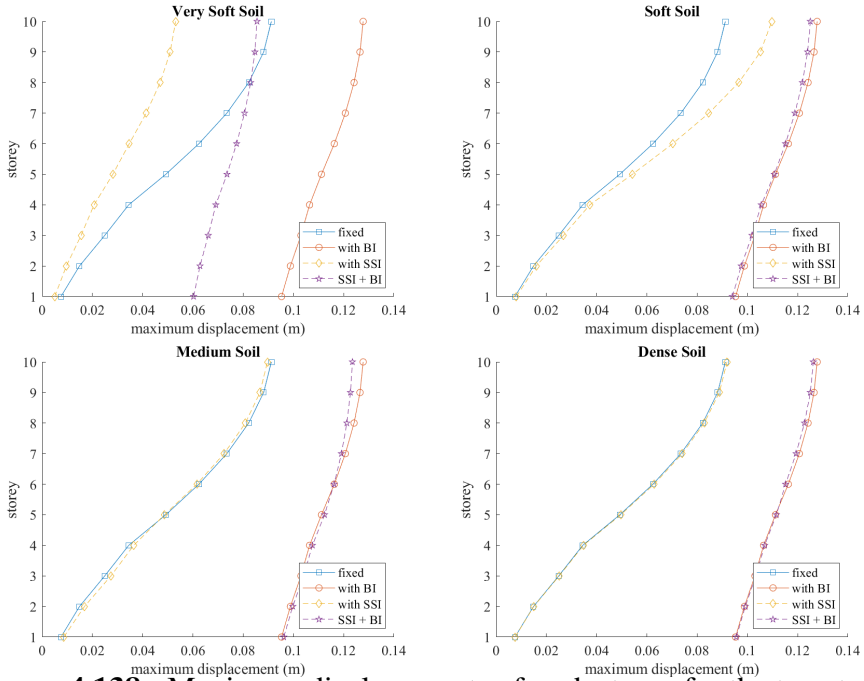

Figure 4.138 : Maximum displacements of each storey for the ten-storey building(Manjil, 1990, far fault).

Figure 4.137 shows comparative displacement-time histories of the ten-storey building for each soil type. Figure 4.138 shows maximum displacement values for each storey.

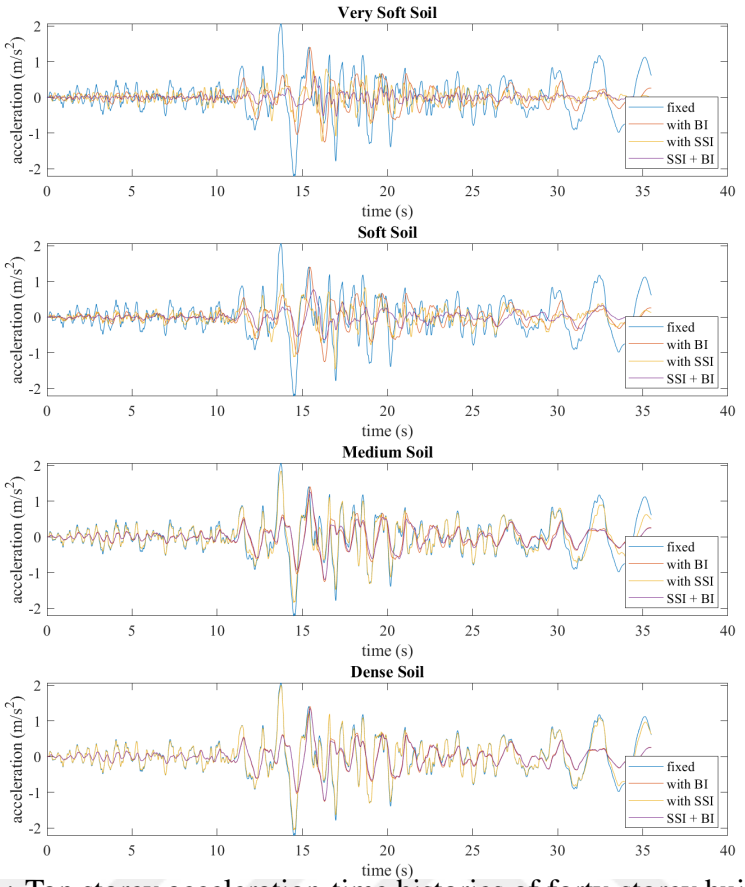

Figure 4.139 : Top storey acceleration-time histories of forty-storey building(Manjil, 1990, far fault).

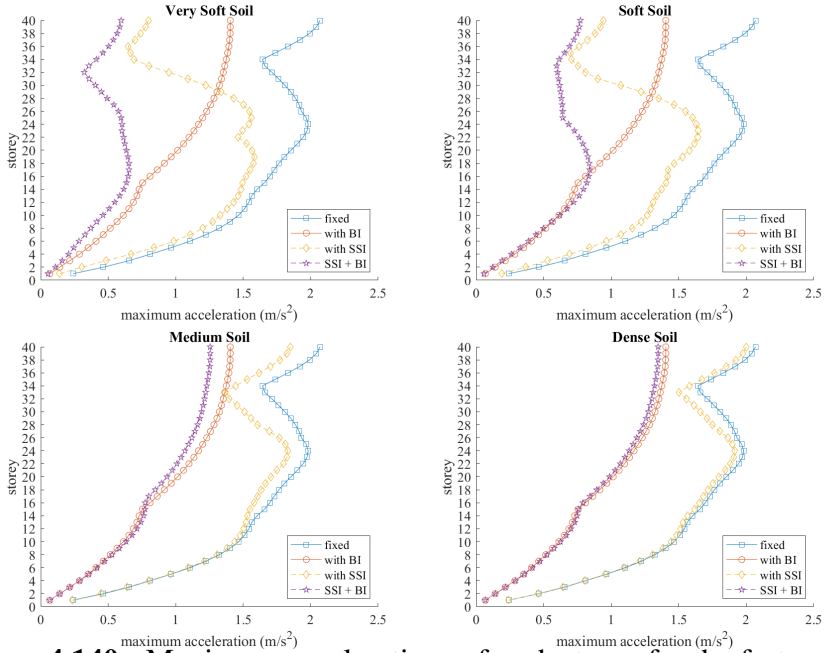

Figure 4.140 : Maximum accelerations of each storey for the forty-storey building(Manjil, 1990, far fault).

Figure 4.139 shows comparative acceleration-time histories of the forty-storey building for each soil type. Figure 4.140 shows maximum acceleration values for each storey.

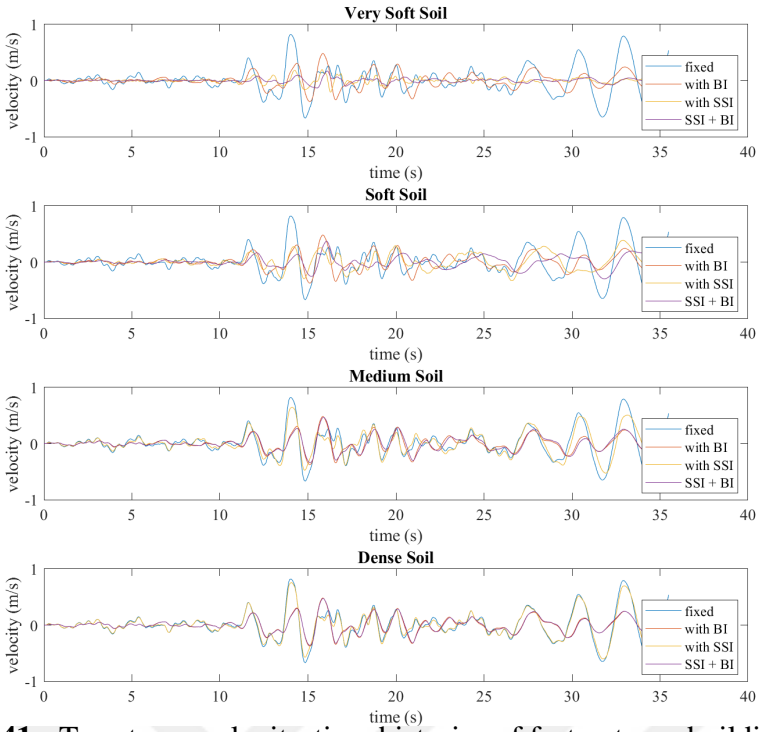

Figure 4.141 : Top storey velocity-time histories of forty-storey building(Manjil, 1990, far fault).

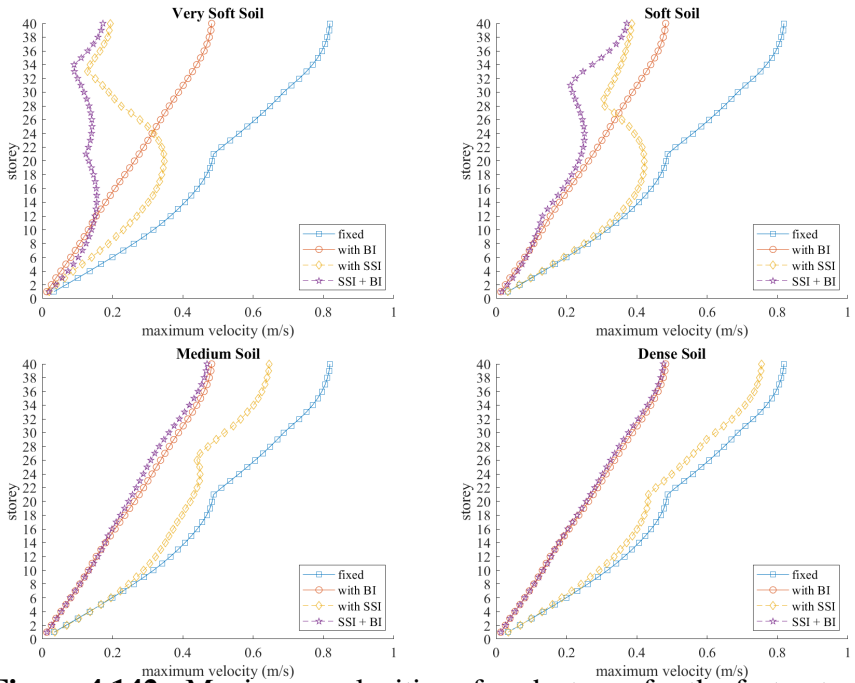

Figure 4.142 : Maximum velocities of each storey for the forty-storey building(Manjil, 1990, far fault).

Figure 4.141 shows comparative velocity-time histories of the forty-storey building for each soil type. Figure 4.142 shows maximum velocity values for each storey.

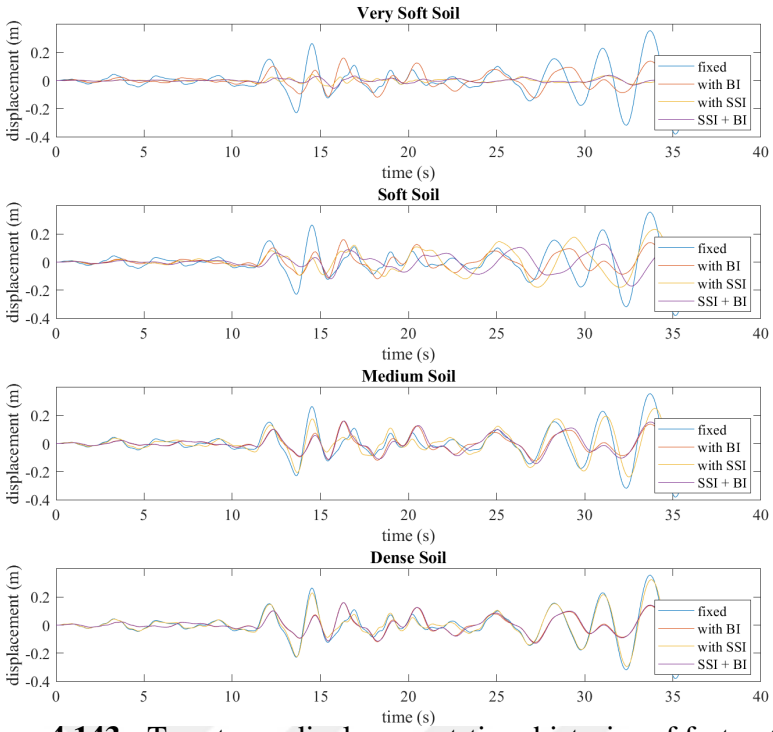

Figure 4.143 : Top storey displacement-time histories of forty-storey building(Manjil, 1990, far fault).

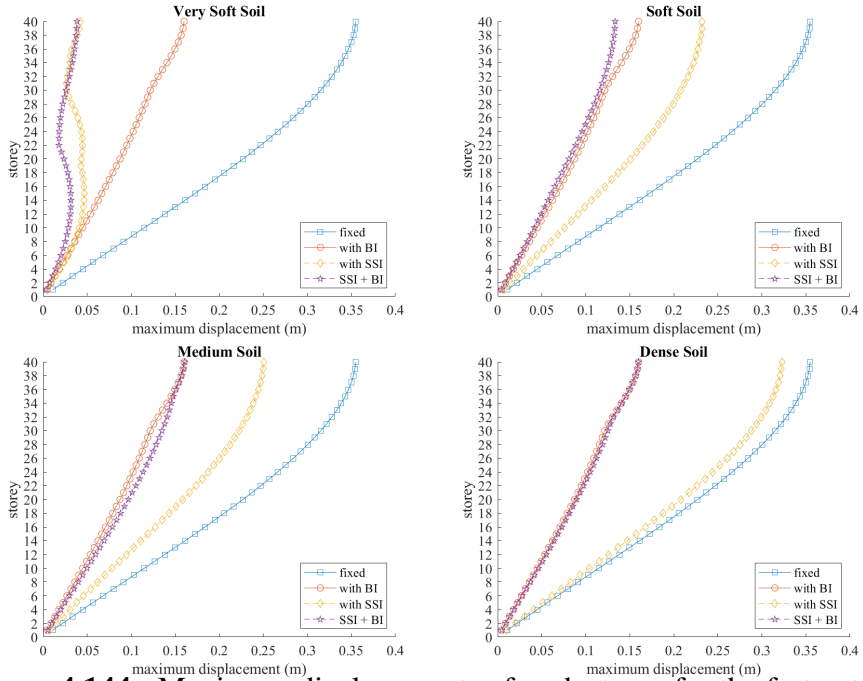

Figure 4.144 : Maximum displacements of each storey for the forty-storey building(Manjil, 1990, far fault).

Figure 4.143 shows comparative displacement-time histories of the forty-storey building for each soil type. Figure 4.144 shows maximum displacement values for each storey.

It can be seen from the results that SSI effects are more pronounced in softer soil conditions. In denser soil conditions, the structure approaches its fixed base conditions. Also it can be seen that SSI is mostly beneficial to the structure. These results does not vary when the rupture distance is changed. Height of the buildings also does not affect the characteristics of the results.

4.2 Spectral Analysis

Response spectra are essentially a collection of responses from single degree of freedom structures under an earthquake excitation. Every single point on the horizontal axis of response spectra is a single degree of freedom structure with a different natural vibration period. The responses of these single degree of freedom structures are calculated and plotted, thus response spectra are created. The responses include acceleration, velocity and displacement. For this task, a Matlab [44] function is written and given in listing 3.7.

Spectral analysis is conducted for the ten-storey building using the 1940 Imperial Valley earthquake and the results are given in figures 4.145 to 4.148.

Results show that the period elongation feature of base isolation and SSI lowers the spectral acceleration response of the structure. Base isolation displacements are higher than fixed conditions which is the same as time history results. The conclusions obtained from this study are given in this section.

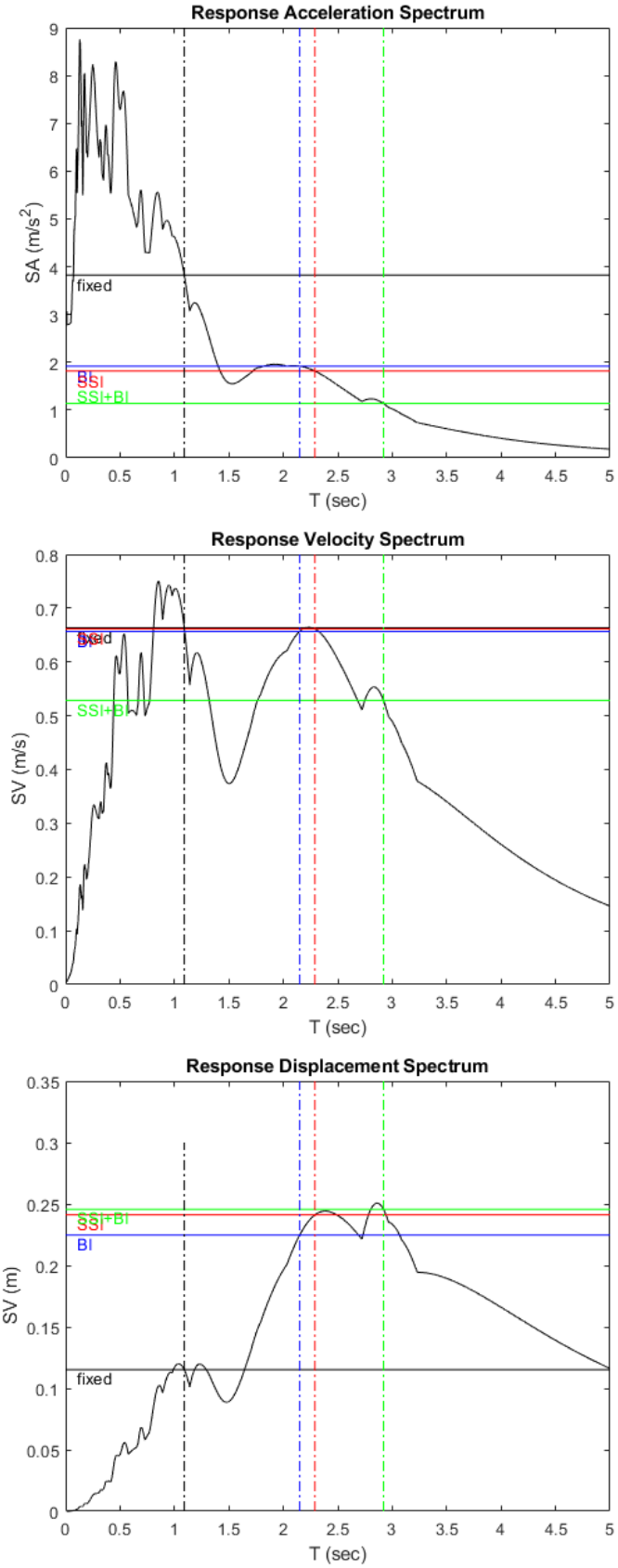

Figure 4.145 : Spectral acceleration, velocity and displacement values for very soft soil conditions.

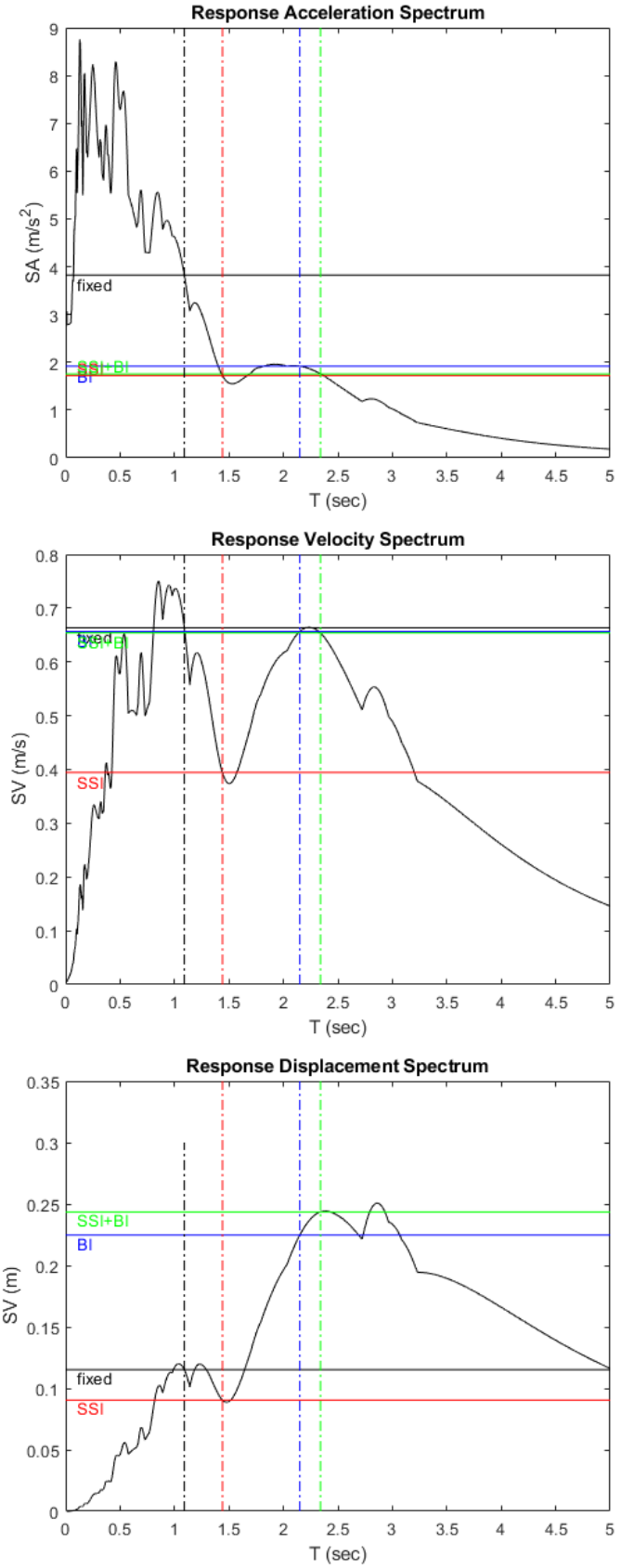

Figure 4.146 : Spectral acceleration, velocity and displacement values for soft soil conditions.

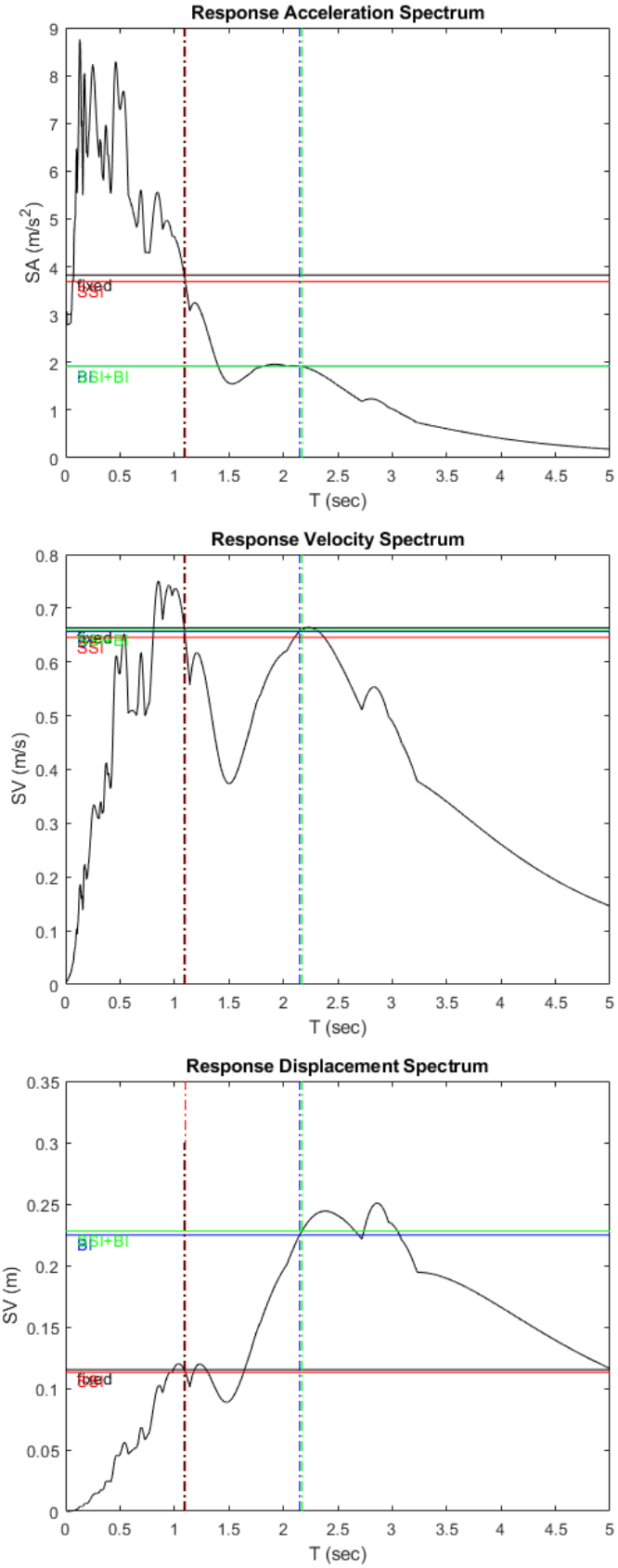

Figure 4.147 : Spectral acceleration, velocity and displacement values for medium soil conditions.

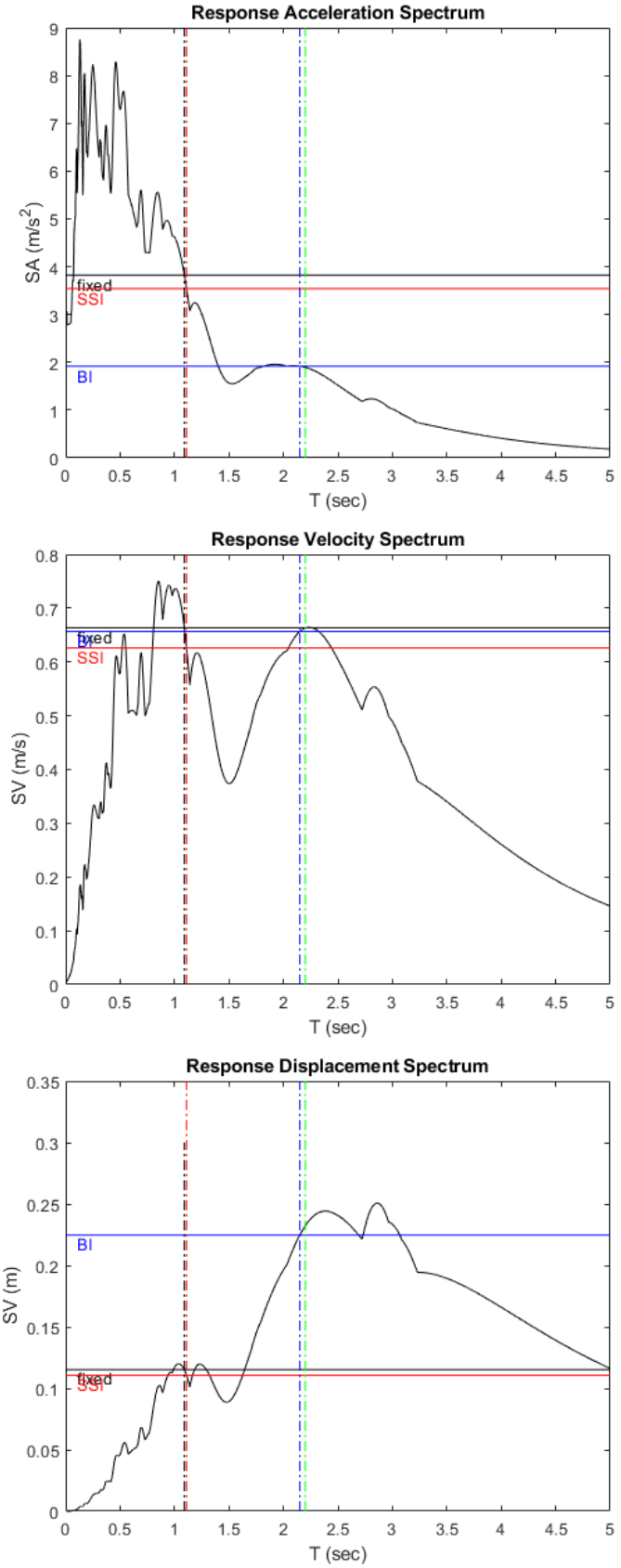

Figure 4.148 : Spectral acceleration, velocity and displacement values for dense soil conditions.

5. CONCLUSIONS AND RECOMMENDATIONS

A large number of numerical analyses are conducted for three different shear frame buildings. It should be noted here that all the conclusions given below are obtained from numerical results that are given in this thesis.

Base isolation may greatly reduce acceleration, velocity and displacements on structures that are induced by earthquakes. Although total displacements might be higher than a fixed structure, most of it happens on the isolation system and the superstructure moves as a whole, resulting in much lower inter-storey drifts compared to the fixed base structure.

SSI may modify the acceleration, velocity and displacement responses of structures. Results show that SSI mostly reduces the effects of earthquakes. For the purpose of staying in the safer side, design codes does not specify SSI analysis procedures, they often briefly state that SSI can sometimes modify earthquake responses and for those rare cases it should be investigated [9]. This study's results are in line with these assumptions. For a small number of cases, SSI may slightly increase the response of structures.

Results show that SSI effects are much more pronounced in soft soil conditions and hardly ever present at dense soil conditions. In dense soil conditions, response of structures eminently approaches to fixed base conditions.

Based on this study, SSI affects the performance of base isolation systems. Effectiveness of base isolation systems is reduced when SSI is considered.

According to this study, both far and near fault earthquakes leads to the responses that have similar characteristics. Height of structures also don't have any significant effects when SSI and base isolation considered.

Spectral analysis results agree with the time history results.

This study does not cover the nonlinearity of structures and isolation systems. This can be covered in future research.

REFERENCES

[1] **Celep, Z.** (2017). *Deprem mühendisliğine giriş ve depreme dayanıklı yapı tasarımı*, Beta Basım Yayım Dağıtım A.Ş.

[2] **Chopra, A.K.** (2013). *DYNAMICS OF STRUCTURES, Theory and Applications to Earthquake Engineering, 4th Edition*, Pearson Education Limited.

[3] **Türkiye Bina Deprem Yönetmeliği**, (2019), Deprem Etkisi Altında Binaların Tasarımı için Esaslar.

[4] **Touaillon, J.**, (1870), Improvement in buildings, United States Patent, No: 99973 dated 15.02.1870.

[5] **Cooper, A.F.**, (1870), Improved foundation for buildings, United States Patent, No: 100262 dated 01.03.1870.

[6] **Naeim F., Kelly J.M.** (1999). *Design of Seismic Isolated Structures: From Theory to Practice*, John Wiley & Sons, Inc.

[7] **Bechtold, J.**, (1907), Earthquake-proof building, United States Patent, No: 845046 dated 26.02.1907.

[8] **Calantarients, J.A.**, (1909), Building construction to resist the action of earthquakes, United States Patent, No: 932443 dated 31.08.1909.

[9] **American Society of Civil Engineers**, (2000), FEMA 356 Prestandard and Commentary for the Seismic Rehabilitation of Buildings.

[10] **Constantinou M., Kneifati M.** (1988). Dynamics of Soil-Base-Isolated-Structure Systems, *Journal of Structural Engineering*, *114*(1), 211–221.

[11] **Bycroft G.** (1977). Soil-structure interaction at higher frequency factors, *Earthquake Engineering and Structural Dynamics*, *5*(3), 235–248.

[12] **Novak M., Henderson P.** (1989). Base-isolated buildings with soil-structure interaction, *Earthquake Engineering and Structural Dynamics*, *18*(6), 751–765.

[13] **Pappin J., Lubkowski Z., King R.** (1997). The Significance of Site Response Effects on Performance Based Design, *Uniform Building Code, International Conference of Building Officials*, Whittier, California.

[14] **Mylonakis G., Gazetas G.** (2000). Seismic Soil-Structure Interaction: Beneficial or Detrimental?, *Journal of Earthquake Engineering*, *4*(3), 277–301.

[15] **Tongaonkar N.P., Jangid, R.S.** (2003). Seismic response of isolated bridges with soil–structure interaction, *Soil Dynamics and Earthquake Engineering*, *23*(4), 287–302.

[16] **Mylonakis G., Voyagaki E., Price T.** (2003). Damage Potential of the 1999 Athens, Greece, Accelerograms, *Bulletin of Earthquake Engineering*, *1*(2), 205–240.

[17] **Syngros K.** (2004). Seismic Response of Piles and Pile-Supported Bridge Piers Evaluated Through Case Histories, *Ph.D. thesis*, Langan Engineering / City College of New York.

[18] **Deb S.** (2004). Seismic base isolation – An overview, *Current Science*, *87*(10), 1426–1430.

[19] **Tsai C., Chen C., Chen B.** (2004). Effects of unbounded media on seismic responses of FPS-isolated structures, *Structural Control and Health Monitoring*, *11*(1), 1–20.

[20] **Dicleli M., Albhaisi S., Mansour M.Y.** (2005). Static Soil–Structure Interaction Effects in Seismic-Isolated Bridges, *Practice Periodical on Structural Design and Construction*, *10*(1).

[21] **Liu M., Chiang W., Hwang J., Chu C.** (2008). Wind-induced vibration of high-rise building with tuned mass damper including soil–structure interaction, *Journal of Wind Engineering and Industrial Aerodynamics*, *96*(6-7), 1092–1102.

[22] **Spyrakos C.C., Koutromanos I.A., Maniatakis C.A.** (2009). Seismic response of base-isolated buildings including soil–structure interaction, *Soil Dynamics and Earthquake Engineering*, *29*(4), 658–668.

[23] **Jeremic B., Jie G., Preisig M., Tafazzoli N.** (2009). Time domain simulation of soil–foundation–structure interaction in non-uniform soils, *Earthquake Engineering and Structural Dynamics*, *38*(5), 699–718.

[24] **Karabörk T., Deneme İ.Ö., Bilgehan R.P.** (2010). Temeli izole edilen yapılarda dinamik yapı-zemin etkileşimi (Turkish), *Erciyes Üniversitesi Fen Bilimleri Enstitüsü Dergisi*, *26*(1), 77–87.

[25] **Kausel E.** (2010). Early history of soil–structure interaction, *Soil Dynamics and Earthquake Engineering*, *30*(9), 822–832.

[26] **Genes M., Doğanay E., Bikçe M., Kaçın S.** (2011). Soil-Structure Interaction in RC Frame Buildings from Strong-Motion Recordings, *KSU. Journal of Engineering Sciences*, *14*(1).

[27] **Matinmanesh H., Asheghabadi M.** (2011). Soil-structure interaction at higher frequency factors, *Procedia Engineering*, *14*, 1737–1743.

[28] **Manolis G., Markou A.** (2012). A distributed mass structural system for soil-structure-interaction and base isolation studies, *Archive of Applied Mechanics*, *82*(10-11), 1513–1529.

[29] **Giarlelis C., Mylonakis G.** (2014). The role of soil-structure interaction in the inelastic performance of multi-storey buildings, *9th International Conference on Structural Dynamics*, Porto, Portugal.

[30] **Li C., Liu W., Wang S., Du D.** (2010). Analysis of Soil-Structure Interaction (SSI) Effects on Seismic Response of Base-Isolated Structures, *Advanced Materials Research*, *163-167*, 4199–4207.

[31] **Luco J.E.** (2014). Effects of soil–structure interaction on seismic base isolation, *Soil Dynamics and Earthquake Engineering*, *66*, 167–177.

[32] **Tsai C.S., Hsueh C.I., Su H.C.** (2016). Roles of soil-structure interaction and damping in base-isolated structures built on numerous soil layers overlying a half-space, *Earthquake Engineering and Engineering Vibration*, *15*(2), 387–400.

[33] **Ashiquzzaman M., Hong K.** (2017). Simplified Model of Soil-Structure Interaction for Seismically Isolated Containment Buildings in Nuclear Power Plant, *Structures*, *10*, 209–218.

[34] **Pioldi F., Salvi J., Rizzi E.** (2016). Seismic Soil-Structure Interaction Analysis of Isolated Nuclear Power Plants in Frequency Domain, *Shock and Vibration*, *2016*.

[35] **Forcellini D.** (2018). Seismic assessment of a benchmark based isolated ordinary building with soil structure interaction, *Bulletin of Earthquake Engineering*, *16*(5), 2021–2042.

[36] **Mckenna F.** (2011). OpenSees: A Framework for Earthquake Engineering Simulation, *Computing in Science & Engineering*, *13*, 58–66.

[37] **Dai W., Rojas F., Shi C., Tan Y.** (2018). Effect of soil structure interaction on the dynamic responses of base isolated bridges and comparison to experimental results, *Soil Dynamics and Earthquake Engineering*, *114*, 242–252.

[38] **Zhenxia S., Haiping D.** The Analysis of Seismic Response for Base-isolated Structure by LS-DYNA, *Indian Institute of Technology, Kanpur*, available from: `http://www.iitk.ac.in/nicee/wcee/article/14_14-0204.PDF`.

[39] **Livermore Software Technology Corporation**, LS-DYNA, `http://www.lstc.com/`.

[40] **Datta, T.** (2010). *Seismic Analysis of Structures*, John Wiley & Sons (Asia) Pte Ltd.

[41] **Pioldi F., Salvi J., Rizzi E.** (2017). Refined FDD modal dynamic identification from earthquake responses with Soil-Structure Interaction, *International Journal of Mechanical Sciences*, *127*, 47–61.

[42] **Bekdaş G., Nigdeli S.M.** (2017). Metaheuristic based optimization of tuned mass dampers under earthquake excitation by considering soil-structure interaction, *Soil Dynamics and Earthquake Engineering*, *92*, 443–461.

[43] **Salvi J., Pioldi F., Rizzi E.** (2018). Optimum Tuned Mass Dampers under seismic Soil-Structure Interaction, *Soil Dynamics and Earthquake Engineering*, *114*, 576–597.

[44] **MATLAB©** (2018). *version R2018a*, The MathWorks Inc., Natick, Massachusetts.

[45] **Pacific Earthquake Engineering Research Center** (2013). *PEER NGA-West2 Database*, https://ngawest2.berkeley.edu/.

APPENDICES

APPENDIX A : DVD containing results and computer program

CURRICULUM VITAE

Yalçıncan Ulus

EDUCATION:

- **B.Sc.:** 2015,Sakarya University, Faculty of Engineering, Department of Civil Engineering